MOLECULAR MECHANISMS OF THE SALT TOLERANCE RESPONSE IN THE HALOPHILE VIBRIO PARAHAEMOLYTICUS

by

Yvon Serge Ongagna Yhombi

A dissertation submitted to the Faculty of the University of Delaware in partial fulfillment of the requirements for the degree of Doctor of Philosophy in Biological Sciences

Spring 2014

UMI Number: 3631201

UMI

Dissertation Publishing

UMI 3631201

ProQuest®

MOLECULAR MECHANISMS OF THE SALT TOLERANCE RESPONSE IN THE HALOPHILE VIBRIO PARAHAEMOLYTICUS

by

Yvon Serge Ongagna Yhombi

Approved: _____
Randall L. Duncan, Ph.D.
Chair of the Department of Department of Biological Sciences

Approved: _____
George H. Watson, Ph.D.
Dean of the College of Arts and Sciences

Approved: _____
James G. Richards, Ph.D.
Vice Provost for Graduate and Professional Education

I certify that I have read this dissertation and that in my opinion it meets the academic and professional standard required by the University as a dissertation for the degree of Doctor of Philosophy.

Signed: _____

E. Fidelma Boyd, Ph.D.
Professor in charge of dissertation

I certify that I have read this dissertation and that in my opinion it meets the academic and professional standard required by the University as a dissertation for the degree of Doctor of Philosophy.

Signed: _____

Daniel Simmons, Ph.D.
Member of dissertation committee

I certify that I have read this dissertation and that in my opinion it meets the academic and professional standard required by the University as a dissertation for the degree of Doctor of Philosophy.

Signed: _____

Melinda K. Duncan, Ph.D.
Member of dissertation committee

I certify that I have read this dissertation and that in my opinion it meets the academic and professional standard required by the University as a dissertation for the degree of Doctor of Philosophy.

Signed: _____

Erica Selva, Ph.D.
Member of dissertation committee

I certify that I have read this dissertation and that in my opinion it meets the academic and professional standard required by the University as a dissertation for the degree of Doctor of Philosophy.

Signed: _____
Michelle A. Parent, Ph.D.
Member of dissertation committee

ACKNOWLEDGMENTS

This document is dedicated to:

My spouse Carol Ann Ongagna-Yhombi, my children Will Sergy Tristan Ongagna, Chanelle Hayey Ongagna, and Christelle Van-nooten Ongagna for their patience, unconditional love, and support.

My loved ones: David Ongagna, Cyr Furet Ongagna, Jeremi Ayossa Ongagna, Constant Jonas Ongagna Otsando, and Rodrigues Armand Ongagna Ndinga. This accomplishment would not have been possible without your unwavering love and support.

My late mother, Atsono Aye Helene, who instilled in me the educational philosophy. Despite being herself victimized and discriminated against as a child by an insensitive society that did not allow the education of young girls, she (my mother) never gave up her strong desire to educate herself and helped make my own journey possible. Lord knows whether my Ph.D. accomplishment would have been possible had it not been for the timeless life lessons she taught me as a child. For that I am forever grateful.

TABLE OF CONTENTS

LIST OF TABLES

LIST OF FIGURES

ABSTRACT

Vibrio parahaemolyticus is a Gram-negative, halophilic bacterium that causes foodborne illness in humans and has become a major public health concern in recent years. This organism is ubiquitous to coastal and marine environments around the world, where fluctuations in salinity are frequent. In addition, as a gut pathogen causing gastrointestinal infections in humans, this bacterium encounters additional stresses in the forms of the host immune response. To thrive in such fluctuating environments, *V. parahaemolyticus* has evolved adaptive strategies such as the uptake and synthesis of protective molecules termed compatible solutes. The genome of *V. parahaemolyticus* contains putative gene clusters for *de novo* synthesis and transport of compatible solutes. The role and full understanding of these specialized genomic features in the overall osmotic stress tolerance of *V. parahaemolyticus* is currently unresolved. We hypothesized that the synthesis and transport systems are essential for *V. parahaemolyticus* growth and survival under osmotic stress conditions.

In order to investigate the functionality of these systems in the osmotic stress tolerance of *V. parahaemolyticus*, we divided the research project in three parts: (1) Examine the role of the ectoine (1, 4, 5, 6-tetrahydro-2-methyl-4-pyrimidine carboxylic acid) and glycine betaine (N, N, N-trimethylglycine) synthesis systems in the NaCl stress response, (2) Determine the role of the four putative Betaine-Carnitine-Choline transporter (BCCT) homologues in the NaCl stress response, and (3) Determine the role of two ProXWV (ProU1 and ProU2) homologues in the NaCl stress response.

Using a combination of different experimental approaches, we examined the functionality of these putative osmotically-controlled systems under conditions that mimicked the increase in NaCl in both defined and complex media.

The role of the two synthesis systems in the NaCl stress response. We demonstrated that *V. parahaemolyticus* had an extended salt tolerance range up to 10.5% NaCl in complex media and a 6% NaCl tolerance in defined M9 minimal media. We demonstrated that exogenously supplied compatible solutes or their precursors in the media relieved the growth constraint caused by high NaCl. By using proton Nuclear Magnetic Resonance spectroscopy (^{1}H-NMR) analysis, we determined for the first time the profile of compatible solutes synthesized and accumulated by this organism. Furthermore, we showed that *V. parahaemolyticus* cells could perform de novo synthesis of ectoine and glutamate in a NaCl-dependent manner.

By comparative growth analysis in defined media amended to high osmolarity containing exogenously supplied compatible solutes or their precursors, we ranked the most effective compatible solutes in *V. parahaemolyticus* in the following order: glycine betaine > choline > proline>glutamate > ectoine. Interestingly, we showed that *V. parahaemolyticus* could use glutamate or proline as a sole carbon source, but not ectoine and glycine betaine suggesting that the latter are bona fide compatible solutes. By expression analysis of the ectoine (*ectA)* and betaine (*betA)* biosynthesis genes we determined that both systems were constitutively expressed at a basal level, but up-regulated upon NaCl upshock. The expression of the *ectA* gene, however, was markedly more induced by NaCl upshock than that of the *betA* under all the conditions examined.

To examine the essentiality of the biosynthesis systems in *V. parahaemolyticus* at high osmolarity, comparative growth analysis was performed between *V. parahaemolyticus* wild-type (WT) and mutant harboring deletion mutations in the glycine betaine synthesis (Δ*betA),* the ectoine synthesis system (Δ*ectB)*, and both systems (Δ*betA*Δ*ectB*). Growth in media of high osmolarity lacking compatible solutes revealed that Δ*ectB* and Δ*betA*Δ*ectB* strains were defective compared to the WT and Δ*betA*. Furthermore, this result indicated that the ectoine synthesis was critical for growth at high osmolarity. Interestingly, the Δ*betA* strain could not grow in high osmolarity media supplied with choline suggesting that choline was toxic to

Δ*betA*. Irrespective of the mutant strains, growth at high osmolarity was rescued to the wild-type level in the presence of glycine betaine. Finally, we performed a phylogenetic survey of the synthesis systems among the members of the genus *Vibrio* and showed the predominance of both systems in these species.

The role of the four putative BCCT homologues in the NaCl stress response. To test the hypothesis that the four Betaine-Carnitine-Choline Transporters (BCCTs) are functional, we examined the role of these systems at high osmolarity. Expression analysis of the four BCCTs subjected to NaCl upshock showed that three of the BCCTs, VP1456, VP1905 and VPA0356 were induced. We constructed in-frame single deletion mutations in all four BCCTs and revealed a behavior similar to wild-type demonstrating redundancy of the systems. However, a triple mutant ΔVP1456ΔVP1723ΔVP1905 was defective in glycine betaine and ectoine uptake. Using *E. coli* MHK13, a betaine synthesis and compatible solute transporter negative strain, we examined the transport specificity of each BCCT in this background. All four BCCTs could transport glycine betaine, but VP1456 had the most diverse substrate transport ability, up-taking glycine betaine, proline, ectoine, and choline.

The role of two ProU homologues in the NaCl stress response. The two ProU transporters identified in *V. parahaemolyticus* are predicted from bioinformatics to function as compatible solute transporters [3]. A *proU1* mutant was previously constructed and showed no distinguishable phenotype compared to the wild-type under high osmolarity [3]. To further understand the role of these systems, we investigated the role of the ProU systems in the osmotic stress tolerance of *V. parahaemolyticus*. We showed that these systems were transcriptionally induced by NaCl upshock. We created several strains carrying deletion mutations in the ProU systems and showed that the Δ*proU1*Δ*proU2* strain exhibited significant growth defect at high osmolarity relative to the wild-type; this result suggested the possibility of additional roles for the ProU systems. Furthermore, we demonstrated that the ability to uptake glycine betaine was retained in both wild-type and Δ*proU1*Δ*proU2* strains at high osmolarity, suggesting that the ProU transport systems are not essential for the

uptake of glycine betaine. Growth in the presence of choline, ectoine, and proline resulted in a slighter reduction in the lag phase in the $\Delta proU1 \Delta proU2$ compared to the wild-type strain.

In summary, our study demonstrated that the putative transporter and synthesis systems found in *V. parahaemolyticus* are transcriptionally induced by NaCl. We demonstrated that these systems are functional and used for biosynthesis and uptake of compatible solutes. We determined for the first time the profile of compatible solutes synthesized and accumulated by this species. Overall, our results indicated that *V. parahaemolyticus* derives osmotic stress protection via the use of the compatible solute biosynthesis and transport systems present in the genome.

Chapter 1

INTRODUCTION

Vibrio parahaemolyticus

Vibrio parahaemolyticus is a Gram-negative, rod-shaped, halophilic bacterium that belongs to the Vibrionaceae family [4, 5, 6; 88]. Members of this family encompass species inhabiting a wide range of aquatic ecosystems [6; 88, 7-10]. *V. parahaemolyticus* is commonly found at the interface of fresh and sea waters, and in sea water, as free living organisms or in associations with fish, and other marine species [7, 9, 10]. In the marine environment, the prevalence of *V. parahaemolyticus* is linearly dependent on both high temperature and salinity [11-13]. As a result, these bacteria are typically absent during the winter months, but are found in great numbers during the warmer months where they are detected in oysters destined for consumption [7-9, 14-19].

Vibrio parahaemolyticus colonization of oysters has been associated with gastrointestinal illness in humans, especially when infected oysters are consumed raw or undercooked. In most cases, these infections are self-limiting in healthy individuals, but can cause serious health complications in immune-compromised subjects. In recent years, *V. parahaemolyticus* infections have drastically increased making *V. parahaemolyticus* the leading cause of bacterial seafood-borne illness in the US, and a major public health concern [11, 20-23]. Besides, *V. parahaemolyticus* colonization of oysters also exerts a huge economic toll to the oyster industries in the US [23, 24].

1

An intriguing aspect of the physiology of *V. parahaemolyticus* is its remarkable adaptation to diverse environments inherent to its ubiquitous lifestyle both as a marine organism where it faces nutrient availability and salinity fluctuations, and as an intestinal human pathogen exposed to *in vivo* immune pressure [10, 18, 24-28]. Therefore, to thrive in such fluctuating environments these bacteria must possess strategies to cope with shifts in osmotic stress, one of the most common stresses in marine environments [29-31].

Typically, bacterial growth and survival in salinity fluctuations requires the maintenance of an intracellular concentration of solutes equal or slightly higher than that of the extracellular milieu in order to maintain a positive turgor pressure [30]. Thus, during situations where the osmolarity of the extracellular milieu drastically increases or drops, bacteria detect these changes and respond swiftly to prevent death by plasmolysis during osmotic upshock or cytolysis during osmotic downshock conditions [29-31]. The ultimate goal of these adaptive responses is the restoration of the cell volume, an intracellular osmotic equilibrium, and a positive turgor pressure-the driving force for normal cell growth and division [30, 32-35].

Two near universal strategies exist to cope with the sudden change in the osmotic pressure in the external environment of the cell; accumulation of K^+ ions in the cytoplasm and/or the uptake/synthesis of compatible solutes [30, 32, 35-37].

Osmotic Stress Strategies

The accumulation of potassium. Bacteria physiological response to the sudden increase in the osmolarity of the environment is the accumulation of K^+ ions in the cytoplasm, coupled with the accumulation of a counter ion such as glutamate. The concomitant accumulation of K^+ ions and glutamate has been observed in *Escherichia*

coli and many bacteria as a primary response during the early phase of osmotic stress [30, 32, 35, 36, 38-45].

In most cases, this early response alone is sufficient to provide temporary relief against low and moderate osmotic stresses [41, 43]. However, as the osmolarity of the external environment steadily increases and extend in duration, the accumulation of high K^+ alone becomes insufficient to counteract osmotic stress constraint. Moreover, the accumulation of extremely high levels of K^+ in the cytoplasm further exacerbates the normal functionality of cellular enzymes [30, 36, 43]. Therefore, bacteria often resort to a second and more sustainable strategy that is the accumulation of compatible solutes, achieved via *de novo* synthesis and uptake [30, 31, 36, 43, 46-48].

Although for the majority of bacteria the K^+ strategy is only a transient response, aerobic Archaean of the order Halobacteriales and certain extremophiles inhabiting extremely high salinity environments have evolved to function only under high potassium content in their cytoplasm, the so-called salt-in strategy[29, 32, 37, 49]. This parallel evolutionary strategy emanates mainly from the makeup of their proteins that contains a high proportion of acidic amino acids over basic residues, making these proteins highly charged [29, 32, 35, 49]. The salt-in strategy also offers little flexibility in the presence to constant salinity fluctuations [29, 32, 49]. But new evidences now suggest that the osmoadaptive strategies among these specialized salt-in taxa are even more complex than initially implied, with subset of the *Halobacteriales* genera using additional strategies such as the compatible solute strategy described below [50].

The accumulation of compatible solutes. The second strategy used by most bacteria to counteract osmotic stress is the accumulation of compatible solutes (CS).

Compatible solutes are low molecular weight organic compounds, soluble in water, that do not carry any charge at physiological pH (Zwitterion) [51]. These compounds are accumulated to high intracellular concentration by most bacteria to protect against osmotic stress [30, 31, 47, 52-61].

A great structural diversity exists among these compounds as they are typically found throughout the three kingdoms of life [51, 62]. Some of the representatives include but not limited to compounds such as trehalose, free amino acids (proline, glutamate, glutamine), and amino acid derivatives (glycine betaine and ectoine) [46, 51]. Depending on the species, these compounds can be used strictly as compatible solutes, or as both compatible solutes and carbon and/or nitrogen sources [51, 56, 63, 64].

Glycine betaine (N, N, N-trimethylglycine) is one of the most efficient compatible solutes used by a wide range of species [65-68]. Besides, compatible solutes also protect against other stressors such as temperature, pH, high pressure, cold, and desiccation depending on the species [52, 53, 55, 66, 69-73].

The mechanisms by which compatible solutes protect against osmotic stress are not yet clearly understood; however, several models have been proposed that suggest that these compounds are preferentially excluded from the protein domain, thus preserving the functionality of cellular enzymes [74, 75, 76-82].
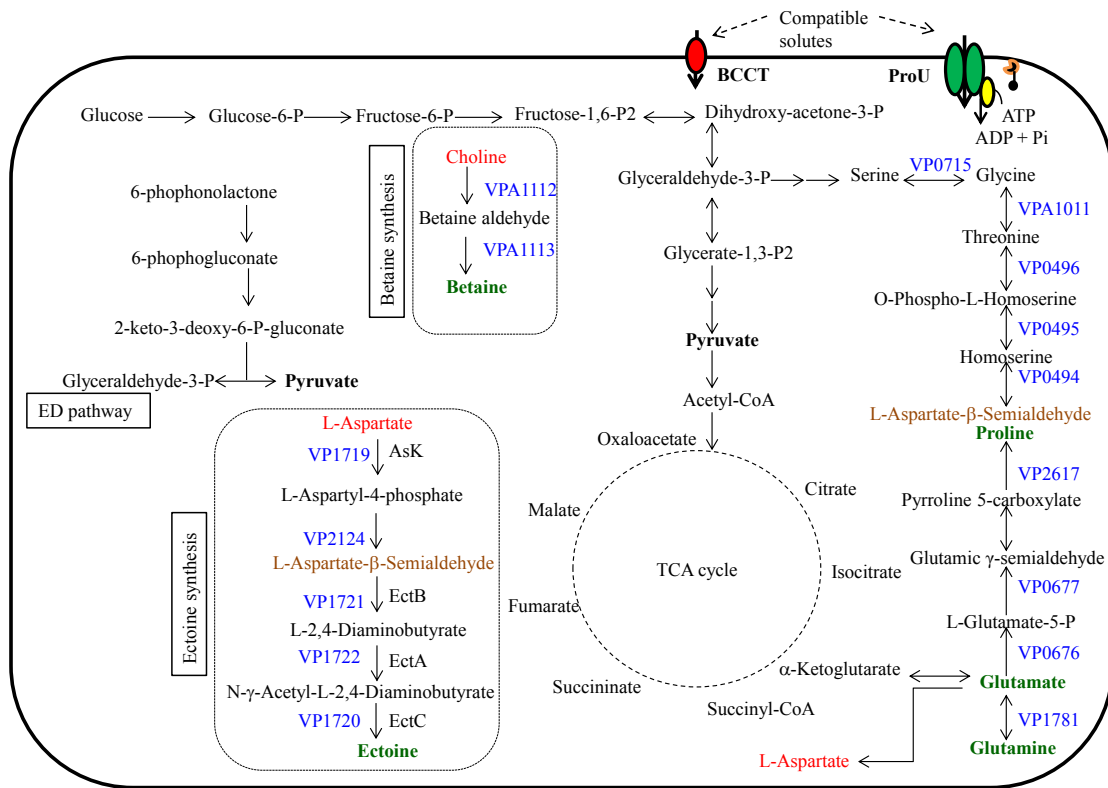
Figure 1 **Schematic representation of the CS pathways in *V. parahaemolytcu*s.** Compatible solutes accumulation is achieved either via uptake by osmotically-controlled transporters (BCCT and PrU), or *de novo* synthesis. *V. parahaemolytcu*s genome contains gene clusters for *de novo* synthesis of ectoine (VP1719-VP1720) and glycine betaine (VPA112-VP114). Additional putative genes of interest that can be utilized to synthesis precursors and relevant amino acids are also shown in the figure. Compatible solutes are shown in green and precursors molecules in red. Gene locus tags are shown in blue

Synthesis Systems

One way by which compatible solutes are accumulated in the cytoplasm is via *de novo* synthesis by biosynthesis gene clusters present in the genome. Some of the pathways used for the synthesis of compatible solutes include but not limited to the trehalose, glycine betaine, and ectoine biosynthesis systems [43, 51, 64, 69, 83, 84].

The trehalose biosynthesis pathway. In *E. coli*, genes encoding the trehalose biosynthesis pathway form a single *OtsBA* operon [84]. This pathway uses UDP-glucose or glucose-6-Phosphate as a precursor molecule to synthesize trehalose in a two-step reaction in which the glucosyltransferase enzyme (trehalose-6-phosphate synthase) encoded by the *otsA* catalyzes the conversion of the precursors to trehalose-6-phosphate, while the trehalose-6-phosphate phosphatase (encoded by the *otsB* gene) carries out the subsequent dephosphorylation of trehalose-6-phosphate to generate trehalose.

Vibrio parahaemolyticus RIMD 2210633 genome does not contain trehalose biosynthetic gene clusters, but contains in chromosome I gene encoding a PTS system trehalose (maltose)-specific transporter subunits IIBC (VP0710) responsible of the import of trehalose (or maltose) into the cell, and its later conversion into trehalose-6-phoshate [85-89]. In the genome, the trehalose-specific PTS transporter is flanked upstream by a trehalose repressor gene *treR* (VP0709) and downstream by a gene encoding a trehalose-6-phosphate hydrolase or TreC (VP0711) capable of the conversion of trehalose-6-phosphate into glucose and glucose-6-phosphate.

The ectoine biosynthesis pathway. This pathway contains genes involved in the synthesis of the ectoine [3, 48, 90]. Biosynthesis genes governing this pathway

cluster in an *ectABC* or *ectABC-aspk* operon depending on the species and use aspartic acid or related molecules as precursors [47, 48, 63, 71, 91].

Ectoine biosynthesis is a multi-step pathway. At the outset of the process, an enzyme called aspartokinase encoded by the *aspk* gene catalyzes the phosphorylation of the L-aspartic acid to L-4-aspartyl-phosphate in a reaction that requires an input of ATP. Next, the aspartate-semi aldehyde dehydrogenase converts the L-4-aspartyl phosphate to L-aspartate-β-semi aldehyde in the presence of NADPH with the release of $NADP^+$ and phosphate. The generated L-aspartate-β-semi aldehyde is located at the junction of many amino acid biosynthesis pathways (methionine, lysine, and threonine) (Fig. 1).

In order to move down the ectoine biosynthesis pathway, a diaminobutyrate-2-oxoglutarate transaminase enzyme (EctB) must catalyze the transamination of L-aspartate-β-semi aldehyde to L-2, 4-diaminobutyrate in the presence of L-glutamate with the release of 2-oxoglutarate. The transamination step is directly followed by the acetylation of L-2, 4-diaminobutyrate (DABA) to Nγ-acetyl-L-2, 4-diaminobutyrate in the presence of the Acetyl-CoA catalyzed by L-2, 4-diaminobutyric acid acetyltransferase (EctA). Finally, the L-ectoine synthase (EctC) catalyzes the cyclization of Nγ-acetyl-L-2, 4-diaminobutyrate to generate L-ectoine with the release of a water molecule.

A subset of ectoine-producing bacteria possesses an additional gene (*ectD*) that encodes an ectoine hydroxylase enzyme responsible of the conversion of ectoine to hydroxyectoine [44, 48, 63, 69, 75, 83, 91-93]. *V. parahaemolyticus* contains *ectABCaspk* ectoine- biosynthetic gene cluster located in chromosome I [3, 94].

The glycine betaine biosynthesis pathway. The canonical glycine betaine

biosynthesis pathway uses choline as a precursor in a two-step oxidation reaction via

betaine aldehyde as intermediate. In *V. parahaemolyticus* and other Gram-negative

bacteria such as *E. coli*, the genes governing this pathway are organized in a *betIBA*

operon [3, 95-97]; the *betA* gene encodes a choline dehydrogenase that catalyzes the

conversion of choline to betaine aldehyde, while the *betB* gene encodes a betaine

aldehyde dehydrogenase enzyme responsible for the conversion of betaine aldehyde to

glycine betaine (Fig. 1) [3, 30, 95-97]. The *betI* gene, however, encodes a

transcriptional repressor that preforms regulatory functions [43, 95, 96]. The

conversion of betaine aldehyde to glycine betaine (the second step of the process) is

mostly conserved between bacteria, mammals and plants and uses the betaine

aldehyde dehydrogenase enzyme, while the first step of the process in not always

conserved [98]. For instance, *Arthrobacter pascens* and *A. globoformis* two Gram-

positive soil bacteria use choline oxidase instead choline dehydrogenase to carry out

the conversion of choline to betaine aldehyde; higher plants use the choline

monooxygenase enzyme to catalyze the first reaction of the pathway [99-105].

Aside from the canonical pathway mentioned above, there exist other

variations in the biosynthesis of glycine betaine found in nature. One such alternative

strategy is the synthesis of glycine betaine from glycine that utilizes a three-step series

of methylation reactions catalyzed by two methyltransferase enzymes, glycine-

sarcosine methyltransferase (GSMT) and sarcosine-dimethylglycine methyltransferase

(SDM), two enzymes with partially overlapping substrate specificity [106 , 107, 108].

This pathway is used by the extreme halophytic phototrophic bacteria such

Halorhodospira halochloris, Methanohalophilus portuclensis and several others [106, 107, 108].

Finally, glycine betaine can also be synthesized from the degradation of carnitine, and this pathway has been described in many bacteria [109, 110]. The key enzyme in this pathway is the carnitine dehydrogenase that converts carnitine to 3-dehydrocarnitine, which is then subsequently broken down to glycine betaine and beyond [110, 111]. The genes governing the synthesis of glycine betaine from glycine and carnitine are absent in *V. parahaemolyticus* [3, 85, 94].

Osmoregulated Transporters

Another means by which bacteria accumulate compatible solutes is through osmotically-controlled transporters, namely the Betaine-Carnitine-Choline Transporter (BCCT) systems and the ATP-Binding Cassette (ABC) family of transporters also known as the ProU transport systems. These specialized transporters scavenge compatible solutes from the external environment during osmotic stress.

Betaine-Carnitine-Choline Transporters (BCCTs). Members of this group belong to the single-component family of secondary transporters that use proton or sodium-motive force to translocate substrates across the membrane [112, 113]. These transporters display certain distinguishing features such as the transport of molecules with quaternary ammonium groups, and encode a protein of 500 amino acid residues on average, organized in 12 putative transmembrane α-helices [113, 114]. In addition, they possess a conserved stretch of tryptophan residues located in the transmembrane domain eight (TM8) believed to be involved in the binding of substrate [114-116]. BCCT proteins have been widely studied in many bacteria such as in *Escherichia coli* (BetT), *Vibrio cholerae* (opuD), *Pseudomonas aeruginosa* (BetT1 and BetT3),

Corynebacterium glutamicum (BetP), and *B. subtilis* (OpuD and OpuE) and shown to carry out uptake of compatible solutes at high osmolarity [54, 58, 114, 116, 117]. *V. parahaemolyticus* genome possesses four putative BCCTs scattered in both chromosomes [3].

   ATP-Binding Cassette (ABC) Transporters. The ABC family of transporters also known as ProU transport systems, named for the ability of these proteins to uptake proline. ProU transport systems constitute are multicomponent transporters that use energy released from ATP hydrolysis to transport substrates across the membrane. These proteins are organized in three separate proteins components encoded by genes organized in *proXWX* operon that includes a periplasmic-binding protein component (ProX*)*, a transmembrane component or permease (ProW*)*, and a nucleotide-binding component or ATPase (ProV) [118-120]. Additional signature motifs include a Q-loop, an H-loop/switch region, a Walker A motif/P-loop, D-loop, and a Walker B motif [119]. Together the Walker A, Walker B, Q-loop, D-loop, and H-loop constitutes the nucleotide binding site/ ATP binding site (chemical binding site) of these proteins. Some of these proteins uptake very specific substrates, while others uptake structurally diverse compounds [119].

   The roles of the ProU transporters in the uptake of compatible solutes during osmotic stress have been widely investigated [116, 118, 121-124]. *V. parahaemolyticus* genome contains two osmoregulated ProU transport systems located in each chromosome whose function is unknown (Fig. 2) [3, 94].

Chromosome 1

ProU1 (ProXWV)

BCCT · DNA pol. III ε · H. Protein · ATPase · Permease · Binding Protein · TH-VPH · LC-FA-CoA ligase

VP1723 · VP1724 · VP1725 · VP1726 · VP1727 · VP1728 · VP1729 · VP1730

Chromosome 2

ProU2 (ProXWV)

H. Protein · NAD(P) H-FR · ATPase · Permease · Binding Protein · Bet A · Bet B · BetI

VPA1107 · VPA1108 · VPA1109 · VPA1110 · VPA1111 · VPA1112 · VPA1113 · VPA1114
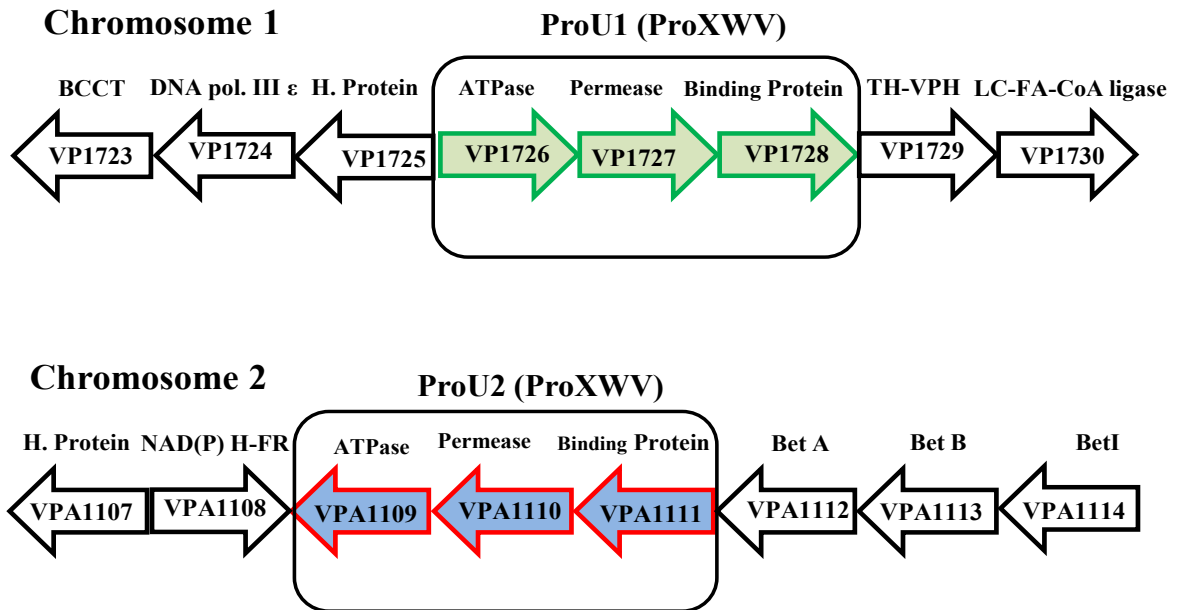
Figure 2   **Organization of the ProU transport systems in *V. parahaemolyticus*.** The ProU1 transport system (located on the positive strand of the DNA) is arranged in VP1726-VP1728 operon. It is flanked on the left by VP1725 (hypothetical protein), VP1724 (DNA polymerase III subunit epsilon, and VP1723 (BCCT), and on the right by VP1729 (thermostable hemolysin delta-VPH) and VP1730 (long-chain-fatty-acid-CoA ligase). The ProU2 transport system (located on the negative strand) is arranged in VPA1109-VPA1111 operon. It is flanked on the left by VPA1108 (NAD (P) H-flavin reductase) and VPA1107 (hypothetical protein), and on the right by the glycine betaine biosynthesis gene clusters (VPA1112-VPA1114). The color green denotes the ProU1 operon, and the red the ProU2 operon. Both operons are boxed in the figures.

Background and Significance

Vibrio parahaemolyticus is a halophilic marine organism that causes gastroenteritis in humans. This bacterium was first described in Japan in the 1950s during a large outbreak associated with the consumption of raw seafood [4, 5, 10, 125, 126]. In the early 1990s, a highly virulent O3:K6 serogroup of *V. parahaemolyticus* emerged in India causing large numbers of hospitalizations and this specific serogroup has since spread worldwide [18, 22, 127, 128].

In recent years, *V. parahaemolyticus* has risen to prominence becoming the leading cause of bacterial seafood-borne gastroenteritis infections in the US, especially during the summer months [12, 13, 20]. One of the main characteristics of *V. parahaemolyticus* is its remarkable ability to survive and thrive in diverse ecosystems marked by abiotic stresses [11, 13, 129]. These stresses are often encountered during fluctuations in salinity, temperature, and nutrient depletion.

The correlation between the rise in temperature and salinity of the oceans and *V. parahaemolyticus* prevalence have been known for some time, but an understanding of the mechanisms driving the ubiquity of this organism are currently lacking [12, 13, 127]. Moreover, the mechanisms that allow *V. parahaemolyticus* to survive and thrive in the presence of high salinity fluctuations remain largely unknown. In many bacterial species, the synthesis and transport of compatible solutes have been shown to provide protection against osmotic stress [30, 43, 55, 130-137]. Furthermore, recent studies have begun to examine extreme halophiles and the role compatible solutes such as ectoine and hydroxyectoine play in the extreme environment these organisms

are found [71, 83, 92, 93l]. Very little is known about the role compatible solute synthesis and transporter systems play in the fitness and survival of *V. parahaemolyticus* and *Vibrio* species in general [3, 54]. This work was undertaken to fill in this gap in our knowledge of this important marine organism.

Previously, it was found that *V. parahaemolyticus* genome contains multiple putative synthesis and transport systems compared to closely related species such as *V. cholerae* and *Vibrio vulnificus* [3]. These systems are used by bacteria to synthesis and scavenge compatible solutes under high osmolarity, which ultimately enhances their survival under stress. Preliminary findings have also suggested a correlation between the presence of these systems and the adaptation of *V. parahaemolyticus* to many stress conditions; for instance, *V. parahaemolyticus* exhibited higher NaCl tolerance and could grow at lower temperature in high NaCl concentrations than species with fewer systems [3]. However, whether these numerous systems work in synergy or individually to protect *V. parahaemolyticus* against NaCl stresses have yet to be examined. We hypothesized that the presence of two synthesis and six transport systems provides *V. parahaemolyticus* with a particular advantage under osmotic stress conditions. A thorough examination of these systems in *V. parahaemolyticus* will provide insight into their physiological significance in osmoadaptation with respect to the diverse ecological niches where these bacteria are found. In addition to addressing the basic research questions aforementioned, the information gained from this study may provide a better understanding of the following aspects related to *V. parahaemolyticus*:

Vibrio parahaemolyticus, the oyster industry, and public health

Vibrio parahaemolyticus is the leading cause of bacterial seafood-borne gastroenteritis infection in the US [138]. Several outbreaks associated with this pathogen have been documented in the US since 1997[138, 139]. *V. parahaemolyticus* proliferates during the warmer months of the year when the temperature and salinity are elevated [140]. Most infections occurred as result of consumption of raw or undercooked and contaminated seafood such as oysters; it is estimated that approximately 4,500 cases/year occur in the US (CDC);however, the exact number could be much higher due to the lack of unified reporting policy across the states. Besides, *V. parahaemolyticus* contamination of oysters exerts a huge economical toll to the oyster industry. The current strategies used by oyster harvesters to substantially reduce vibrio's contamination in oysters and ensure oyster safety rely on consumer education and on postharvest processing methods [17]. Postharvest processing methods use an array of techniques such as quick freezing, frozen storage, high hydrostatic pressure, mild heat, or low dose gamma irradiation [15, 17]. Although these techniques have been widely used by oyster harvesters with relative success, the high cost associated with their implementation has widened the discord between the FDA and the oyster industry. Additionally, some customers have complained about the organoleptic impact of these invasive treatments in oysters. Thus, the results from the study of osmotic stress tolerance in *V. parahaemolyticus* could further our current understanding of the relationships of vibrio proliferation in oysters during the warmer months, where temperature and salinity are elevated. Furthermore, the knowledge gained may also help the oyster industry develop new and cost efficient postharvest strategies.

Vibrio parahaemolyticus and *in vivo* stress tolerance

As a gastrointestinal pathogen, *V. parahaemolyticus* is subjected to a myriad of host eradication strategies whose goals are to eliminate, stop, or circumvent the infection. Among the stresses encountered by *V. parahaemolyticus* in the human body are bile and acid stresses, antimicrobial peptides*,* and reactive oxygen species, among others [141, 142, 143]. The knowledge gained from the study of these systems could lend support towards understanding whether or not the numerous compatible and transporter systems found in *V. parahaemolyticus* are part of the "arsenal" that allow this organism to cope with the stresses encountered during the course of the infection in human. Already in *Listeria monocytogenes*, the presence of numerous osmoregulatory systems has been shown to play a critical role in the pathogenicity of this species [53, 57].

Vibrio parahaemolyticus and biotechnology

From a biotechnological standpoint, the studies of the two synthesis systems within a single organism carries potential biotechnological implications; compatible solutes, owing to their ability to preserve cellular molecules against heat, cold, dehydration, salinity, and other abiotic stresses are widely used in biotechnology [144]. Some of the applications involve their use in cosmetic to make skin lotion, in molecular biology as DNA stabilizer, in pharmaceutical industry, and in agriculture to create genetically modified stress-tolerant crops [69, 99, 100, 103, 144]. Consequently, their wide use in biotechnology has resulted in the development of optimized industrial approaches [145]. However, most of the current bioprocesses produce only one compatible solute at a time [91, 144, 146]. The ability to optimize

the production of multiple compatible solutes from a single organism has very attractive biotechnological applications.

Dissertation Work

This research work was undertaken to address the as-yet unanswered questions related to the complex physiology of *V. parahaemolyticus*, especially the mechanisms that control growth and survival in high salinity environments.

Vibrio parahaemolyticus is a bacterium predominant in marine and estuarine environments around the world, ecosystems exposed to constant fluctuations in salinity. Additionally, as a gut pathogen causing gastroenteritis illness in human hosts, this bacterium encounters additional stresses in the form of antimicrobial peptides, acid stresses, and oxygen reactive species.

The full understanding of the mechanisms that drive the ubiquity of these organisms in these fluctuating ecosystems, especially in relation to salinity remains poorly understood. To investigate these questions, different research avenues have been proposed and are currently being pursued in our laboratory to look into the mechanisms that control the physiology and ecology of this important marine organism. One of those research avenues has focused on the investigation of the mechanisms that allow *V. parahaemolyticus* to cope with constant salinity fluctuations in the environment.

Bioinformatics appraisal of the genomic features of *V. parahaemolyticus* and other Vibrionaceae had previously identified the genomic features of interest [3, 85, 94]. Furthermore, ensuing studies have provided additional information on the possible contribution of these systems in *V. parahaemolyticus* ability to grow and survive over a broad range of salinity conditions relative to closely related species [3]. Furthering on those preliminary studies, we set to broaden the study to the mechanisms of osmoadaptation in *V. parahaemolyticus* by examining the functionality of the compatible solute synthesis and transport systems.

We hypothesized that the presence of two putative compatible solute synthesis systems and six transport systems is important for *V. parahaemolyticus* growth and survival under osmotic stress conditions.

We devised an experimental strategy that included conditions that mimicked NaCl shifts to look into the cues that induced these systems. Furthermore, we employed molecular and evolutionary genetic approaches to examine the functionality, the distribution and evolutionary relatedness of these systems.

Interestingly, we provided experimental support that demonstrated the functionality of these systems under NaCl-induced conditions, and also the type of compatible solutes synthesized or transported.

Finally, we laid out the foundation and provided insights for future directions to be pursued to gain a complete understanding of these systems.

In chapter 2, we investigated the roles of the ectoine and betaine synthesis systems and showed that they are functional. Furthermore, we created synthesis systems single and multiple deletion strains and demonstrated that the ectoine synthesis was critical for growth under high salinity conditions. We examined the expression of the synthesis genes under normal and upshock conditions and showed that these genes were osmotically induced. Moreover, we determined the most effective compatible solutes used by *V. parahaemolyticus.*

In chapter 3, we examined the role of the four putative osmoregulated Betaine-Carnitine-Choline transporter (BCCT) homologues in the osmotic stress tolerance of *V. parahaemolyticus.* We showed that three out of four BCCTs were markedly induced upon NaCl upshock, indicating that high osmolarity was the trigger for induction of these systems. We created single in-frame deletions of these systems and

showed by comparative growth analysis that they are functionally redundant. Furthering on these results, we created two triple BCCT mutants and showed that these systems are involved in the uptake of compatible solutes at high osmolarity. We cloned individual BCCTs into an inducible vector and transformed a compatible solute synthesis system-and uptake-deficient *E. coli* MKH13 strain and determined their substrate specificity in this background. We demonstrated herein that the four BCCT are involved in the uptake of compatible solutes, but VP1456 was a broad-range transporter. Finally, we determined the affinity of these transporters for glycine betaine and showed that VP1456 was again the most efficient of all.

In chapter 4, we investigated the functionality of the two putative osmoregulated ProU (ABC transporters) in *V. parahaemolyticus*. We showed that, as seen with the four BCCTs, the two ProU single mutants were also functionally redundant. We created a double ProU mutant, lacking both systems, and noticed extended lag phase relative to the wild-type strain at high osmolarity in defined media; this phenotype suggested the possibility of additional roles for the ProU other than the uptake of compatible solutes. Interestingly, growth of the double ProU mutant in high osmolarity in the presence of exogenously supplied compatible solutes resulted in a somewhat reduced in the lag phase compared to the wild-type, suggesting that these systems are involved in uptake of compatible solutes. Conversely, growth of the double ProU mutant in the presence of glycine betaine resulted in an identical reduction in the lag phase as in the wild-type, which suggested that these systems are not involved in the uptake of glycine betaine.

Overall, this dissertation work furthered the current understanding of the role of the synthesis and transport systems in *V. parahaemolyticus* ability to withstand

constant salinity fluctuation in the marine ecosystems. We determined for the first time the profile of the compatible solute accumulated by this species, and most of all showed that NaCl was the trigger for induction of these systems. Future research will be needed to tie together the data generated herein, especially with respect to understanding how these systems sense, regulate, and orchestrate the overall osmoadaptation strategy in this organism.

Chapter 2

THE BIOSYNTHESIS OF THE OSMOPROTECTANT ECTOINE BUT NOT GLYCINE BETAINE IS CRITICAL FOR THE SURVIVAL OF OSMOTICALLY STRESSED VIBRIO PARAHAEMOLYTICUS

Introduction

Vibrio parahaemolyticus is a halophile that is abundant in the aquatic environment and has been isolated from the water column, sediment and in association with crustaceans, mollusks, fish and planktonic copepods [7-9]. In the marine and estuarine environments, *V. parahaemolyticus* must navigate changing salinities, temperatures and nutrient limitations and is known to proliferate during the warmer months of the year when the salinity and temperature are elevated [4, 8, 147, 148]. *V. parahaemolyticus* levels in marine and estuarine waters are linearly dependent on both salinity and water temperature, and in winter months the bacterium is rarely isolated from the water column and is typically only found in small numbers in sediment [4, 8, 16].

Global climate change has resulted in the overall increase in ocean temperatures as well as the acidification of these waters, which impacts the distribution of marine species [149-153]. In recent years, outbreaks of *V. parahaemolyticus* have been documented as far north as Alaska and this northward migration trend has been mainly attributed to the rise in ocean temperature [139, 148, 154]. Interestingly, it was demonstrated that growth in differing NaCl concentrations alters the susceptibility of *V. parahaemolyticus* to other environmental stresses [155].

It has been documented that growth of *V. parahaemolyticus* in 3% NaCl compared to 1% NaCl increased survival under both inorganic (HCl) and organic (acetic acid) acid conditions. In addition, at 42°C and -20°C, growth of *V. parahaemolyticus* in 1% NaCl compared to 3% NaCl had a detrimental effect [155]. It has also been suggested that temperature may play a role in virulence gene regulation [156]. *V. parahaemolyticus* is of significant medical importance as it is the leading cause of seafood-associated bacterial gastroenteritis worldwide [20, 27, 138].

Generally, the bacterium infects the host through the gastrointestinal tract, where it encounters stress conditions such as low pH, bile salts, antimicrobial peptides, and low salinity as well as challenges from the host immune system. Most infections of *V. parahaemolyticus* occur as a result of consumption of raw or undercooked contaminated seafood. Bioinformatics analysis has shown that the *V. parahaemolyticus* genome contains two compatible solute biosynthesis gene clusters; ectoine (encoded by *ectABCaspK*) and glycine betaine (encoded by *betIBA*) [3, 94, 157]. In addition to these synthesis systems, the genome encodes two putative glutamine synthetase genes (VP0121 and VP1781), a glutamate synthetase gene (VPA0765) and a glutamate synthase gene cluster (VP0481-VP0484), as well as a putative bifunctional proline dehydrogenase/pyrroline-5-carboxylate dehydrogenase that can perform the reversible reaction of proline to glutamate. Six putative compatible solute transporters including four betaine-carnitine-choline transporters (BCCTs) and two ProXWV (also known as ProU) transporters are contained also within the genome [3, 94].

In many Proteobacteria, the response to osmotic stress has two phases; the first is the short term response resulting in the accumulation of K^+. The second (prolonged

22

strategy) is the synthesis and/or accumulation of compatible solutes that can be amassed in high concentrations without disturbing vital cellular functions [62]. Compatible solutes include but are not limited to trehalose, glycerol, mannitol free amino acids such as glutamate, glutamine, and proline, and their derivatives betaine, glycine betaine, and ectoine [31, 47, 51, 62, 130, 158]. It has been proposed that most bacteria use the trimethylammonium compound glycine betaine (N, N, N-trimethylglycine) as their preferred compatible solute [33, 51, 130]. However, one of the most widespread compatible solutes is ectoine (1, 4, 5, 6-tetrahydro-2-methyl-4-pyrimidinecarboxylic acid) [31, 33, 47, 51, 130, 158]. Ectoine is the only compatible solute synthesized in *V. cholerae* and *V. fischeri*, and in *V. cholerae* it was shown to play a role in osmotolerance [159].

Previously, we demonstrated using comparative physiological analysis that *V. parahaemolyticus* compared with *V. vulnificus* YJ016, *V. cholerae* N16961 and *V. fischeri* ES114, which all contain fewer compatible solutes systems had a growth advantage under different salinity concentrations and temperatures [3]. We showed using one dimension nuclear magnetic resonance (^{1}H-NMR) that at high salinity *V. parahaemolyticus* is capable of *de novo* synthesis of ectoine whereas a Δ*ectB* strain was not [3].

In this study, we examined the role of compatible solute synthesis in the *V. parahaemolyticus* NaCl tolerance response and determined the compatible solutes synthesized and utilized to greatest effect by this bacterium. It was determined using ^{1}H-NMR analysis the major compatible solutes synthesized by *V. parahaemolyticus* when cells were osmotically challenged. We examined whether *V. parahaemolyticus* could synthesize both ectoine and glycine betaine in the presence of their precursors

23

aspartic acid and choline, respectively. It was established the conditions under which the ectoine and glycine betaine biosynthesis genes are expressed and whether NaCl induces expression. Using a molecular genetic approach, constructed deletions in each of the biosynthesis systems were examined for their effect on growth and survival.

Materials and Methods

Bacterial strains, plasmids, and growth conditions

Bacterial strains and plasmids used in this work are listed in Table 1. *Vibrio parahaemolyticus* RIMD2210633 serotype O3:K6[85] and generated mutants were routinely grown at 37°C with aeration in Luria-Bertani (LB) broth (Fisher Scientific, Fair Lawn, NJ) with 3% NaCl (w/v)*,* or in M9 minimal medium containing 47.8 mM Na_2HPO_4, 22 mM KH_2PO_4, 18.7 mM NH_4Cl, 8.6 mM NaCl (Sigma-Aldrich, USA) supplemented with 2 mM $MgSO_4$, 0.1 mM $CaCl_2$, and 0.4% (w/v) glucose as a sole carbon source designated M9G with 3% NaCl (w/v). To recreate conditions of elevated osmotic strength, LB and M9G media were prepared with increasing concentrations of NaCl ranging from 1% to 11% NaCl (w/v). Compatible solutes or their precursors were added to growth media at the following concentrations: glycine betaine 100 µM, ectoine 100 µM, choline 1000 µM, aspartic acid 1000 µM, glutamate 1000 µM, glutamine 1000 µM and proline 1000 µM (Sigma-Aldrich, USA). *Escherichia coli* DH5α λpir used in this study was grown in LB media containing 1% NaCl at 37°C under aerobic condition and *E. coli* β2155*,* an auxotroph for diaminopimelic acid (DAP), was grown at 37°C in LB 1% NaCl broth supplemented with 0.3 mM DAP. All antibiotics were used at the following concentrations:

Ampicillin (Amp), 100 µg/ml; Chloramphenicol (Cm), 25 µg/ml; and Streptomycin (Str), 200 µg/ml.

Growth analysis

Growth analysis of *V. parahaemolyticus* RIMD2210633 and mutants was performed in a 96-well Tecan Sunrise microplate reader (Tecan US Inc., Durham, NC) in LB or M9G media adjusted to a desired NaCl concentrations and in the absence or presence of compatible solutes or their precursors. Briefly, pre-cultures of *V. parahaemolyticus* were grown overnight in LB or M9G media and 2% of inoculum of stationary phase cells were used to inoculate fresh media and grown for 5 h at 37°C with aeration. A 2.5% inoculum was subsequently used to inoculate a 96-well microliter plate filled with 200 µl/well of media adjusted to different NaCl concentrations. Bacterial growth was monitored hourly by measuring the optical densities (OD_{595}) for a period of 24 h or longer. All measurements were done in triplicate using at least two biological replicates. The data obtained were then computed statistically and plotted as average of means using Origin 8.5 software program (Origin Lab Corporation, MA, USA).

Nuclear magnetic resonance spectroscopy (NMR) analysis

Cellular extracts of *V. parahaemolyticus* RIMD2210633 were prepared for NMR analysis, as previously described [3, 159]. In brief, *V. parahaemolyticus* was cultured to logarithmic or stationary phase at 37°C in M9G supplemented to a NaCl concentration as indicated. Bacterial cells were then pelleted by centrifugation for 10 min at 1000 *xg*, and the cell pellets were washed once with fresh media of equal salinity. Cells were then lysed by freeze-thaw cycles three times in dry ice and

subsequently suspended in 750 μl of ethanol. After centrifugation at 4000 *xg*, ethanol extracts free of cellular debris were transferred into clean tubes and ethanol was removed by evaporation in a Savant SpeedVac concentrator (Thermo Scientific, Waltham, MA) for ~4 h. The resulting dried pellet material was suspended in 500 μl of deuterium oxide (D_2O) solvent (Cambridge Isotope Laboratories Inc., Andover, MA), and insoluble material was removed by centrifugation. The suspended organic materials were transferred into a 5 mm NMR tube (Wilmad LabGlass, Vineland, NJ) and ^{1}H-NMR spectral data were obtained by running samples in a Bruker Avance 400 NMR spectrometer at 400 MHz. Acquired ^{1}H-NMR spectra were processed and analyzed by ACD/NMR Processor Academic Edition software version 12.01 (ACD/Labs, Canada).

RNA isolation and cDNA synthesis

Vibrio parahaemolyticus RIMD2210633 Wild-type was grown overnight at 37°C with aeration in LB or M9G media containing 3% NaCl (w/v). A 2% aliquot of the overnight culture was then used to inoculate fresh LB or M9G 3% NaCl (w/v) and allowed to grow for 4 h (log phase) or 10 h (stationary phase). Cells were grown in LB 3% NaCl (w/v) or M9G 3% NaCl (w/v) media to either log or stationary phase, and subjected to osmotic upshock conditions in 6% NaCl (w/v) for 30 min at 37°C. For all conditions examined, total RNA was isolated by adding two volumes of RNAprotect Bacteria Reagent (Qiagen) to the cell culture according to the manufacturer's instructions. Isolated RNA was quantified by Nanodrop spectrophotometer (Thermo Scientific, Waltham, MA) and examined by gel electrophoresis on 0.8% agarose to assess quality. RNA was treated with DNase kit (Invitrogen) to remove any genomic DNA contaminant as per the manufacturer's

protocol. The first-strand cDNA synthesis reaction was initiated with 500 ng of purified RNA as a template in a reaction primed with 200 ng of random hexamers, according to the manufacturer's protocol (Superscript II reverse transcriptase kit, Invitrogen).

Gene expression analysis

Transcriptional analysis was performed to assess the expression levels of ectoine and glycine betaine synthesis genes of *V. parahaemolyticus* RIMD2210633 in response to both high NaCl concentrations and different growth phases (log and stationary phase cells). Reverse Transcriptase-PCR gene-specific primers were designed to amplify a 250-270-bp region of *ectA* and *betA* genes (Table 2). RT-PCR assays were then performed on cDNA diluted to 1:25 and 1:125. To assure equal loading of the cDNA template in the RT-PCR reaction and to correct for sampling errors, the expression level of each gene was compared to the level of 16S rRNA control. Following RT-PCR amplification, the expression levels of the genes tested were assayed by running the samples on 1.8% agarose gel. RT-PCR cycling conditions used in these experiments were as follows: 95°C/3 min one cycle; followed by 94°C/30 sec, 55°C/30 sec, 72°C/1 min for 29 cycles; and 72°C/5 min last cycle. To quantify expression levels of *ectA* and *betA* genes after NaCl upshock quantitative real-time PCR (QPCR) was performed. QPCR analysis was performed in a 20 μl reaction to assess the fold change in expression levels of *ectA* and *betA* transcripts after salt upshock in log and stationary phase cultures of *V. parahaemolyticus*; diluted cDNA template was mixed with HotStart-IT SYBR green qPCR master mix (USB, Santa Clara, CA) in a 96-well plate and the Q PCR analysis performed using an Applied Biosystems 7500 fast real-time PCR system (Foster City, CA). The following

cycling conditions were used for the real-time PCR assay: 95°C/2 min one cycle; followed by 95°C/10 sec; 60°C/30 sec for 40 cycles. At the completion of the assay, the generated threshold cycle (C_T) mean values were normalized across the samples with the 16S rRNA control, and the gene expression levels relative to culture grown in 3% NaCl for 4 h was performed using the $\Delta\Delta C_T$ method[160-162]. Two technical replicates and at least two biological replicates were performed for all assays. The significance of the different treatments was statistically computed using an unpaired Student's t test.

Mutant construction

A mutant harboring an in-frame non-polar deletion in the choline dehydrogenase gene (*betA)* of *V. parahaemolyticus* was constructed by Splicing by Overlap Extension (SOE) PCR and homologous recombination [163, 164]. The 1746-bp gene sequence for choline dehydrogenase encoded by *vpa1112* (*betA*) located on the chromosome II of *V. parahaemolyticus* was retrieved from the NCBI GenBank (reference sequence: NC_004605.1). SOE PCR primers along with screening primers were then designed and analyzed using Primer Quest from Integrated DNA Technologies (IDT, USA) (Table 2). The VPA1112A primer was designed to include an XbaI restriction site at the 5'-end, while the VPA1112B primer was modified at the 5'-end by addition of 18-nucleotides tag. The VPA1112C primer was modified at the 5'-end to include a complementary sequence of the 18 nucleotides tag. Finally, the VPA1112D primer was designed to include a SacI restriction site at the 5'-end (Table 2). For SOE PCR amplification, *V. parahaemolyticus* RIMD2210633 genomic DNA was used as a template. Two rounds of PCR amplifications [95°C/5 min; 94°C/30 sec (94°C/30 sec, 51°C/30 sec, 72°C/2 min) x 29 cycles; 72°C/10 min] were performed

first using primer pairs VPA1112A/VPA1112B and VPA1112C/ VPA1112D generating products AB of 379-bp and CD of 334-bp. In the subsequent PCR amplification, primer pair VPA1112A/VPA1112D was used to generate a product (betA-AD) of 713-bp in size containing at the 5' and 3'ends restriction sites for *Xba*I and *Sac*I, respectively. The purified betA-AD truncated DNA fragment was subcloned into the pJET1.2 vector (Fermentas, Glen Burnie, MD). The resulting recombinant plasmid pΔ*betA* was then transformed into *E. coli* DH5α-λpir strain and cloned into a suicide vector pDS132[165]. The recombinant plasmid pDS132Δ*betA* was subsequently used to transform *E. coli* β2155 λpir DAP auxotroph strain, which was conjugated into *V. parahaemolyticus* using a contact-dependent biparental mating by cross-streaking the two strains on LB agar with 1% NaCl 0.3 mM DAP. Following a series of selections on chloramphenicol and sucrose plates, the recombinant clones that underwent double crossover (*ΔbetA*) were selected for the phenotype sucrose resistant (SacB^r) chloramphenicol sensitive (Cm^s), and confirmed by colony PCR and DNA sequencing. Similarly, *ΔectBΔbetA*, devoid of both *betA* and *ectB* genes, was constructed by conjugating *E. coli* β2155 λpir pDS132Δ*ectB* [3] with *V. parahaemolyticus* mutant strain *betA* using the same protocol. The generated *ΔectBΔbetA* was confirmed by PCR and DNA sequencing.

Phylogenetic tree construction

Detection of homologous protein sequences from compatible solute biosynthesis pathways was performed using EctA (VP1722) and BetA (VPA1112) sequences as templates in searches performed with the BLASTP program at the National Center for Biotechnology Information (NCBI) (www.ncbi.nlm.nih.gov/BLAST). Sequences with minimum E values of 0.0001

without filtering were identified. We constructed a phylogenetic tree based on three housekeeping genes of all Vibrionaceae species whose genome sequence is complete. The three housekeeping genes used were RNA polymerase subunit beta (*rpoB*), malate dehydrogenase (*mdh*), both present on chromosome I, and dihydrorotase (*pyrC*) present on chromosome II. Phylogenetic analysis was performed using complete concatenated sequences aligned by ClustalW 2.0 and the neighbor-Joining (NJ) method for tree construction as implemented in MEGA 5[166]. The Bootstrap values for NJ trees were obtained after 1000 generations and MEGA 5 tree viewer was used to visualize the trees and calculate confidence values [166]. The locus tags for each of the genes examined are as follows: ***rpoB***: VSAL_I2866, VHA_000316, YP_131518, V12G01_00020, VAA_00351, VIBR0546_19107, VIBC2010_11541, VC0328, VIC_000047, VcycZ_010100012493, VF_2414, VFA_003646, VME_32530, VIBHAR_00225, VII00023_15976, VII_003403, VINI7043_00277, VordA3_010100006710, ZP_05946651, VPMS16_1850, VP2922, VrotD_010100000953, VIS19158_14047, VISI1226_14532, AND4_18793, VEJY3_14765, VEA_002173, MED222_00572, VIBRN418_07985, VCJ_000034, VS_2963, VT1337_16523, VV3159. ***mdh***: VSAL_I0359, VHA_002058, PBPRA0391, V12G01_12048, VAA_01685, VIBR0546_19297, VIBC2010_15622, VC_0432, VIC_004828, VcycZ_010100009988, VF_0276, VFA_000332, VME_16640, VIBHAR_00795, VII00023_17031, VII_003296, VINI7043_19588, VordA3_010100015387, VIA_003995, VPMS16_415, VP0325, VrotD_010100003320, VIS19158_04331, VISI1226_19579, AND4_18426, VEJY3_01590, VEx25_0219, MED222_17215, VIBRN418_11585, VCJ_000156, VS_0358, VT1337_16653, VV0467. ***pyrC***: VSAL_II0468, ZP_06053391,

30

PBPRA2405, V12G01_05941, VAA_00972, VIBR0546_14415, VIBC2010_09342, VCA0925, VIC_003248, VcycZ_010100004852, VF_A0412, VFA_003087, VME_35630, VIBHAR_05227, VII00023_05282, VII_000508, VINI7043_04290, VordA3_010100001797, ZP_05943435, VPMS16_875, VPA0408, VrotD_010100021328, VIS19158_18031, VISI1226_03785, AND4_06254, VEJY3_22466, VEA_001337, ZP_01062853, VIBRN418_08787, VCJ_003244, VS_II0272, VT1337_19727, VVA0407.

Results

Vibrio parahaemolyticus has a higher salt tolerance in complex media

We wanted to determine the role of nutrient availability in salt stress tolerance of *V. parahaemolyticus*. To examine this, growth of *V. parahaemolyticus* was analyzed in the presence of increasing NaCl concentrations (3%-11%) in LB media at 37°C with aeration (Fig. 3A). It was found that under these conditions *V. parahaemolyticus* can grow in up to 10.5% NaCl (w/v). Next, we examined the NaCl tolerance range of *V. parahaemolyticus* in M9G containing 3 to 9% NaCl (w/v) at 37°C with aeration (Fig. 3B). Under these conditions in M9G, where compatible solutes and their precursors were not exogenously present, *V. parahaemolyticus* could grow at an upper maximum of 6% NaCl, but with an extended lag phase of ~5 h (Fig. 3B). This extended lag phase was reduced to 2.5 h or less when ectoine, glycine betaine or their precursor aspartic acid or choline was exogenously supplied (Fig. 3C). These data showed that *V. parahaemolyticus* cells had a broad salt stress tolerance range when grown in complex media compared with defined media. In addition, these data suggested that *V. parahaemolyticus* can synthesize both ectoine and glycine

31

betaine since the addition of their precursors to the media reduced the lag phase in M9G 6% NaCl.

Vibrio parahaemolyticus **synthesizes ectoine and glutamate** *de novo*

The major compatible solutes synthesized by stationary phase *V. parahaemolyticus* cells was investigated by proton NMR (^{1}H-NMR) at 400 MHZ in the presence of Deuterium Oxide as solvent (D$_2$O). From cells grown in M9G 1% NaCl, no known major compatible solutes were found to be present (Fig. 4A). Protons peaks corresponding to alanine and other organic compounds were noted, which are likely metabolic products produced in these stationary phase cells (Fig. 4A). In M9G 3% and 6% NaCl, protons peaks corresponding to ectoine and glutamate, as illustrated by their chemical shift values expressed in ppm, were identified (Fig. 4B and 4C). It appears also that in M9G 6% NaCl the intensity and peak size increased for ectoine and decreased for glutamate, suggesting that ectoine is produced in a NaCl-dependent manner. Also, an examination of exponential phase *V. parahaemolyticus* cells was performed by ^{1}H-NMR and a similar pattern was found for all three conditions (Fig. 5).

We determined whether the reduction in the lag phase seen when cells were grown in the presence of choline or aspartic acid was due to conversion of these two precursors to glycine betaine and ectoine, respectively and not the result of these compounds being used as carbon and energy sources (Fig. 3C). To examine this, *V. parahaemolyticus* was cultured in M9G 6% NaCl supplemented with 1mM of choline or aspartic acid, and the presence of glycine betaine and ectoine was evaluated by ^{1}H-NMR. It was found that both glycine betaine and ectoine were synthesized in the presence of their respective precursors (Fig. 6A and 6B). To address the question of

32

whether *V. parahaemolyticus* can simultaneously synthesize both ectoine and glycine betaine, *V. parahaemolyticus* cells were grown in M9G 6% NaCl supplemented with 1 mM of choline and 1 mM of aspartic acid. By ^{1}H-NMR analysis, it was shown that *V. parahaemolyticus* was able to synthesize both compatible solutes, however, the normalized intensity of the proton peaks corresponding to glycine betaine were much larger than that of the ectoine peaks, suggesting that more glycine betaine was produced than ectoine **(**Fig. 7).

To examine whether compatible solutes or their precursors can be used as sole carbon and energy sources, *V. parahaemolyticus* cells were grown in M9 1% NaCl media supplemented with glycine betaine, choline, ectoine, aspartic acid, proline, glutamate or glutamine as the sole carbon source. We found that glutamate, aspartic acid, and proline could be used as sole carbon sources. After an 18 h lag phase *V. parahaemolyticus* grew poorly in M9 1% NaCl media supplemented with glutamine. There was no detectable growth from cultures containing choline, ectoine, or glycine betaine as carbon sources. This indicates that ectoine and glycine betaine are *bona fide* compatible solutes, and choline is used solely as a precursor for glycine betaine synthesis (Fig. 8).

Ectoine synthesis gene *ectA* is highly induced by NaCl upshock

To determine whether there is differential expression of the ectoine and glycine betaine synthesis genes, we examined expression of *ectA* and *betA* genes from cells grown under different salinity conditions. First, we examined expression from log and stationary phase cells grown in LB 3% NaCl (Fig. 9A). Reverse transcriptase PCR (RT-PCR) and quantitative Real-time PCR (qPCR) were utilized to determine the transcript levels of *ectA* and *betA*. It was found that both genes were more highly

33

expressed in log phase cells compared to stationary phase cells in LB media (Fig. 9A). Then, we examined expression of these genes under the same conditions after a 30 min upshock in 6% NaCl. The *ectA* gene showed increased expression in log and stationary phase cells after NaCl upshock. The *betA* gene also showed increased expression after NaCl upshock in log phase cells, but not in stationary phase cells (Fig. 9A).

Next, the expression pattern of *ectA* and *betA* genes was examined in log and stationary phase cells grown in M9G 3% NaCl (Fig. 9B). It was found that in defined media, the expression level of *ectA* gene was up-regulated in log phase compared to stationary phase cells, whereas *betA* gene showed low levels of expression in log phase and stationary phase cells. Similarly, we found differential expression under the same conditions after a 30 min upshock in 6% NaCl. Both *ectA* and *betA* genes showed increased expression after the NaCl upshock during log phase growth, with the *ectA* gene showing the higher level of expression. In stationary phase cells after the 30 min upshock in 6% NaCl only the *ectA* gene was expressed (Fig. 9B).

Using qPCR we quantified these expression patterns and demonstrated that the *ectA* gene was significantly more induced under all conditions examined (Fig. 9C and 9D). For example, *ectA* gene showed approximately 200-fold and 60-fold change in expression after NaCl up shock in complex LB and defined media, respectively (Fig. 8C and 8D). Whereas, under the same conditions, *betA* gene showed a 14-fold and 1.75-fold change. Together, these results demonstrated that the expression of both genes were growth phase-dependent and induced by NaCl (Fig. 9C and 9D).

Ectoine synthesis is essential for growth in high salt in defined media

We determined whether synthesis of both ectoine and glycine betaine was critical for *V. parahaemolyticus* growth under osmotic stress. To achieve this, first Δ*betA,* Δ*ectB,* Δ*ectB*Δ*betA* deletion strains were constructed (Fig. 10A and 10B). Then, Δ*betA* strain (defective in glycine betaine synthesis), Δ*ectB* strain (defective in ectoine synthesis), and Δ*ectB*Δ*betA* strain (defective in both glycine betaine and ectoine synthesis) were examined. Growth of the wild-type strain was then compared with that of the Δ*betA* in M9G 6% NaCl media and both strains were comparable (Fig. 11A). However, when Δ*betA* was cultured in the presence of the precursor choline, no growth occurred indicating that choline was toxic to the cell, and further examination of these cultures determined that choline accumulation was bacteriostatic (Fig. 12).

To investigate whether this bacteriostatic effect was due to internal accumulation of choline, ^{1}H-NMR analysis was performed; Δ*betA* cells were grown to exponential phase in M9G 6% NaCl, pelleted, suspended in M9G 6% NaCl supplemented with 1 mM choline for 1 h, and analyzed by ^{1}H-NMR. Our results indicated that choline had accumulated internally in the *betA* mutant cells, but no choline was present in wild-type cells grown under the same conditions (Fig. 10). In M9G 6% NaCl supplemented with glycine betaine, the Δ*betA* strain grew better than wild-type, which was demonstrated by a reduction in the lag phase from ~5 h to ≤1 h (Fig. 11A). In the same media supplemented with either ectoine or aspartic acid Δ*betA* strain also had a reduced lag phase, but not to the same extent as glycine betaine did (Fig. 11A). Overall, these data suggest that the betaine synthesis system is not essential for growth in high salt in defined media. However, glycine betaine is a more effective compatible solute than ectoine in *V. parahaemolyticus*.

We examined the role of the ectoine synthesis system in the growth of *V. parahaemolyticus* under high salt and in defined media. A deletion mutation was constructed previously in the *ectB* gene, which knocked out the synthesis system [3]. This deletion mutant grew similar to wild-type in M9G 3% NaCl demonstrating that there is no overall growth defect. However, it was found that, unlike the Δ*betA*, the Δ*ectB* strain could not grow in M9G 6% NaCl, suggesting that ectoine synthesis is essential (Fig. 11B). We investigated the importance of both synthesis systems by examining the growth of Δ*ectB*Δ*betA* under the same growth conditions described above; the double mutant grew similar to wild-type in M9G 3% NaCl, but showed no growth in M9G plus 6% NaCl (Fig. 11C). The ability of different compatible solutes (glycine betaine, ectoine, proline, glutamate, glutamine) and their precursors (aspartic acid and choline) to rescue growth of the double mutant in M9G 6% NaCl was tested (Fig. 11C). It was found that in the presence of glycine betaine (open circles), proline (closed squares), ectoine (open squares), or glutamate (closed triangle) the double mutant strain grew (Fig. 11C). The compatible solutes demonstrated the following effectiveness as determined by lag phase time reduction and overall final optical density (OD$_{595}$): glycine betaine>proline>ectoine >glutamate. In the presence of ectoine there was a slight defect in Δ*ectB*Δ*betA* since the mutant did not show the same reduction in the lag phase as the Δ*ectB* strain (Fig. 11C). In summary, under the conditions examined herein, our data show that the ectoine synthesis system is essential for growth under osmotic stress conditions and ectoine, glycine betaine and proline are effective compatible solutes used by this species.

Ectoine and betaine synthesis systems are predominant in Vibrios

Of the 33 species of the family Vibrionaceae whose complete genome
sequences are available in the NCBI genome database, we identified the ectoine
cluster alone in 7 species, the glycine betaine cluster alone in 5 species, both gene
clusters in 20 species and neither gene cluster in 1 species (Fig. 13). Depending on the
species, the ectoine synthesis system could be present in either chromosome I or II,
although for most species it was present in chromosome II. Only in *V.
parahaemolyticus, V. alginolyticus and V. harveyi* was it contained in chromosome I
where it was always adjacent to a BCCT transporter. The ectoine genes were present
amongst all strains of a given species with the exception of *V. harveyi* HY01 and two
strains of *V. splendidus*. In *V. harveyi* HY01, the genes appear to be deleted as we
found partial sequence of *aspK* and a homologue of the BCCT transporter encoded by
VP1723 in the expected location in the genome as is present in *V. parahaemolyticus*.
The two strains of *V. splendidus* have incomplete genome sequences so we cannot
speculate on their absence. In cases where it could be determined from the genome
sequence, the glycine betaine gene cluster was always present on chromosome II. The
genes were present in all representatives of the species. We reconstructed the
evolutionary history based on three housekeeping genes, *rpoB, mdh and pyrC* of the
33 species examined. Onto this tree we mapped the distribution of ectoine and betaine
biosynthesis gene clusters. The predominant distribution is the presence of both
systems in most species. This is true for the most divergent species within the group
analyzed, *Photobacterium angustum* and *Grimontia hollisae*, which strongly suggests
that both systems are ancestral (Fig. 13). The presence of only the ectoine system in
both *V. cholerae* and *V. mimicus,* but the presence of both synthesis systems in their
close relative *V. furnissii* suggests that deletion of the betaine synthesis system

37

occurred in the last common ancestor to give rise to these species. A similar evolutionary scenario can be proposed for the presence of only the ectoine system in *V. ichthyoenteri, Vibrio sp N418* and *V. scophthalmi*. It is of interest to note that *V. fischeri* also only contains the ectoine system, but its closest relative on the tree *V. salmonicida* contains neither the ectoine nor betaine synthesis systems. This is the only species examined within this family that contained neither system. Interrogation of the genome sequence of *V. salmonicida* did uncover a potential proline synthesis system, ProAB and ProI, which would allow the conversion of glutamate to proline for use as a compatible solute.

Discussion

Synthesis and accumulation of compatible solutes are widely used by bacteria as strategies to relieve the growth constraint imposed by increased osmolarity[33, 57, 58, 62, 130, 167]. This study showed that the addition of exogenous compatible solutes and their precursors to M9G 6% NaCl resulted in the reduction of the lag phase growth, indicating that *V. parahaemolyticus* is able to transport, accumulate, and synthesize compatible solutes (Fig. 3). Using ^{1}H-NMR analysis we showed that ectoine and glutamate were synthesized in M9G 6% NaCl. The role of glutamate in osmotic stress has been described, for example in *E. coli* it acts as a K^+ counter anion during the early stage of NaCl stress [38, 43]. The moderate halophile *Halobacillus halophilus*, under moderate salinities, accumulates glutamate and glutamine to adjust turgor[168].

In this organism one of the major roles of glutamate is to induce proline synthesis at high salinity [46]. However, in *V. parahaemolyticus*, the accumulation of glutamate is not sufficient for long-term survival since the *ectA* mutant cannot grow in

defined media under high NaCl stress, but the *betA* mutant can, indicating that ectoine is the main compatible solute synthesized *de novo*. We examined the NMR profile of wild-type cells grown in the presence of equal concentration of the precursors aspartic acid and choline and found that both ectoine and glycine betaine can be synthesized simultaneously. We demonstrated that ectoine and glycine betaine are *bona fide* compatible solutes, that along with choline cannot be used as sole carbon and energy sources, whereas glutamate, aspartic acid, proline and, to a much lesser extent, glutamine can be used as sole carbon sources. The use of choline and glycine betaine as sole carbon sources in *Pseudomonas aeruginosa* has been documented and is facilitated in this species by the presence of high affinity choline and glycine betaine transporters [117, 169]. This species can also use these substrates as effective compatible solute, but cannot synthesize them *de novo*. *V. parahaemolyticus* can synthesize ectoine, and glycine betaine from choline, and does so quite effectively, but cannot uses these compounds as sole carbon sources. Our data showed that *V. parahaemolyticus* can use proline as a sole carbon source and an effective compatible solute, but it cannot synthesize it *de novo*. Since *V. parahaemolyticus* contains at least six putative compatible solute transporters, uptake of proline may be an important osmotic tolerance strategy for this organism, which needs to be examined further [3, 155]. We showed that both *ectA* and *betA* genes are constitutively expressed in LB and M9 media, and both are more highly expressed in log phase cells compared to stationary phase cells. Although we did find that the NaCl upshock induces expression of both genes in all conditions examined, it was found that the *ectA* gene was always more highly expressed than *betA*. Together with the growth assay and

NMR analyses, these data demonstrated that ectoine synthesis is critical for growth under osmotic stress conditions.

The contribution of both *V. parahaemolyticus* synthesis systems to high salt stress survival was examined via the use of in-frame single and double deletion mutants. These data indicated that the glycine betaine synthesis system was not essential for growth under osmotic stress conditions. We found that the Δ*ectB* strain did not grow under high NaCl stress conditions, indicating that this system is essential. To determine if there was any cumulative effect in deletion of both *ectB* and *betA,* we examined the double mutant and found that the addition of glycine betaine restored growth similar to wild-type levels. We also found that the addition of proline was highly effective in rescuing the double mutant indicating that this is a powerful osmotic tolerance solute in this species. Glutamate could rescue the double mutant somewhat, but the data suggest that this solute is likely not an important compatible solute for this organism. Overall, these data indicated that glycine betaine, proline, ectoine and, to a much lesser extent, glutamate can act as compatible solutes in *V. parahaemolyticus*.

Previously, it was suggested that the ability to synthesize ectoine is specific for halophilic bacteria, and our analysis suggested it is essential for moderate halophile survival [62, 144]. In our analysis of the distribution of EctA and BetA among the family Vibrionaceae*,* we found that of 33 species examined 20 species contained both systems with nearly 70% containing the ectoine system. This percentage of ectoine synthesis ability was much higher than within the Gamma-Proteobacteria in general. Of 284 species examined 43% contained the ectoine synthesis genes. Since we found that most species examined encoded both systems and the two most divergent species

within the family (*P. angustum and G. hollisae*) further suggests that both systems are ancestral and important for these diverse marine organisms.
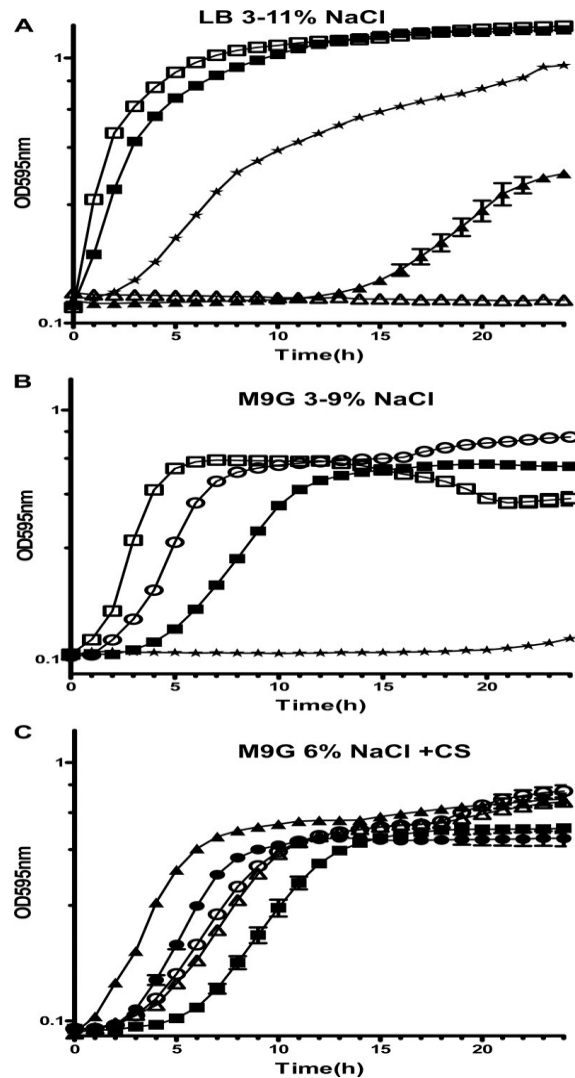
Figure 3   *V. parahaemolyticus* **WT in LB3-11% NaCl (A), M9G3-9% NaCl (w/v) (B), and M9G 6% NaCl±CS or precursors (C).** Symbols: **Panel A**. (□) 3% NaCl; (■) 6% NaCl; (★) 9% NaCl; (▲) 10.5 % NaCl; (△) 11% NaCl; **Panel B.** (□) 3% NaCl; (○) 5.5% NaCl; (■) 6% NaCl; (★) 9% NaCl; **Panel C**: (■) 6% NaCl; (▲) glycine betaine added; (●) choline added; (○) aspartic acid added; (△) ectoine added. Values represent the mean optical densities (OD$_{595}$) from triplicate technical replicates and at least two biological replicates, and error bars show the standard deviations and may be obscured by symbols.
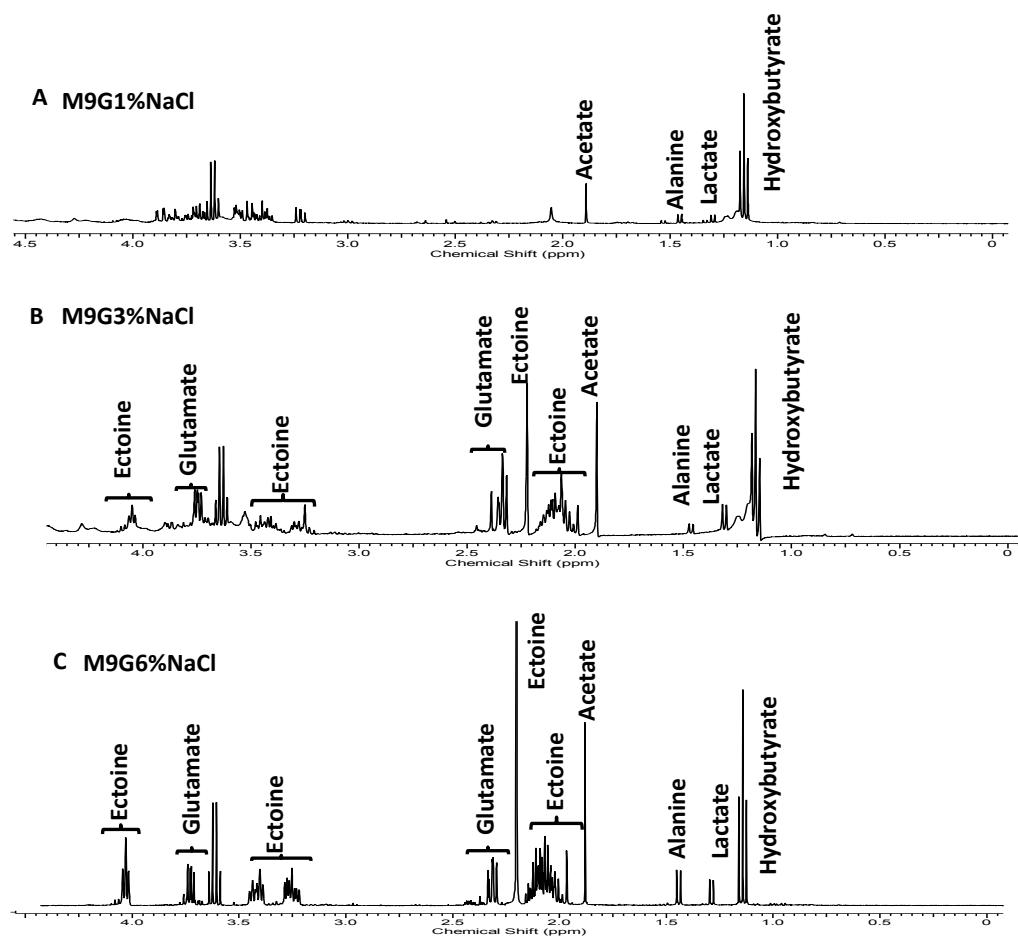
Figure 4   **400-MHz ^{1}H-NMR of stationary phase *V. parahaemolyticus* cells in M9G 1, 3, and 6% NaCl**. The spectral peaks were recorded for cells grown in M9G 1% NaCl (**A**), M9G 3% NaCl (**B**), and M9G 6% NaCl (**C**). The chemical environments of each type of proton or chemical shifts (δ) are expressed in ppm in the figure. The spectral peaks corresponding to the different compounds are labeled with the names of the compounds.
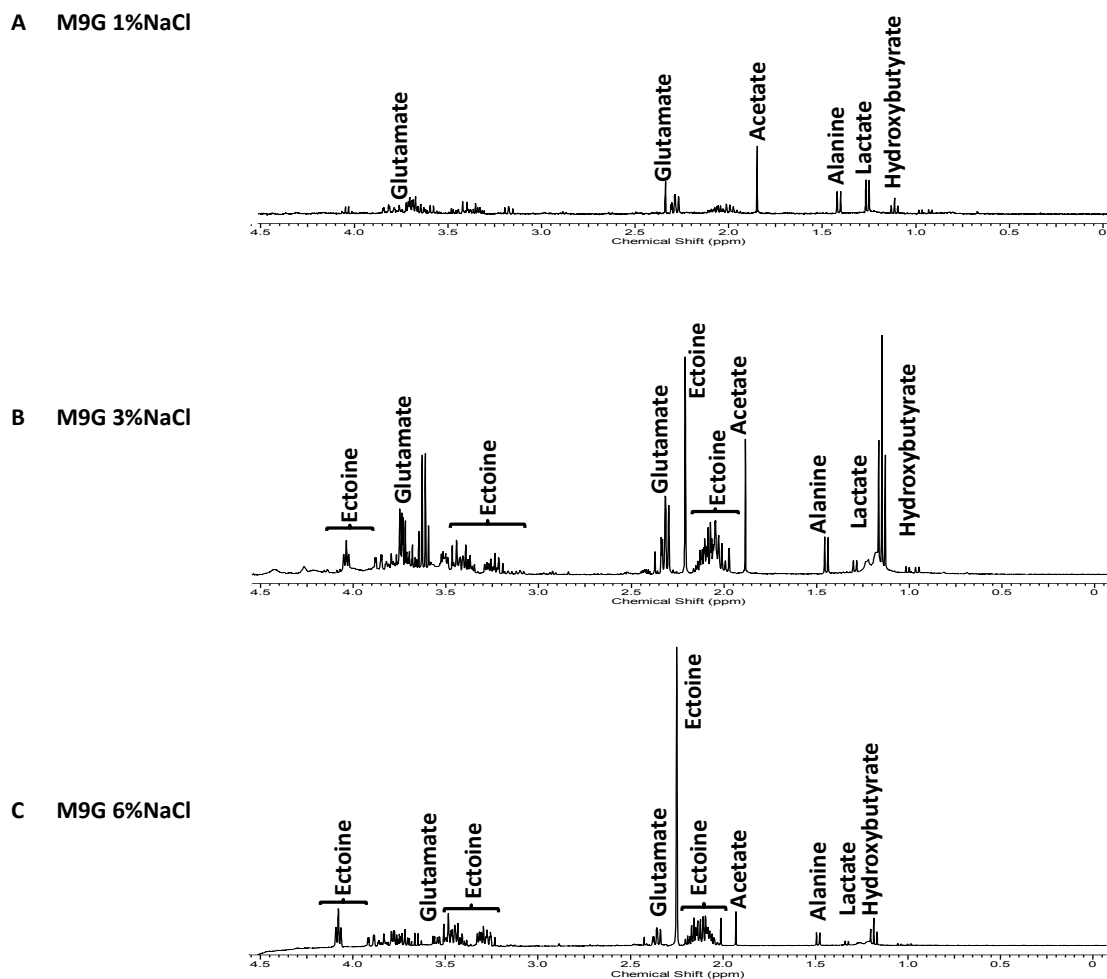
Figure 5   **400-MHz ^{1}H-NMR of log phase *V.parahaemolyticus* cells in M9G 1, 3, and 6% NaCl**. The spectral peaks were recorded for cells grown in log phase in M9G 1% NaCl (**A**), M9G 3% NaCl (**B**), and M9G 6% NaCl (**C**). The chemical environments of each type of proton or chemical shifts (δ) are expressed in ppm in the figure. The spectral peaks corresponding to the different compounds are labeled with the names of the compounds.

A WT in M9G3%NaCl + Aspartic acid

B WT in M9G3%NaCl + Choline
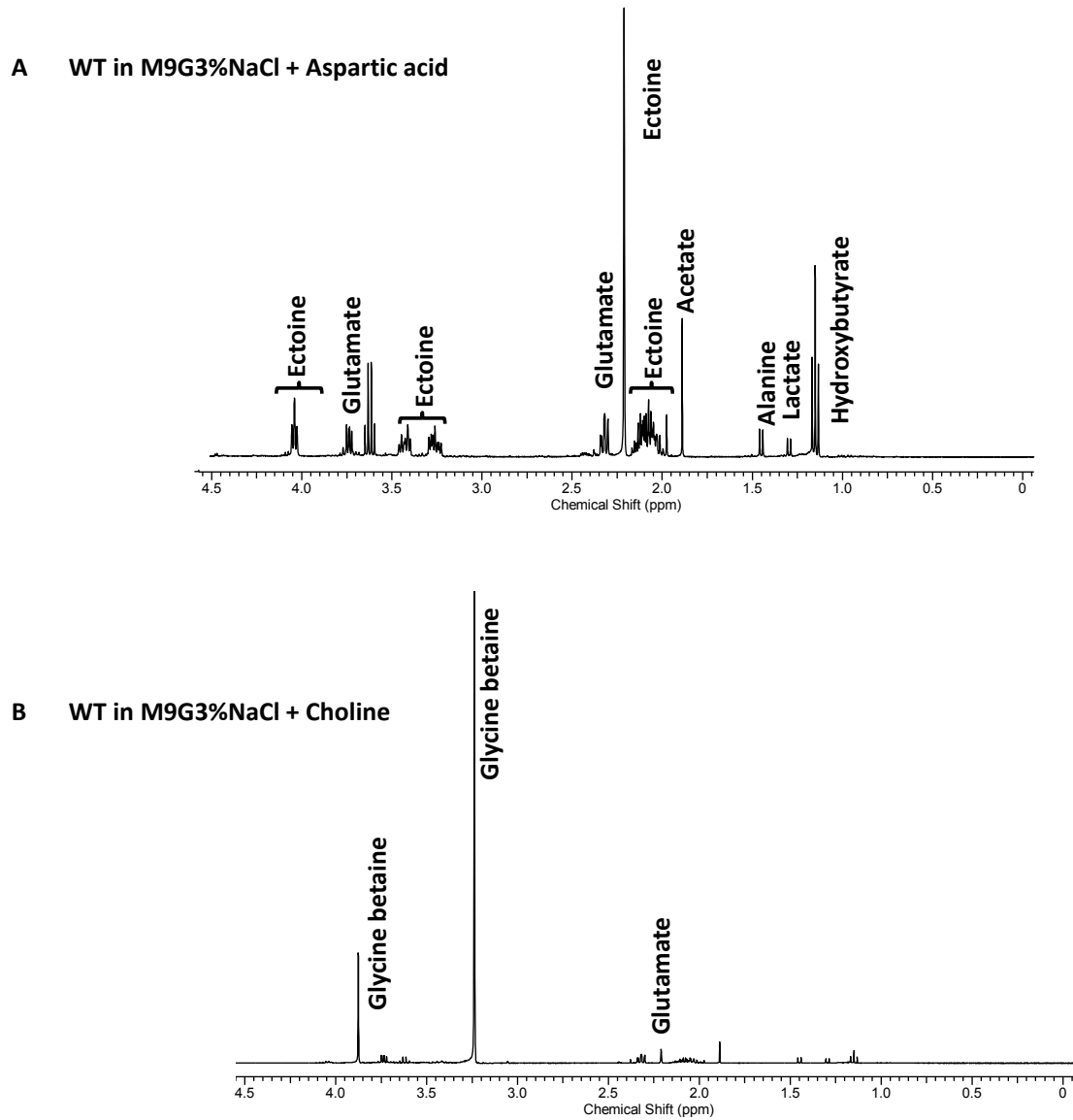
Figure 6   **400-MHz ^{1}H-NMR of *V. parahaemolyticus* WT in (A) M9G 6% NaCl+Aspartic acid (B) and M9G 6% NaCl+Choline**. The spectral peaks were recorded for cells grown in (**A**) M9G 6% NaCl+Aspartic acid and (**B**) M9G 6% NaCl+Choline. The chemical environments of each type of proton or chemical shifts (δ) are expressed in ppm in the figure. The spectral peaks corresponding to the different compounds are labeled with the names of the compounds
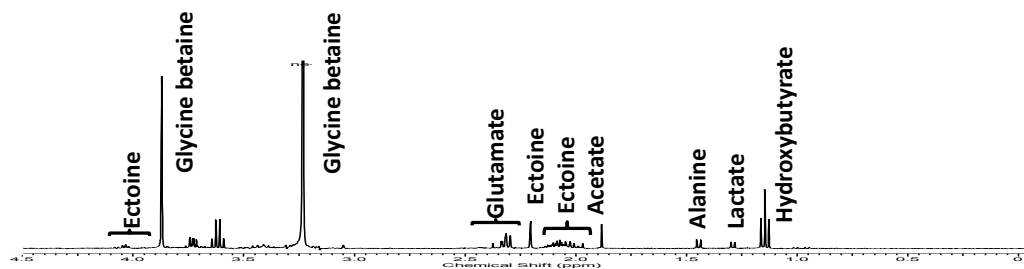
Figure 7   **400-MHz ^{1}H-NMR of *V. parahaemolyticus* in M9G 6% + Choline Aspartic acid**. The spectral peaks were recorded for *V. parahaemolyticus* grown in M9G 6% NaCl supplemented with aspartic acid and choline. The chemical environments of each type of proton or chemical shifts (δ) are expressed in ppm in the figure. The spectral peaks corresponding to the different compounds detected are labeled with the names of the compounds.
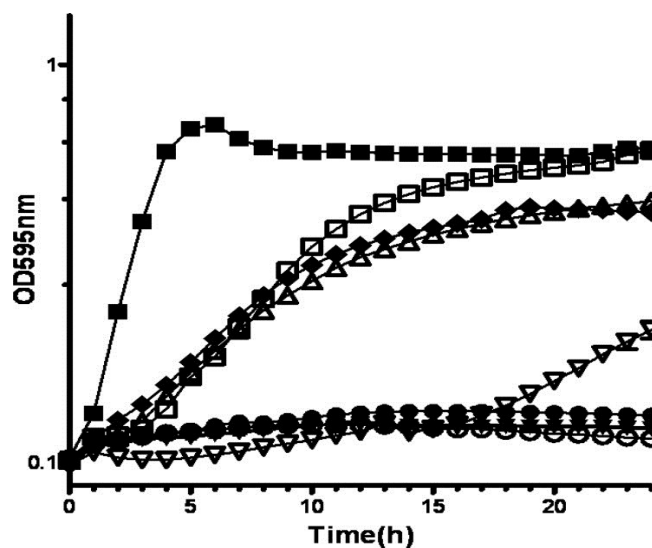
Figure 8   **Growth of *V. parahaemolyticus* in M9 1% NaCl containing 20 mM of CS or precursors as sole carbon sources**. Symbols: (■) glucose; (□) glutamate; (◆) aspartic acid; (△) proline; (▽) glutamine. Some of the following symbols that represent no growth may be obscured; (●) no glucose; (▲) choline; (▼) glycine betaine; (○) ectoine.

46
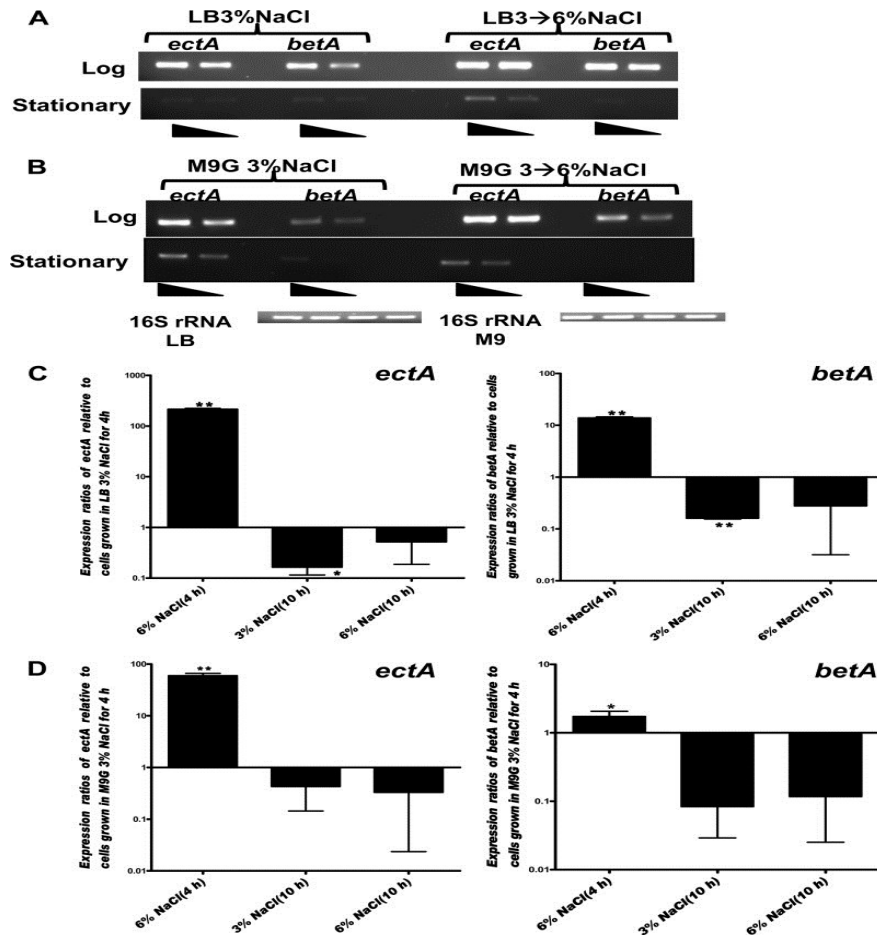
Figure 9   **Expression analysis of *ectA* and *betA* genes**. RT-PCR of *ectA* and *betA* genes from *V. parahaemolyticus* cells grown to log or stationary phase in LB (**A**) or M9G (**B**) and subjected to 30 min upshock in 6% NaCl. The cDNA templates were diluted 1:25 and 1:125 as indicate by triangles. The 16S rRNA control is shown for each sample. (**C**) qPCR of *ectA* and *betA* from cells grown to log or stationary phase in LB and subjected to 30 min upshock in 6% NaCl. (**D**) qPCR of *ectA* and *betA* from cells grown to log or stationary phase in M9G and subjected to 30 min upshock in 6% NaCl. Bars represent the expression of the indicated genes normalized to 16S rRNA and are relative to those of log-phase cells. Error bars indicate standard deviations. *P* values were calculated using an unpaired Student's *t*-test with a 95% confidence interval. Asterisks denote significant differences as follows: *, $P < 0.05$; **, $P < 0.02$.
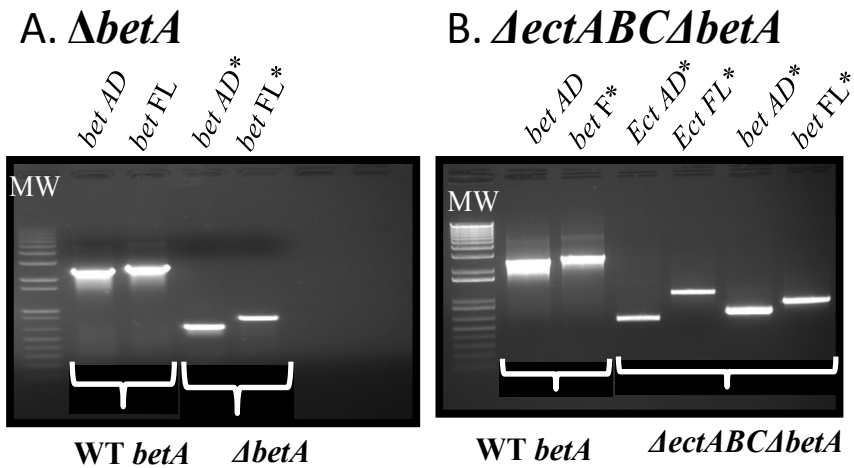
Figure 10   **PCR confirmation of *V. parahaemolyticus* RIMD2210633 WT and *ΔbetA* and *ΔectBΔbetA*.** Mutants were by generated by Splicing by Overlap Extension (SOE) PCR and homologous recombination. (**A**) ΔbetA (single mutant). (B) ΔectBΔbetA (double mutant). Legend. MW: Molecular weight 1kb ladder (Invitrogen); bet AD: WT betA (AD) fragment; bet FL: WT betA flanking (FL); bet AD*: truncated betA fragment; bet FL*: truncated betA flanking fragment; Ect AD*: truncated ectB AD fragment; Ect FL* truncated ectB flanking fragment. (*): Truncated.

48
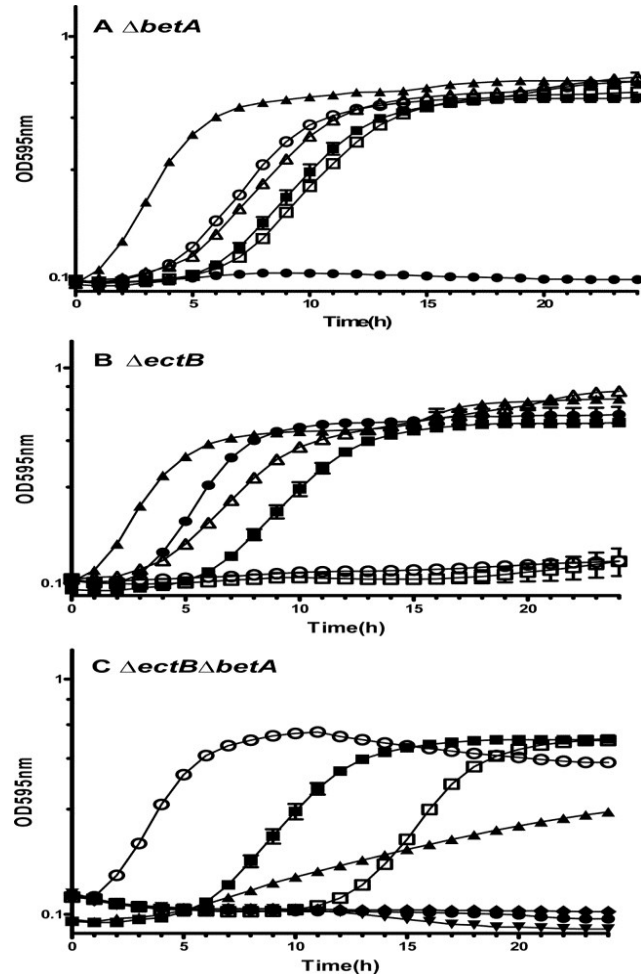
Figure 11   **Growth of ΔbetA (A), ΔectB (B), and ΔbetAΔectB (C) strains in M9G 6% NaCl in the presence or absence of CS or their precursors. Panel A**: (■) WT; (□) ΔbetA; (●) ΔbetA with choline added; (○) ΔbetA with ectoine added; (▲) ΔbetA with glycine betaine added; (△) ΔbetA with aspartic acid added. **Panel B**: (■) WT; (□) ΔectB; (●) ΔectB with choline added; (○) ΔectB with aspartic acid added; (▲) ΔectB with glycine betaine added; (△) ΔectB with ectoine added. **Panel C**: (■) ΔbetAΔectB with proline added; (□) ΔbetAΔectB with ectoine added; (○) ΔbetAΔectB with glycine betaine added; (●) ΔbetAΔectB ;(▲) ΔbetAΔectB with glutamate added; (▼) ΔbetAΔectB with choline added; (◆) ΔbetAΔectB with aspartic acid. Values represent the mean optical densities at 595 nm from triplicate technical replicates and at least two biological replicates, and error bars show the standard deviations.
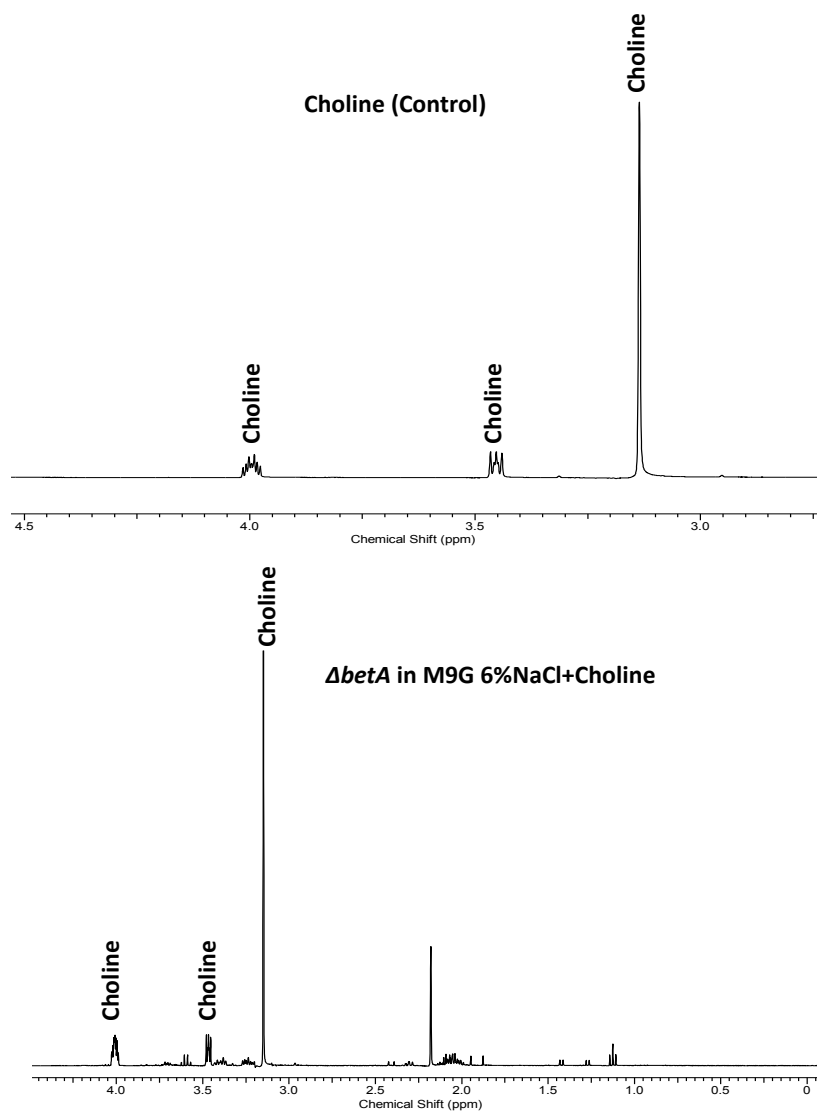
Figure 12   **400-MHz ^{1}H-NMR spectroscopy of *V. parahaemolyticus* Δ*betA* strain in M9G 6% NaCl+Choline**. The spectral peaks were recorded for cells grown in M9G 1% NaCl overnight, washed and suspended in M9G 6% NaCl+Choline. The uptake assay for carried for 1 hour at 37˚C with aeration (250 rpm). Cells were collected and processed for ^{1}H-NMR. (**A**) Choline control (SIGMA); (**B**) Δ*betA* in M9G 6% NaCl+Choline. The chemical environments of each type of proton or chemical shifts (δ) are expressed in ppm in the figure. The spectral peaks corresponding to the different compounds are labeled with the names of the compounds.
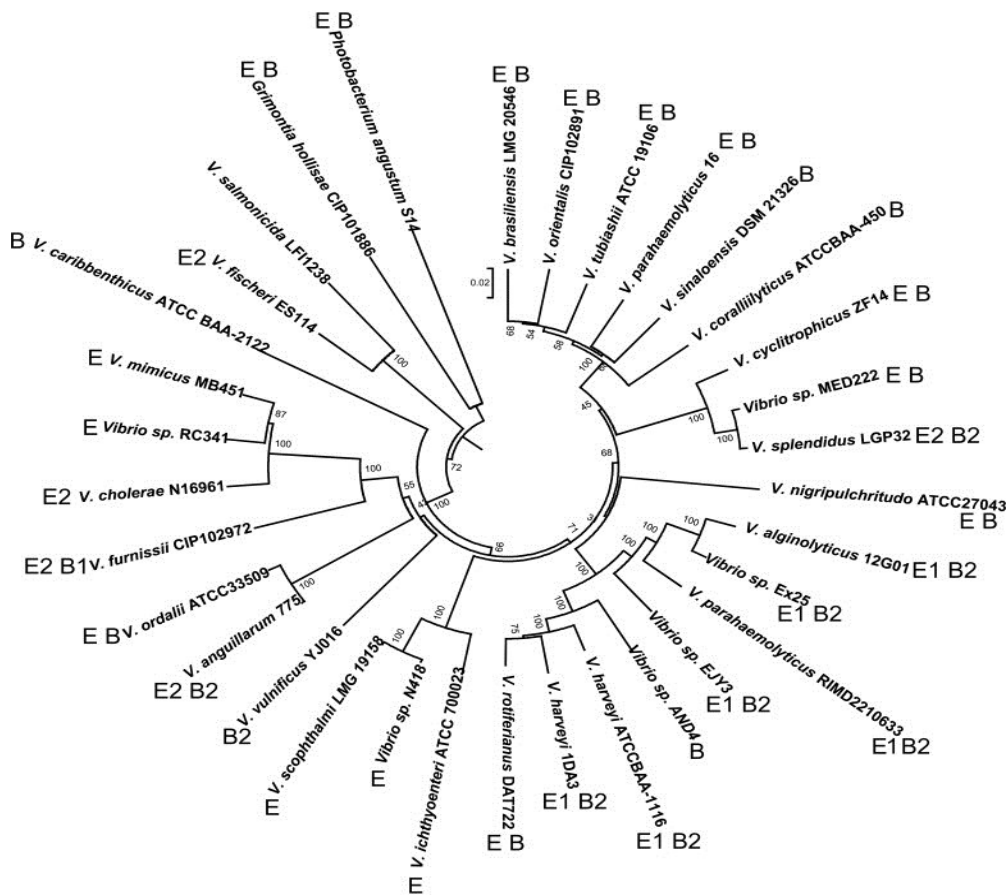
Figure 13   **Phylogenetic tree based on the concatenated sequences of three housekeeping genes, *rpoB*, *mdh*, and *pyrC*, for 33 species from the family Vibrionaceae**. Almost all the species shown in the tree are *Vibrio* species. The evolutionary history was inferred using the neighbor-joining method [170]. The bootstrap consensus tree inferred from 1,000 replicates is taken to represent the evolutionary history of the taxa analyzed. The percentages of replicate trees in which the associated taxa clustered together in the bootstrap test (1,000 replicates) are shown next to the branches. The tree is drawn to scale, with branch lengths in the same units as those of the evolutionary distances used to infer the phylogenetic tree. The evolutionary distances were computed using the Jukes-Cantor method and are in the units of the number of base substitutions per site. All positions containing gaps and missing data were eliminated. Evolutionary analyses were conducted in MEGA5 [166]. **E**, ectoine cluster; **B**, betaine cluster; **B1** and **E1**, chromosome 1; **B2** and **E2**, chromosome 2.

Table 1   **Bacterial strains and plasmids used in this study**

Strains	Genotypes	Reference
V. parahaemolyticus		
RIMD2210633	O3:K6 clinical isolate	[85]
Δ*betA*	RIMD2210633 Δ*betA* (VPA1112)	This study
Δ*ectB*Δ*betA*	RIMD2210633Δ*betA* (VPA1112) Δ*ectB* (VPA1721)	This study
Δ*ectB*	RIMD2210633 Δ*ectB* (VPA1721)	[85]
Escherichia coli		
DH5α-λpir	λ*pir*φ80d*lacZ*ΔM15Δ(*lacZYA-argF*)*U169recA1* *hsdR17 deoR thi-1 supE44 gyrA96 relA1*	
DH5α λpir Δ*betA*	DH5α λpir containing pDS132Δ*betA*	
DH5α λpir Δ*betA*	DH5α λpir containing pΔ*betA*	
β2155 DAP	Donor for bacterial conjugation; *thr1004 pro thi strA hsdS lacZ*ΔM15 (F′ *lacZ*ΔM15 *lacTRQJ*Δ36 *proA*+ *proB*+) Δ*dapA* Erm[r] *pirRP4* (Km[r] from SM10)	This study
β2155 DAP-Δ*betA*	β2155 harboring pDS132Δ*betA*	This study
β2155 DAP-Δ*betA*	β2155 harboring pDS132Δ*ectB*	This study
Plasmids		
pJET1.2	General cloning vector, Amp[R]	
pΔ*betA*	*betA* mutant cloned into pJET1.2	This study
pDS132	Suicide vector for conjugal transfer and integration: R6K γ*ori mobRP4 sacB* Cm[r].	[165]
pDS132Δ*betA*	pDS132 harboring truncated *betA* gene	This study
pDS132Δ*ectB*	pDS132 harboring truncated *ectB* gene	[85]

Table 2   **Primers pairs used in this study**

Target	Primer[a]	Sequence (5→3')[b]	Product (bp)[c]
VPA1112	VPA1112A	TCTAGACCACGTACAGCAAGAGATCT	SOE AB: 379
	VPA1112B	**cagctgagatctggtacc**TTTCATTTTGTGTCTCCTA	
	VPA1112C	**ggtaccagatctcagctg**TCTTAATCTTTAAAAACTG	SOE CD: 334
	VPA1112D	GAGCTCTCGTTGGCATCCAGTTACC	
	VPA1112FL-F	AACCGTATTTATCGAC	SOE AD: 713
	VPA1112FL-R	TTCCAGGTCAGCAAAGCTC	
VPr001	VPr001RT-F	ACCGCCTGGGGAGTACGGTC	234
	VPr001RT-R	TTGCGCTCGTTGCGGGACTT	
VPA1112	VPA1112RT-F	AAAGAGGCGGGCTATCCAGAAACT	264
	VPA1112RT-R	TTTCTCAAATTCAACGCCGACCGC	
VP1721	VP1721RT-F	CCAATGGCGGTTGTACTGCTGAAA	269
	VP1721RT-R	TCACCGTGAATACACTCGATGCCA	

[a]: At the end of the primer designations, F stands for forward and R stands for reverse.
[b]: Lowercase bold letters indicate complementary sequence tags.
[c]:SOE AB product of SOE PCR using VPA1112A and VPA1112B primers; SOE CD product of SOE PCR using VPA1112C and VPA1112D primers; SOE AD product of SOE PCR using VP1112FL-F and VP1112FL-R primers. F: Forward; R: Reverse; RT: Reverse Transcriptase.

Chapter 3

DECIPHERING THE ROLE OF MULTIPLE BETAINE-CHOLINE-CARNITINE TRANSPORTER (BCCT) HOMOLOGUES IN THE HALOPHILE VIBRIO PARAHAEMOLYTICUS

Introduction

Vibrio parahaemolyticus is a Gram-negative, halophile bacterium that belongs to the Vibrionaceae family of bacteria that includes species inhabiting a wide range of aquatic ecosystems [6]. These bacteria are commonly found at the interface of fresh and sea waters, and in sea water, as free living organisms or in associations with fish, and other marine species [5, 7-10, 19, 171]. *V. parahaemolyticus* is an etiological agent of bacterial seafood borne gastroenteritis infection in humans. In recent years there has been an increase in the incidence of *V. parahaemolyticus* infections worldwide, mostly during the warmer summer months [13, 20-23, 128, 140, 172-174, 175 , 176, 177].

Infection by *V. parahaemolyticus* usually occurs via consumption of contaminated, undercooked seafood, particularly oysters [23, 24, 27, 178-180]. While in healthy individuals the infection is self-limiting, with remission usually occurring within days, in individuals with underlining medical conditions it can lead to serious health complications and even death. In addition to health-related issues, *V. parahaemolyticus* also causes huge economic losses annually to the oyster industries [23, 24].

Vibrio parahaemolyticus encounters constant fluctuations in nutrient availability and salinity and, as an intestinal pathogen, this bacterium faces additional stresses related to the *in vivo* pressures in the form of bile salts, pH and antimicrobial peptides stresses [4, 8, 25, 26].

Salinity shifts in the external environment pose tremendous osmotic challenges to bacteria that must respond swiftly to equate their intracellular osmotic potential with that of the external environment in order to maintain a positive turgor pressure required for normal growth [61, 67, 73]. This is typically achieved via two strategies namely the accumulation of inorganic ions such as potassium ions (K^+) concomitant to the counter ion glutamate, and the accumulation of low-molecular weight organic compounds, termed compatible solutes [29-32, 36, 37, 41, 61, 62]. The accumulation of compatible solutes is achieved either by *de novo* synthesis or via uptake from the environment by specific transporters [33, 65, 83, 113, 124, 181-184]. Transport of compatible solutes is a strategy that is widespread among distinct evolutionary taxa of bacteria and has a lower energetic cost to the cell [29, 32, 67, 68]. Some important compatible solutes used by bacteria include but not limited to trehalose, free amino acids (glutamate, glutamine, and proline), and their derivatives glycine betaine and ectoine[31, 47, 51, 62, 64, 158].

Vibrio parahaemolyticus possesses the genetic information for both the synthesis and transport of compatible solutes [3, 94, 157]. We previously described the presence of six putative compatible solute transporter systems and two synthesis systems within *V. parahaemolyticus* genome [3, 94, 157]. The two compatible solute biosynthesis gene clusters encode the *ectABCaspK* required for ectoine and the *betIBA* for glycine betaine biosynthesis. A study by Naughton and colleagues using one

dimension nuclear proton magnetic resonance (^{1}H-NMR) demonstrated that at high salinity *V. parahaemolyticus* is capable of *de novo* synthesis of ectoine, whereas a Δ*ectB* knockout (impaired in L-2,4-diaminobutyric acid acetyltransferase) was not[3]. In *V. parahaemolyticus*, both ectoine and glycine betaine are bona fide compatible solutes (that is they cannot be used as carbon source), and the most effective compatible solutes/precursors in *V. parahaemolyticus* are in the order: betaine > choline > proline= glutamate > ectoine [90]. Expression analysis showed that the *ectA* and *betA* biosynthesis genes were more highly expressed in logarithmic phase cells and both were induced by NaCl upshock [90].

Four of the six transport systems identified in *V. parahaemolyticus* belong to the Betaine-Carnitine-Choline transporter (BCCT) family, and the remaining two represent the members of the ATP-Binding Cassette (ABC) transporters also known as ProU component systems; ProU1 is located in chromosome I and ProU2 is located in chromosome II [3]. Three out of four BCCTs (VP1456, VP1723, and VP1905) are located in chromosome I, while VPA0356 is the only BCCT found in chromosome II [3].

The Betaine-Carnitine-Choline transporter (BCCT) family uses proton or sodium-motive force to translocate substrates across the membrane [113]. These proteins displayed certain distinguishing features such as the transport of quaternary ammonium molecules, and encode an average protein of 500 amino acid residues in size organized in 12 putative transmembrane α-helices [114, 116]. Furthermore, they possess a conserved stretch of tryptophan in their transmembrane domain (TM8) believed to be involved in the binding of substrates [114].

The Studies of the roles of the BCCTs in osmotolerance have been conducted mostly in Gram-positive and a handful of Gram-negative bacteria [54, 57, 95, 114, 116, 117, 185]. For example, in *Corynebacterium glutanicum* and *Bacillus subtilis*, the BCCTs transporters (BetP and OpuD) were shown to uptake glycine betaine at high osmolarity [114, 116]. Studies in *E. coli* demonstrated that the BCCT transporter, BetT, mediated high affinity uptake of choline [95]. In *Vibrio cholerae*, OpuD (VC1279), the only BCCT present in this species, was shown to play a role in the uptake of glycine betaine at high osmolarity [54]. In *Pseudomonas aeruginosa*, an organism that contains three BCCTs, BetT3 was demonstrated to function as the major choline transporter under hyperosmolar conditions [117].

The function of each of the four BCCTs in *V. parahaemolyticus* is currently unresolved. To address this, we examined the role of VP1456, VP1723, VP1905, and VPA0356 in the osmotic stress response of this species by using deletion mutations and heterologous expression analyses. Furthermore, the expression pattern of each of the transporters after high salt upshock was also examined.

Materials and Methods

Bacterial strains, plasmids, and growth conditions

Bacterial strains and plasmids used in this study are listed in Table 3. A clinical isolate of the O3:K6 of *V. parahaemolyticus* strain RIMD2210633 streptomycin-resistant (Str^R) was used as wild-type [85, 155]. Using this strain as a background, several derivative mutant strains harboring either a single or multiple in-frame deletions in their BCCT genes were constructed. Unless otherwise stated, all strains were routinely cultured aerobically (250 rpm) at 37°C either in complex Luria-

Bertani (LB) medium (Fisher Scientific, Fair Lawn, NJ) or defined M9 salts base minimal medium (47.8 mM Na_2HPO_4, 22 mM KH_2PO_4, 18.7 mM NH_4Cl, 8.6 mM NaCl; Sigma) supplemented with 2 mM $MgSO_4$, 0.1 mM $CaCl_2$, and 0.4% glucose (w/v) final concentration as sole carbon source designated M9G. Genetic manipulations used *Escherichia coli* strains MKH13, DH5α λpir, and the diaminopimelic acid (DAP) auxotroph β2155 λpir. *E. coli* β2155 was grown in media supplemented with 0.3 mM DAP (Sigma Aldrich). The following antibiotics were used: ampicillin (100 μg/ml), chloramphenicol (25 μg/ml), and streptomycin (200 μg/ml). Solutions of compatible solutes (Sigma) were prepared, sterilized by filtration with a 0.2 μm filter (Corning, NY), and added to the growth media at the following concentrations unless otherwise stated: 100 μM betaine, 1000 μM choline, 100 μM ectoine, 1000 μM proline, 1000 μM glutamic acid, or 1000 μM L-carnitine, or 1000 μM aspartic acid.

Bacterial growth analysis

Growth analysis of *V. parahaemolyticus* and deletion mutant strains was carried out from cultures grown to exponential phase. A single bacterial colony was used to inoculate M9 salts minimal medium containing 0.4% (w/v) glucose containing 1% (w/v) NaCl (M9G 1% NaCl), and grown overnight at 37ºC. A 2% inoculum of the overnight culture was subsequently used to inoculate an isosmotic M9G media, and grown at 37ºC to logarithmic phase for 5 h to an optical density (OD_{600}) of ~1. A 2.5% aliquot of the 5 h pre-culture was used to inoculate a 96-well microtiter plate containing 200 μl of M9G media with 6% NaCl in the absence or presence of compatible solutes. Growth analysis was carried out at 37ºC with intermittent shaking for 24 h using a Tecan Sunrise microplate reader (Tecan US Inc). Samples were

tested in triplicate wells from at least two biological replicates. The hourly optical densities (OD_{595}) of bacterial growth cultures were measured in the course of the 24 h period. Graphing and statistical analyses of the data were performed using Prism 5 as averages of means of two biological replicates.

Mutant construction

Vibrio parahaemolyticus RIMD2210633 strains harboring a single or multiple in-frame deletions in the BCCT genes were constructed by Splicing by Overlap Extension (SOE) Polymerase Chain Reaction (PCR) and homologous recombination [163, 164]. SOE PCR primers listed in Table 4 were designed to create deletions that removed most of the gene sequence of VP1456, VP1723, VP1905, and VPA0356 using methods previously described [3, 90, 155]. Briefly, using *V. parahaemolyticus* RIMD2210633 genomic DNA as template, two PCR products (AB and CD) flanking the region of the BCCT gene to be deleted were generated using SOE A and B and SOE C and D primer pairs in the first PCR reaction and are listed in Table 4. In the second PCR reaction, the generated fragments of the first round PCR were spliced together to create a truncated version of the gene AD via their overlapping complementary tag sequences using SOE A and D primer pairs. The resultant fragment was ligated into the suicide vector pDS132 [165] and transformed into an E. *coli* β2155, a DAP auxotroph. The recombinant pDS132 plasmid containing the truncated AD fragment was subsequently introduced into a *V. parahaemolyticus* background by conjugation and homologous recombination. The positive colonies resulting from homologous recombination to replace the wild-type gene with a truncated version were subsequently screened on selective agar plates and confirmed by PCR and DNA sequencing.

Cloning of BCCT genes in pBAD33 vector and transformation of *E. coli* MKH13

To clone the individual BCCT genes (VP1456, VP1723, VP1905, and

VPA0356), *V. parahaemolyticus* RIMD2210633 genomic DNA was used as template

for PCR amplification of each gene. Specific PCR primers were designed to amplify

the full-length BCCT fragment containing ~60-100 base pairs (bp) located upstream of

the BCCT gene containing the ribosome binding site (Table 4). Using a Hot Start

High Fidelity polymerase kit (Qiagen), an average fragment of ~1500 bp in length was

generated from each gene by PCR. For the four BCCT genes studied herein, the

following set of primer pairs containing restriction enzyme sites for downstream

cloning steps listed in Table 4 were utilized: VP1456F/VP1456R

(XbaI/HindIII);VP1723F/ VP1723R (XbaI/SphI), VP1905F/ VP1905R (KpnI/PstI),

and VPA0356F/ VPA0356R (XbaI/HindIII). The generated PCR product was excised

from agarose gels, gel-eluted (Qiagen), and sub-cloned into a pJET1.2 blunt end

vector using the CloneJET PCR cloning kit (Thermo Fisher Scientific). A

recombinant pJET1.2 plasmid containing individual BCCT gene was later transformed

into *E. coli* DH5α strain and plated onto LB1% NaCl agar containing 100 μg/ml

ampicillin. The positive colonies were screened by colony PCR and restricted by

double digestion, and ligated into an arabinose-inducible pBAD33 vector also

restricted with the same enzymes. The resulting pBAD33-BCCT recombinant

plasmids were subsequently used to transform a compatible solute synthesis-and

transporter-deficient *E. coli* MKH13 strain [135] and streaked onto LB 1% NaCl agar

plate containing 25 µg/ml chloramphenicol. The chloramphenicol positive colonies were selected from the plate, screened by colony PCR, and confirmed by sequencing.

Functional complementation in *E. coli* MKH13 strain

The transport properties of *V. parahaemolyticus* BCCTs (VP1456, VP1905, VP1723 and VPA0356) were assayed using the heterologously expressed loci in *E. coli* MKH13. The *E. coli* MKH13 strain is a derivative of *E. coli* MC4100 (genotype F⁻, *araD*139 Δ (*argF-lac*) U169 *rpsL*150 *relA1 deoC1 ptsF25 rbsR flbB5301*); the large *argF-lac* deletion Δ (*argF-lac) 169* includes the *betTIBA* locus, and thus this strain cannot convert choline to glycine betaine nor transport choline [135, 186, 187]. Besides, the *E. coli* MKH13 genome contains deletions of genes encoding PutP, ProP, and ProU transport systems, making it unable to transport proline, glycine betaine, or choline [135, 186, 187]. Functional complementation experiments of *E. coli* MKH13 harboring either the empty pBAD33 plasmid vector or pBAD33 containing the BCCT gene were achieved by growing cells overnight in M9G adjusted to 1% NaCl in the presence of 25 µg/ml chloramphenicol (Thermo Fisher Scientific). A 2.5% inoculum from these overnight cultures (OD_{600} ~1.0) was used to inoculate 96-well micro-plate filled with 200 µl of M9G adjusted to 4% NaCl with or without 500 µM of compatible solute. The arabinose promoter of pBAD33 vector was induced by the addition of arabinose to a final concentration of 0.05% (w/v). Bacterial growth was carried out at 37ºC and the OD_{595} measured hourly for a period of 24 h. For each condition tested, the sample was assayed in triplicate wells with at least two biological replicates.

Determination of the affinity of the BCCTs for glycine betaine

To determine the affinity of each BCCT transporter for glycine betaine, growth analyses of *E. coli* MKH13 recombinant strains were performed in the presence of limiting glycine betaine concentrations (0, 5, 25, 50, 75,100, 125, and 150 µM) as previously described [188]. A 2.5% inoculum of overnight cultures of *E. coli* MKH13 strains grown in M9G 1% NaCl (OD_{600}~1.0) was used to inoculate a M9G 4% NaCl media containing 0.05% arabinose and supplemented with different concentrations of glycine betaine. Data collected in the course of 24 h were used to calculate the specific growth rates µ (h^{-1}) of the *E. coli* MKH13 recombinant strains for a given glycine betaine concentration using a nonlinear Monod's regression. The maximum specific growth rate μ_{max} (h^{-1}), and the saturation constant (K_s), which denotes the substrate concentration [S] when $\mu=\mu_{max}/2$ (µM), were empirically determined by fitting the specific growth rates µ (h^{-1}) as a function of glycine betaine concentration [S] in µM. The Eadie Hofstee linear regression plot was generated by fitting the specific growth rates data µ (h^{-1}) against individual specific growth rates µ (h^{-1}) divided by each glycine betaine concentration [S] expressed in µM ([S] µM /µ h^{-1}). Using the Eadie Hofstee plot the following parameters of the bacterial growth kinetics were also deduced: (1) the maximum specific growth rate (μ_{max}) deduced as the y axis intercept, (2) the μ_{max}/K_s from the x axis intercept, and finally (3) the negative slope, which equates to the saturation constant K_s.

Extraction and identification of compatible solutes by ^{1}H-NMR

Proton Nuclear Magnetic Resonance (^{1}H-NMR) spectroscopy was performed on cellular extracts of *V. parahaemolyticus* RIMD2210633 and *E. coli* MKH13 pBCCT strains. For *V. parahaemolyticus* RIMD2210633 and isogenic mutants,

proton NMR experiments, a single bacterial colony was used to inoculate 50 ml LB media of specified salinity. The culture was grown to stationary phase overnight at 37˚C with aeration to an OD_{600} ~1. The resulting cells were harvested by centrifugation for 10 min at 1000 xg and washed once with media of equal salinity. In the case of ^{1}H-NMR experiments examining ectoine and choline uptake in *E. coli* MKH13 pVp1456, a single colony was used to inoculate M9G 1% NaCl media and grown at 37˚C aerobically to an OD_{600} of ~1.0. The cells were pelleted, washed once with M9G 1% NaCl media, and then subjected to an osmotic upshock in M9G 4% NaCl containing ectoine or choline for 1 h. Cells were recovered by centrifugation and the pellet washed once with M9G 4% NaCl media. From this point forward, cell pellets from *V. parahaemolyticus* RIMD2210633 wild-type and E*. coli* MKH13 pBCCT cells were similarly processed. The pelleted cells were lysed by a series of freeze-thaw cycles (three times) in dry ice, and cellular extracts were solubilized in 750 μl ethanol. After a 10 min centrifugation at 4000 xg, ethanol fraction containing organic compounds free of cellular debris was transferred into a clean tube. Ethanol was removed via evaporation in a rotary evaporator. The resulting dried organic materials were subsequently dissolved in 500 μl of deuterium oxide (D_2O) solvent (Cambridge Isotope Laboratories, Inc) and insoluble materials removed by centrifugation. Organic compounds (compatible solutes) dissolved in D_2O were transferred into a 5 mm NMR tube (Wilmad Lab Glass) and ^{1}H-NMR spectral data were recorded with Bruker Advance AVIII 400 MHz NMR spectrometer equipped with a Bruker BBFO probe. The spectrometer was run on Bruker Topspin software. Acquired ^{1}H-NMR spectra were processed using ACD/Lab processing software academic edition (Advanced Chemistry Development, Inc).

Isolation of RNA and gene expression analysis

RNA isolation and VP1456, VP1723, VP1905, and VPA0356 gene expression

analysis under optimal and NaCl upshock growth conditions were carried out using *V.*

parahaemolyticus cultures grown to either logarithmic (log) or stationary phase. A

single bacterial colony was used to inoculate LB media adjusted to 3% NaCl, and

grown aerobically overnight at 37ºC. The resulting culture was diluted 1:50 in LB 3%

NaCl media and grown at 37ºC to logarithmic (4 h) or stationary (10 h) phase.

Osmotic upshock experiments were performed on logarithmic or stationary phase

cultures harvested by centrifugation at 1000 x*g* for 10 min, and transferred into a

media with 6% or 9% (w/v) NaCl final concentrations. The osmotic upshock

experiment was carried out for 30 min at 37ºC with shaking. Total RNA was isolated

from different bacterial growth conditions using the RNAprotect Bacteria reagent and

RNeasy mini kit (Qiagen) following the recommended protocol. Isolated RNA was

quantified by Nanodrop spectrophotometer (Thermo Fisher Scientific) and examined

by gel electrophoresis on 0.8% agarose to assess quality. The first strand cDNA

synthesis was carried out from 500 ng of total RNA as template in a reaction primed

with 200 ng of random hexamers (Invitrogen) using Superscript II Reverse

Transcriptase (Invitrogen). The expression analysis of the BCCT genes was assayed

using synthesized cDNA diluted to 1:125 as template by Reverse Transcriptase (RT)

PCR and real-time PCR. Real-time PCR utilized the Hot Start-IT SYBR green qPCR

master mix reagent (USB, Santa Clara, CA) and BCCT gene-specific primer pairs

listed in Table 4 was carried out on an Applied Biosystems (ABI) 7500 Fast real-time

PCR system (Foster City, CA). The threshold cycle (C_T) values were determined

using the 7500 Software v2.0 (ABI) and the relative quantification of gene expression

was calculated by the $2^{-\Delta\Delta CT}$ method [161, 162] with normalization across samples

using 16S rRNA transcript levels. Real-time PCR was performed with duplicate wells per sample and repeated with at least two biological replicates. The significance of the different treatments was statistically computed using an unpaired Student's *t*-test.

Amino acid alignment of the betaine-carnitine-choline transporters

BCCT amino acid sequences were retrieved from The National Center for Biotechnology Information (NCBI) website (http://www.ncbi.nlm.nih.gov/) using their designated locus tags. EMBOSS Water-Pairwise Protein Sequence Alignment from the European Molecular Biology Laboratory (EMBL) and the European Bioinformatics Institute (EBI) was used for multiple sequence alignment and determination of percentages amino acid identity. The locus tags for the BCCTs and ProUs are listed. BCCT: VP1456, VP1723, VP1905, and VPA0356.

Statistical analysis

An unpaired student's *t*-test was used to compare the means between two treatments (treated and untreated). A one-way analysis of variance (one-way ANOVA) followed by a Bonferroni's multiple comparison posttest was used to analyze multiple groups. The significance of the data was computed as P-values and represented by the asterisk. *, $P<0.05$; **, $P<0.01$; ***, $P<0.001$. Graphing and statistical analyses of the data was performed using Prism 5 software.

Results

Four BCCTs homologues are present in *V. parahaemolyticus*

We previously demonstrated by ^{1}H-NMR analysis that *V. parahaemolyticus* can accumulate glycine betaine, choline, proline, ectoine and glutamate, but we did not identify the transporters involved[90]. Bioinformatics analysis identified four single-component BCCT transporters in *V. parahaemolyticus* RIMD2210633, ORFs VP1456, VP1723, VP1905, and VPA0356 [3, 94]. All four transporters are common to *V. parahaemolyticus* since they are present in all available sequenced genomes. Three of the four BCCT of *V. parahaemolyticus* shared between 50 and 80% identity at the amino acid level to each other, VP1456, VP1723 and VP1905. VP1456 and VP1905 sharing the highest sequence identity of 80% to each other. VPA0356 shared the lowest sequence identity with the other three (between 29 to 30%). Of the four BCCTs examined, VP1456 yielded the highest amino acid identity with the *E. coli* BCCT ProP at 44%. The percentage of identity at the amino acid level among the four BCCTs VP1456, VP1723, VP1905, and VPA0356 with the single *V. cholerae* BCCT OpuD (VC1279) was also determined. The OpuD (VC1279) of *V. cholerae* was previously shown to be involved in the uptake of glycine betaine in this species [54]. VP1905 shared the highest amino acid identity with VC1279 at 82% identity withVP1456 next at 68%, then VP1723 at 49% and lastly VPA0356 at 29%.% (Table 5). Bioinformatics data demonstrated highly variable proteins, which may suggest possible substrate transport differences.

V. parahaemolyticus accumulation of glycine betaine is NaCl-dependent

To examine whether the accumulation of compatible solutes by *V. parahaemolyticus* cells during growth in LB media was NaCl-dependent, ^{1}H-NMR

analysis was performed; *V. parahaemolyticus* cultures were grown in LB at 1%, 3%, and 6% NaCl. It was found that *V. parahaemolyticus* accumulated glycine betaine starting at salinity of 3% NaCl and above, but not at 1% NaCl (Fig. 14 A-D). To ensure that glycine betaine was not synthesized internally, but was transported into the cell from the media, we performed a similar experiment using a *V. parahaemolyticus* Δ*ectB*Δ*betA* double knockout previously described [90]. We found that the Δ*ectB*Δ*betA* double knockout accumulated glycine betaine in LB 6%NaCl. These results indicate that glycine betaine is transported into the cell at high NaCl concentrations (Fig. 14D).

VP1456, VP1905, and VPA0356 are induced by NaCl upshock

To address the question of whether the four putative BCCT genes found in *V. parahaemolyticus* are induced by NaCl upshock, QPCR analysis was performed on *V. parahaemolyticus* cultures grown to logarithmic and stationary phases in LB 3% NaCl and subjected to 6% and 9% (w/v) NaCl upshock. It was found under these conditions that VP1456, VP1905, and VPA0356 were up-regulated upon NaCl upshock, while VP1723 was either unchanged or down-regulated (Fig. 15A-B). For instance, logarithmic phase expression analyses upon upshock in 6% NaCl gave the following fold induction 4, 3.8, and 5.5-fold increase for VP1456, VP1905, and VPA0356, respectively. Logarithmic phase expression analyses at 9% NaCl upshock gave fold change increases of 5 for VP1456, 3.2 for VP1905, and 3.3 for VPA0356 gene; the VP1723 was unchanged. Similarly, expression analysis of stationary phase cells subjected to 6% NaCl upshock yielded similar expression trends as described above for VP1905 and VPA0356 with a 6.5, 5.5, and 7 Log_2 fold increases. The VP1723 was unchanged after 6% NaCl upshock, but showed a 2.5 Log_2 fold decrease after a 9%

NaCl upshock. Overall, these data demonstrated induction of VP1456, VP1905, and VPA0356 from log and stationary phase cells after NaCl upshock.

BCCT are functionally redundant in *V. parahaemolyticus*

To examine the question of whether the four BCCTs present in *V. parahaemolyticus* are essentials, in-frame single deletions of each of the genes were constructed (Fig.16A-D). Growth analysis of each single mutant with that of *V. parahaemolyticus* wild-type in M9G 6% NaCl media was examined in the absence or presence of compatible solutes or their precursors. No noticeable growth difference was found between the wild-type and the single mutant strains, indicating a functional redundancy (Fig.15A-H). We next constructed two *V. parahaemolyticus* triple BCCT mutants, ΔVP1456ΔVP1723ΔVPA0356 and ΔVP1456ΔVP1723ΔVP1905. Several attempts were made to create a quadruple mutant strain, devoid of all the four BCCT genes by using each of the triple BCCT mutant strains, but were unsuccessful each time; it appears that the presence of at least one BCCT protein is required for this species to carry out its physiological function. All mutants were tested under optimal growth conditions in complex LB 3% NaCl and in M9G 3% NaCl and were found to grow similar to the wild-type (Fig. 17).

The two triple mutant strains were then compared to the wild-type in M9G 6% NaCl media in the absence or presence of compatible solutes (glycine betaine, ectoine, proline, and the glycine betaine precursor choline). Growth analyses of the wild-type and both triple mutants in M9G 6% NaCl media lacking compatible solutes yielded similar growth patterns indicating no overall defect in the mutants (Fig. 18A-H). In M9G 6% NaCl media supplemented with 100 μM glycine betaine, the lag time for WT was reduced from ~7 h to 2 h, whereas for ΔVP1456ΔVP1723ΔVPA0356 strain the

lag time was reduced from ~7 h to 4 h. This result indicates that glycine betaine is still transported into the cell but not at the same level as the wild-type, suggesting that at least one of the BCCTs VP1456, VP1723, or VP0356 may be required for maximum uptake but none of the three are essential for uptake (Fig. 18A). Interestingly, for the second triple mutant ΔVP1456ΔVP1723ΔVP1905 growth under the same conditions barely showed a reduction in the lag time, indicating that glycine betaine uptake is very weak; this result suggests that at least one if not all three BCCTs VP1456, VP1723, and VP1905 are important glycine betaine transporters (Fig. 18B).

Comparison of growth data of the wild-type with the two triple mutants in M9G 6% NaCl media supplemented with 1000 μM proline or choline yielded a reduction in the lag time for all three strains, but not to the same extent as for glycine betaine (Fig. 18C-18F). In addition, the wild-type strain showed a greater reduction in lag phase than either of the triple mutants indicating that these BCCTs may be required for proline and choline uptake. Comparison of growth in M9G 6% NaCl media supplemented with 100 μM ectoine, yielded no reduction of the lag time for the triple BCCT mutants compared to the wild-type (Fig. 18G and 18H). This result suggests that neither VP1905 nor VPA0356 is involved in ectoine uptake. Taken together, the growth analysis data demonstrate that VP1456, VP1723, and VP1905 are likely involved in glycine betaine, proline, and choline transport in *V. parahaemolyticus*.

BCCTs are compatible solute transporters

To examine the transport specificity of each BCCT in relation to a given compatible substrate, functional complementation analyses of *E. coli* MKH13 harboring individual BCCTs were performed. The *E. coli* MKH13 strain is a Δ*putPA*,

Δ*proP*, and Δ*proU* mutant in an MC4100 background and is thus unable to transport proline, glycine betaine and choline, nor convert choline to glycine betaine. Each BCCT gene was cloned, transformed into *E. coli* MKH13, and grown in M9G 4% NaCl media in the presence of compatible solutes. Under these conditions, only *E. coli* MKH13 strains transformed with functional BCCTs were able to grow in high NaCl concentrations (Fig. 19A-D). It was found that *E. coli* MKH13 complemented with pVP1456, pVP1723, pVP1905, or pVPA0356 grew in the presence of glycine betaine (Fig. 19A). In the presence of proline, *E. coli* MKH13 pVP1456 or pVP1723 grew significantly better than the control indicating that these BCCTs can transport proline (Fig. 19B), which was also suggested by the triple mutant analysis. VP1905 and VPA0356 do not appear to be involved in proline transport. Only *E. coli* MKH13 pVP1456 grew significantly better than the negative control in the presence of ectoine (Fig. 19C), while VPA0356 was the only transporter of glutamate (Fig. 19D).

To determine whether any of the BCCTs uptake choline, we performed ^{1}H-NMR analyses since choline is toxic to *E. coli* MKH13 lacking *betIBA*since it cannot convert choline to glycine betaine [97]. Purposely, *E. coli* MKH13 transformed with individual BCCTs were grown in M9G 1% NaCl to early exponential phase and then switched in M9G 4% NaCl supplemented with 1000 μM choline for 1 h before ^{1}H-NMR analyses were carried out on these cells. It was found that *E. coli* MKH13 cells transformed with VP1456 (but not VP1723, VP1905, or VPA0356) accumulated choline intracellularly (Fig. 21A). ^{1}H-NMR uptake analyses of *E. coli* MKH13 recombinant cells containing individual BCCT in M9G 4% NaCl supplemented with 1000 μM ectoine also demonstrated accumulation of ectoine only in VP1456

70

transformed cells (Fig. 21B). Together, these data demonstrate that VP1456 is a transporter for both choline and ectoine.

VP1456 and VP1905 transport glycine betaine with high efficiency

Glycine betaine is one of the most commonly used compatible solutes among a wide range of evolutionary distinct groups of bacteria. To examine whether the four BCCTs found in *V. parahaemolyticus* take up glycine betaine with high or low efficiency, growth analyses of individual BCCT transformed into compatible solute synthesis-and transporter-deficient *E. coli* MKH13 in the presence of limiting concentrations of glycine betaine was performed, as previously described[188]. Using Monod's nonlinear regression and the Eadie Hofstee linear plots, the parameters of bacterial growth kinetics in glycine betaine limiting concentrations were empirically determined and the binding affinities of each BCCT inferred. It was found that VP1456 transported glycine betaine with high an affinity of K_s=5.9±1.8 μM, VP1723 with affinity of K_s =14.0 ±5.0 μM, and VP1905 with an affinity of K_s =8.4±0.9 μM (Fig. 20A-D). Based on these data it was concluded that the BCCT binding affinities for glycine betaine were in the descending order: VP1456>VP1905>VP1723.

Discussion

The uptake and/or synthesis of compatible solutes are paramount to the growth and survival of bacteria under high salinity conditions [30, 31, 47, 54, 58, 60, 61, 131, 158]. *V. parahaemolyticus* inhabits a wide range of ecosystems subjected to constant shifts in salinity. In this study, we investigated the specific role of the four betaine-carnitine-choline transporters (BCCTs) and showed by amino acid sequence comparisons that three out of four BCCTs (VP1456, VP1723, and VP1905) shared

high amino acid sequence identity with the OpuD of *V. cholerae*. We found that VPA0356 only shared around 30% amino acid identity. Moreover, we demonstrated in this study that all four BCCTs can accumulate glycine betaine.

To examine whether the BCCT genes found in *V. parahaemolyticus* were inducible by NaCl, expression analysis of each gene was carried out by quantitative real-time PCR on cells subjected to NaCl upshock. The data revealed that three out of four genes, VP1456, VP1905, and VPA0356, were induced by NaCl upshock over a wide range of salinity conditions examined. Interestingly, VP1723 showed reduced expression at high salinity suggesting that this is not a trigger for expression but is induced by other factors such as the presence of compatible solutes. In fact, it has been shown that certain BCCTs are not induced at the level of transcription but at the level of activity when compatible solutes are supplemented in the media under high salinity [117].

To further investigate the function of the four BCCTs in the uptake of compatible solutes, single in-frame deletion mutations were created but found to be functionally redundant. We were unable to construct a quadruple mutant, thus we constructed two different BCCT triple mutants and examined these mutants at high salinity. A promising phenotype emerged in the ΔVP1456ΔVP1723ΔVP1905 triple knockout, which showed uptake of glycine betaine was nearly completely lost, suggesting that at least one of the above BCCTs was important for uptake. Interestingly, in both ΔVP1456ΔVP1723ΔVP1905 and ΔVP1456ΔVP1723ΔVPA0356 triple knockouts no uptake of ectoine was noted suggesting that at least one of these transporters is required for uptake. To more closely examine the contribution of individual BCCTs in the uptake of compatible solutes, we performed functional

complementation in the *E. coli* MKH13 compatible solute synthesis-and transporter-deficient strain with each BCCT [135, 186, 187]. This strain is defective in glycine betaine biosynthesis from choline and in transport of glycine betaine, choline and proline into the cell. From these assays, we found that all four BCCTs could transport glycine betaine with varying degrees of efficiency. VP1723 could uptake proline and glycine betaine, while VP1905 could only transport glycine betaine. VPA0356 transported glutamate and glycine betaine. Finally, VP1456 transported not only glycine betaine, but also proline and ectoine, which was suggested by the triple mutant growth analysis studies. Since *E. coli* MHK13 cannot convert choline to glycine betaine [97], we examined uptake of choline by the BCCT transporters using ^{1}H-NMR analysis by exposing exponential phase cells to choline for an hour. We found that only *E. coli* MKH13 complemented with VP1456 could transport choline into the cell. These data suggest that VP1456 has a diverse substrate range.

Glycine betaine is among the most abundant compatible solutes present in the environment; we sought to investigate the affinity of each BCCT to glycine betaine by growth analysis in media of high osmolarity with limiting concentrations of glycine betaine. This analysis demonstrated that VP1456, V1905, and VP1723 were the main glycine betaine transporters in this species with respective affinities of K_s of 5.9 ± 1.8 µM for VP1456, K_s of 8.4 ± 0.9 µM for VP1905, and K_s of 14.0 ± 5.0 µM for VP1723. These affinity constants are in the range of what have been previously described [114, 116, 183].

In this study, we undertook the examination of the four putative betaine-carnitine-choline transporters in *V. parahaemolyticus*, with a focus on their role in the uptake of compatible solutes during growth at high salinity. Using a combination of

73

technical approaches, we showed that the BCCT are functional and involved in the uptake of compatible solutes at high osmolarity. We demonstrated that the expression of three BCCTs was induced by high NaCl. Furthermore, in-frame deletion mutations in these systems demonstrated a functional redundancy.
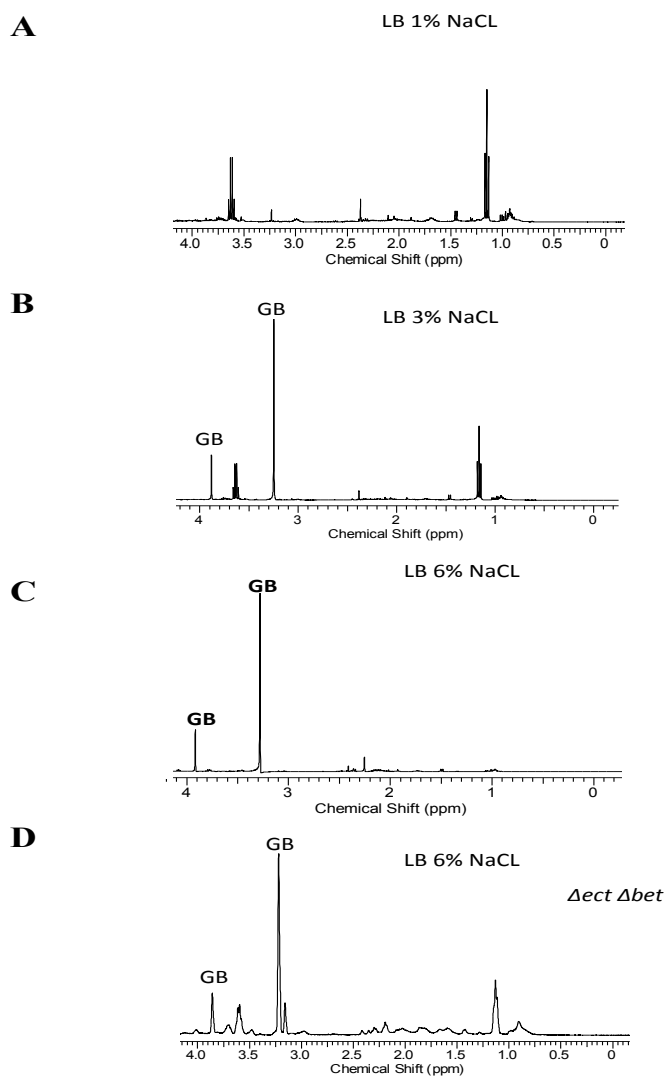
Figure 14   **¹H-NMR of *V. parahaemolyticus* WT and Δ*ect*Δ*bet* in LB media**. (**A**) WT in LB 1% NaCl; (**B**) WT in LB 3% NaCl; (**C**) WT in LB 6% NaCl; (**D**) Δ*ect*Δ*bet* in LB 6% NaCl. GB: Glycine betaine. Experiments were repeated with two biological replicates.
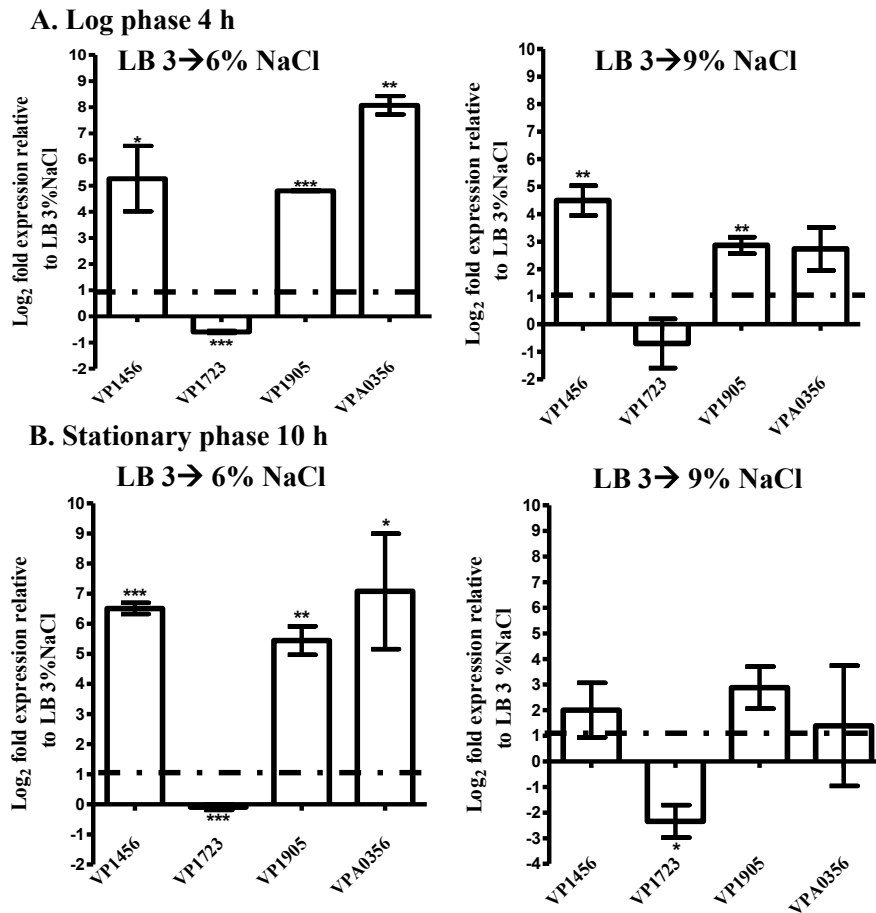
Figure 15   **Expression analysis of BCCT genes in *V. parahaemolyticus* following NaCl upshock in LB media**. Cultures were grown in LB media 3% NaCl to log phase 4 h (**A**) or stationary phase 10 h (**B**) and then subjected to 6% and 9% NaCl upshock. At least two biological replicates were used. Changes in expression levels are relative to expression levels in either log phase (**A**) or stationary phase cultures (**B**) cells not subjected to osmotic upshock. Data were statistically analyzed using an unpaired student's *t*-test with a 95% confidence interval. The *P* values are shown as asterisks and denote the significant difference between upshocked samples relative to untreated control. The error bars indicate mean $\pm$ standard error. *, $P \leq 0.05$; **, $P \leq 0.01$; ***, $P \leq 0.001$.
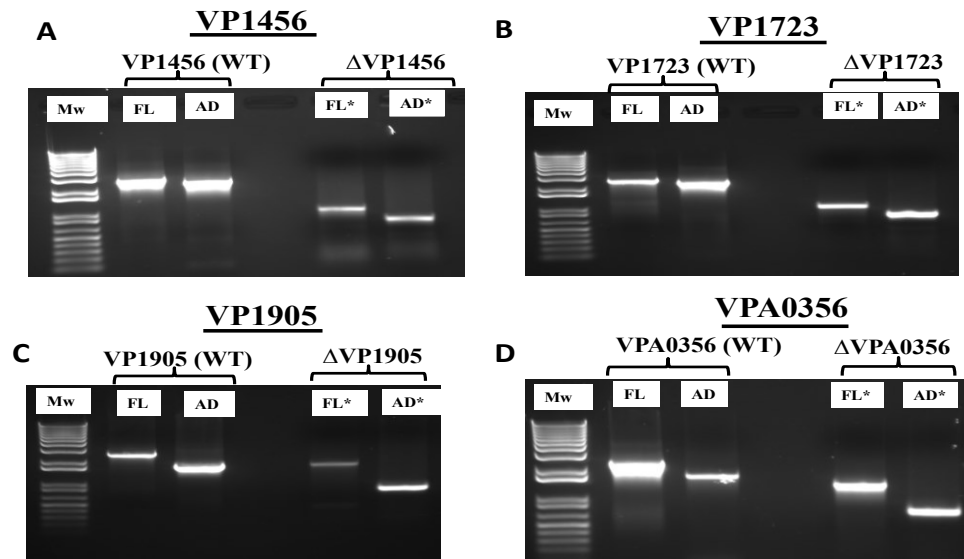
Figure 16   **PCR confirmation gels of *V. parahaemolyticus* RIMD2210633 wild-type (WT) and BCCT deletion bands**. ΔVP1456, ΔVP1723, ΔVP1905, and ΔVPA0356 created by SOE PCR and homologous recombination. Legend. (**A**): VP1456 WT and ΔVP1456; (**B**): VP1723 WT and ΔVP1723; (**C**): VP1905 WT and ΔVP190; (**D**): VPA0356 WT and ΔVPA0356. Mw: 1kb molecular weight ladder (Fermentas); FL: WT flanking band generated with SOE flanking primers; AD: AD WT band generated with SOE A and SOE D primers; FL*: truncated flanking band generated with SOE flanking primers; AD*: AD truncated band generated with SOE A and SOE D primers.
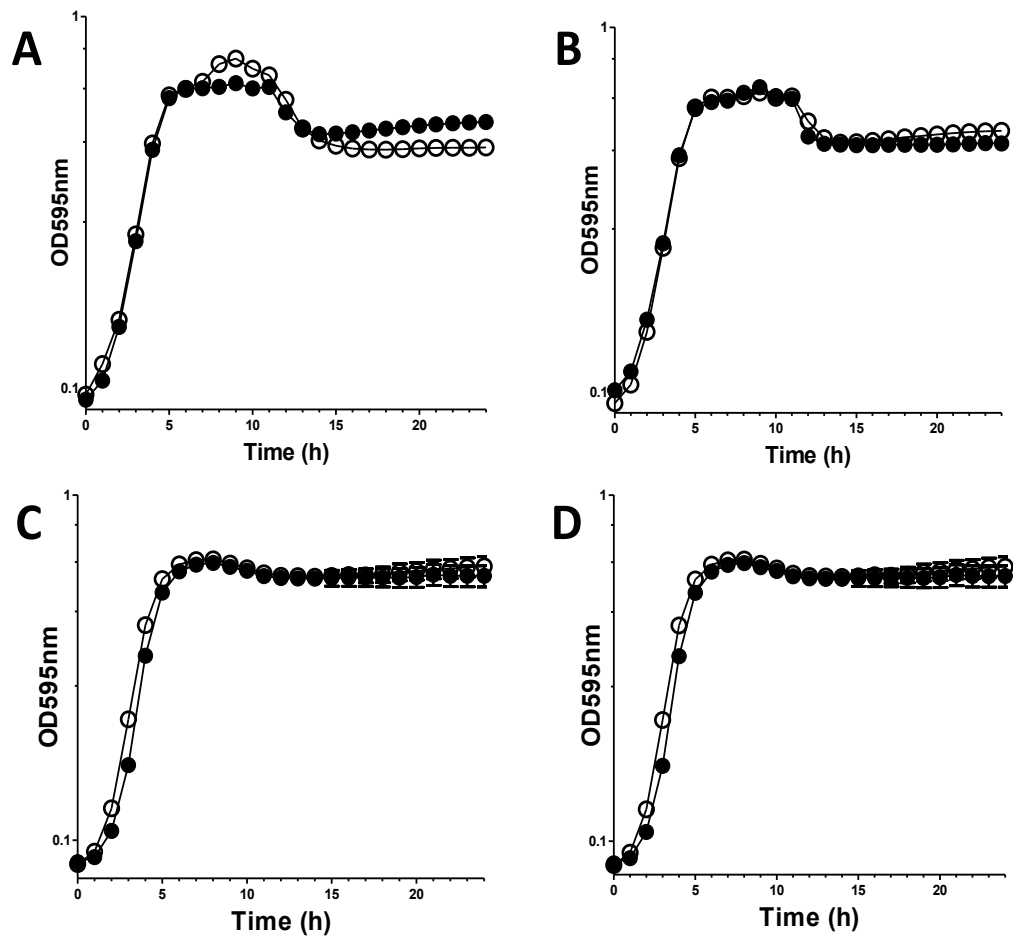
Figure 17   **Growth analysis of *V. parahaemolyticus* WT and single ΔBCCTs in M9G 3% NaCl. A**. (●): WT; (○): ΔVP1456; **B**. (●): WT; (○): ΔVP1723; **C**. (●): WT; (○): ΔVP1905; **D**. (●): WT; (○): ΔVPA0356.

78
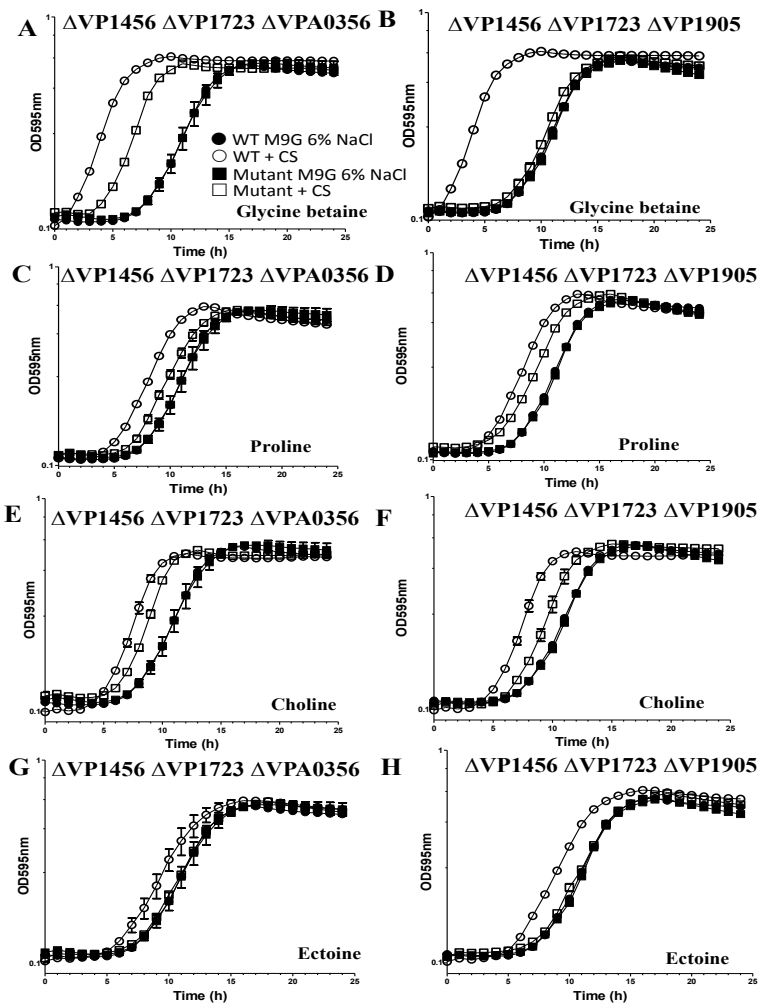
Figure 18 **Growth analyses of *V. parahaemolyticus* and triple ΔBCCTs in M9G 6% NaCl ±CS**. Strains were grown in M9G 1% NaCl overnight and then inoculated in M9G 6% NaCl ±CS for 24 h are shown in graphs **A-H**. Each assays were performed in triplicate and data are shown as the pooled data from two biological replicates
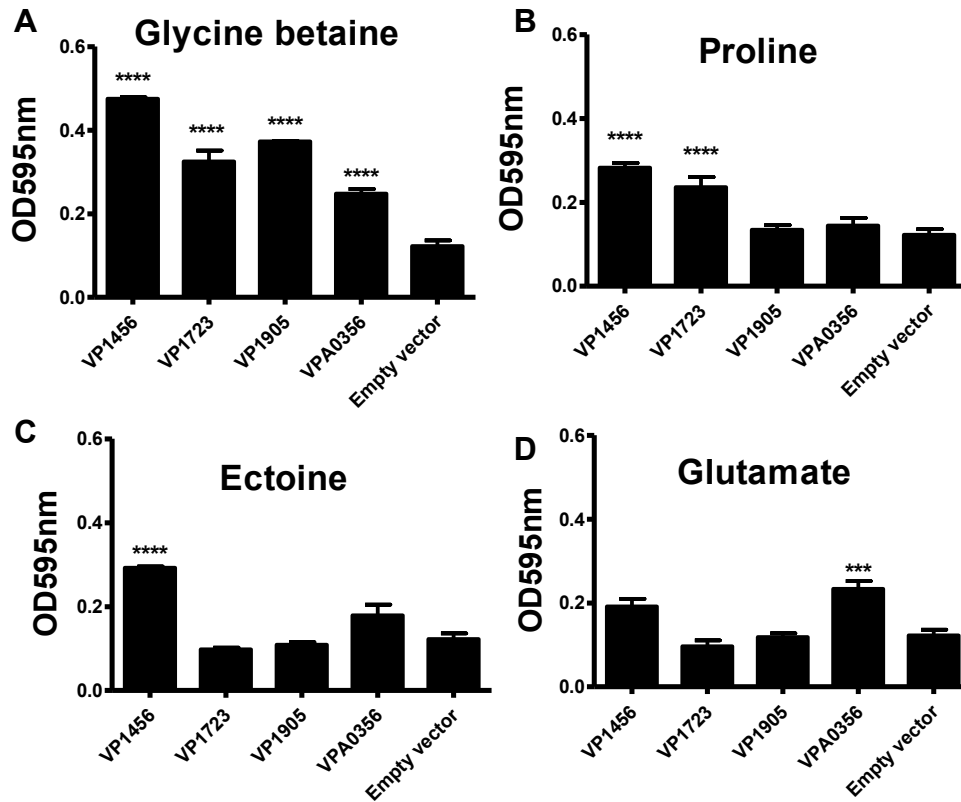
Figure 19   **Functional complementation of BCCT in *E. coli* MKH13**. *E. coli* MKH13 strains harboring either an empty pBAD33 vector or a pBAD33-BCCT recombinant plasmid were grown in M9G 4% NaCl ± CS. For each condition tested, the sample was assayed in triplicate from at least two biological replicates and compatible solute uptake was assessed relative to empty vector controls. **A**. M9G 4% NaCl+500 μM Glycine betaine; **B**. M9G 4% NaCl+500 μM Proline; **C**. M9G 4% NaCl+500 μM Ectoine; **D**. M9 G 4% NaCl+500 μM Glutamate. The P values were calculated using one-way analysis of variance (one-way ANOVA) followed by a Bonferroni's multiple comparison posttest. The error bars represent mean ± standard error. ***, $P \leq 0.001$.
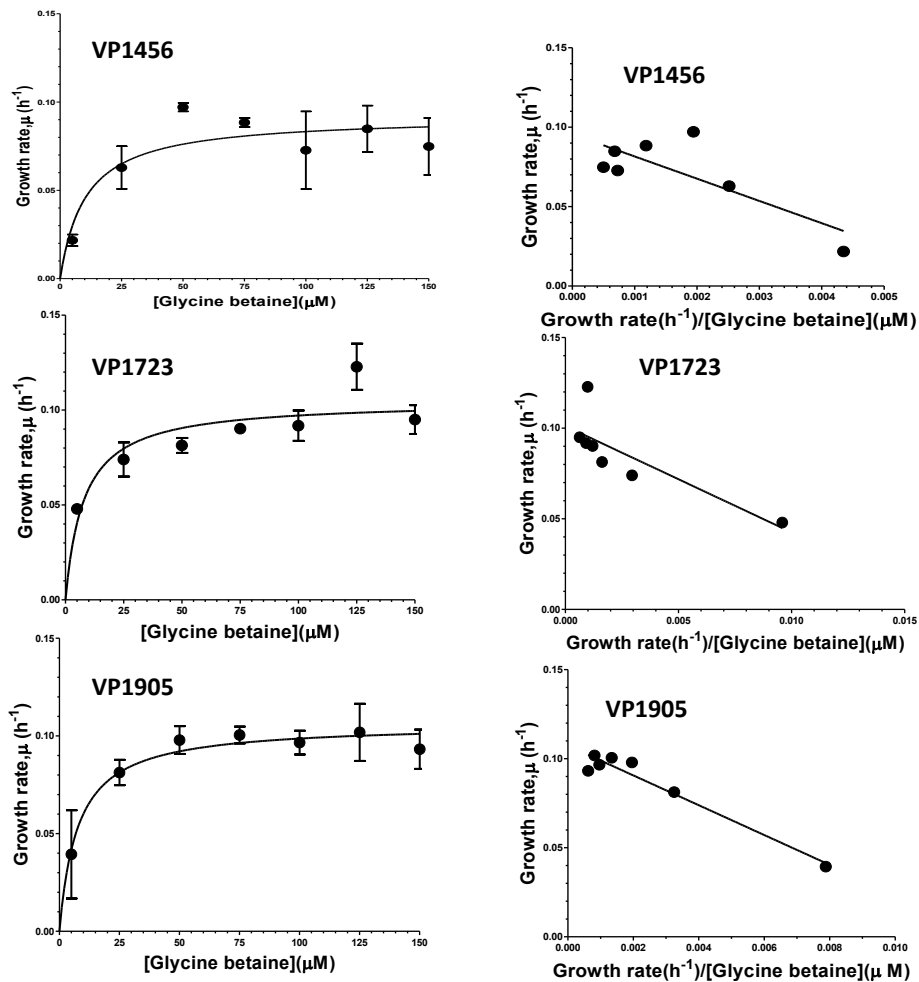
Figure 20   **Determination of the affinity of BCCTs for glycine betaine**. *E. coli* MKH13 pBCCT recombinant strains were M9G 4% NaCl containing varying concentrations of glycine betaine (0, 5, 25, 50, 75,100, 125, and 150 μM). Measured OD595 were converted in specific growth rates μ (expressed in h-1) and plotted against the glycine betaine concentration in a nonlinear Monod regression. A corroborative Eadie Hofstee plot was also fitted. Each experimental condition was tested in triplicate wells and the assay repeated with at least two independent biological replicates. The affinity Ks (saturation constant) and μmax (maximal specific growth rate) were deduced from the plots.
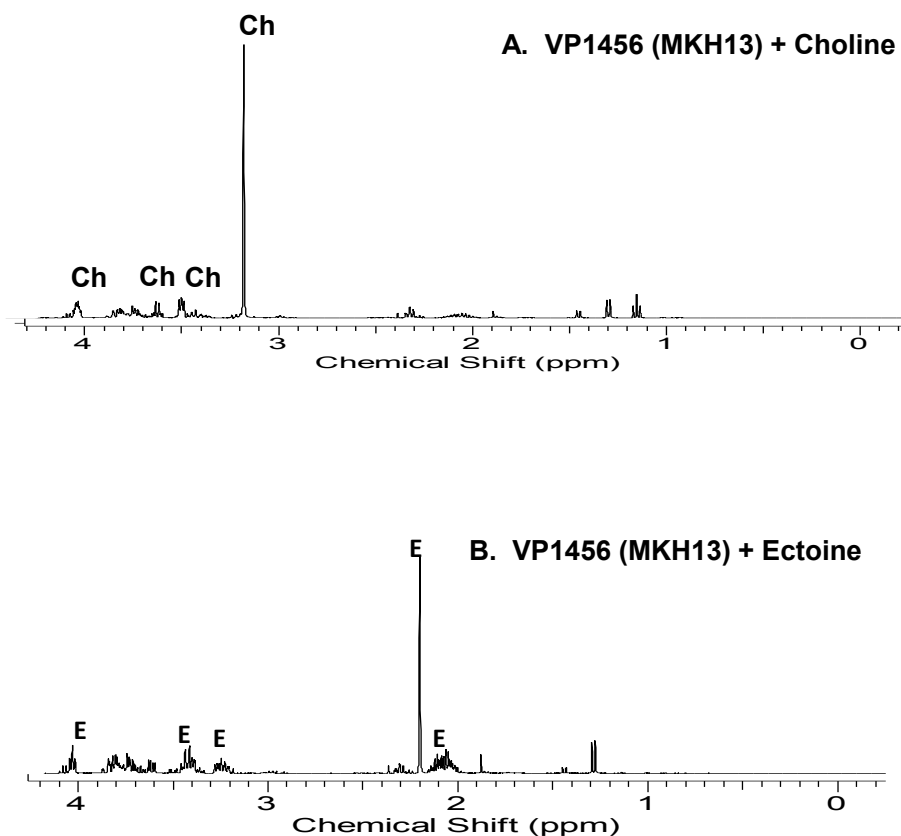
Figure 21 ^{1}H-NMR of *E. coli* **MKH13 pVP1456 strain in (A) M9G 4%**
NaCl+Choline and (B) M9G 4% NaCl+Ectoine. ^{1}H-NMR spectra
were acquired with a Bruker AVANCE III-400 MHz NMR Spectrometer
and the data processed with ACD/Labs software. Chemical shifts (δ) are
expressed in ppm. Experiments were performed at least twice with two
biological replicates. The initials: **E**: Ectoine peaks; **Ch**: Choline peaks.

Table 3   **Bacterial strains and plasmids used in this study**

Strain or Plasmid	Genotypes	Reference
Strains		
V. parahaemolyticus		
RIMD2210633	WT O3:K6 clinical isolate Str^R	[85]
SOY1456 (ΔVP1456)	WT with a VP1456 deletion	This study This
SOY1723 (ΔVP1723)	WT with a VP1723 deletion	study This study
SOY1905 (ΔVP1905)	WT with a VP1905 deletion	This study
SOYA0356 (ΔVPA0356)	WT with a VPA0356 deletion	This study
SOYBCCT12	WT with ΔVP1456ΔVP1723	This study
SOYBCCT124	WT with ΔVP1456ΔVP1723ΔVPA0356	This study
SOYBCCT123	WT with ΔVP1456ΔVP1723ΔVP1905	This study
Δ*ect* Δ*bet*	WT with ectoine and betaine synthesis deleted.	[90]
Escherichia coli		
DH5α-λpir	λpir φ80dlacZΔM15 Δ (lacZYA-argF) U169 recA1 hsdR17 deoR thi-1 supE44 gyrA96 relA1.	
pJΔVP1456 (DH5α-λpir)	pJET-ΔVP1456 transformed into *E. coli* DH5α-λpir	This study
pJΔVP1723 (DH5α-λpir)	pJET-ΔVP1723 transformed into *E. coli* DH5α-λpir	This study
pJΔVP1905 (DH5α-λpir)	pJET-ΔVP1905 transformed into *E. coli* DH5α-λpir	This study
pJΔVPA0356 (DH5α-λpir)	pJET-ΔVPA0356 transformed into *E. coli* DH5α-λpir	This study
β2155 DAP auxotroph	Donor for bacterial conjugation; thr1004 pro thi strA hsdS lacZΔM15 (F′ lacZΔM15 lacTRQJΔ36 proA$^+$ proB$^+$) ΔdapA Erm^r pirRP4 (Km^r from SM10).	
pDS1ΔVP1456 (β2155)	pDSΔVP1456 transformed into *E. coli* β2155	This study
pDSΔVP1723 (β2155)	pDSΔVP1723 transformed into *E. coli* β2155	This study
pDSΔVP1905 (β2155)	pDSΔVP1905 transformed into *E. coli* β2155	This study
pDSΔVPA035 (β2155)	pDSΔVPA0356 transformed into *E. coli* β2155	This study
MKH13	MC4100 (Δ*betTIBA*) Δ(*putPA)101*Δ(*proP)2*Δ(*proU)*,Sp^R	[135]
pBAVP1456 (MKH13)	pBAVP1456 transformed into MKH13	This study
pBAVP1723 (MKH13)	pBAVP1723 transformed into MKH13	This study
pBAVP1905 (MKH13)	pBAVP1905 transformed into MKH13	This study
pBAVPA0356 (MKH13)	pBAVPA0356 transformed into MKH13	This study
Plasmids		
pDS132	R6K γ**ori mobRP4 sacB** Cm^r; suicide vector for conjugal transfer and integration.	
pDSΔVP1456	ΔVP1456 cloned into pDS132 suicide vector	This study
pDSΔVP1723	ΔVP1723cloned into pDS132 suicide vector	This study
pDSΔV1905	ΔV1905 cloned into pDS132 suicide vector	This study
pDSΔVPA0356	ΔV1905 cloned into pDS132 suicide vector	This study
pJET1.2	General cloning vector (Fermentas), Amp^R	
pJEΔVP1456	ΔVP1456 cloned into pJET1.2vector	This study
pJEΔVP1723	ΔVP1723 cloned into pJET1.2 vector	This study
pJEΔVP1905	ΔVP1905 cloned into pJET1.2 vector	This study
pJEΔVPA0356	ΔVPA0356 cloned into pJET1.2 vector	This study
pBAD33	Expression vector, AraC, Cm^R	[189]
pBAVP1456	VP1456 cloned into pBAD33	This study
pBAVP1723	VP1723 cloned into pBAD33	This study
pBAVP1905	VP1905 cloned into pBAD33	This study
pBAVPA0356	VPA0356 cloned into pBAD33	This study

Table 4   **Primers used in this study**

Cloning primers		
Target	**Primer Name**	**Sequence (5'→3')**
VP1456 (BCCT1)	VP1456F (XbaI)	**TCTAGA**TCTTGTGAGTTGAAGACACTTG
	VP1456R (Hind III)	**AAGCTT**AAAAATGCCGAGCAATGAAT
VP1723 (BCCT2)	VP1723F (XbaI)	**TCTAGA**AACTTGTGCTTGGTGATGTG
	VP1723R (SphI)	GAGCTCACGGCACACTTTCGCATG
VP1905 (BCCT3)	VP1905F (Kpnl)	GAGA**GGTACC**GATCTTCCGCTTTCAC
	VP1905R(Pstl)	GAGA**CTGCAG**AGCAGGGTGCTGGCTTC
VPA0356 (BCCT4)	VPA0356F (XbaI)	**TCTAGA**AGCGGCTTTTTGAACATCCT
	VPA0356R (Hind III)	**AAGCTT**CCAATTAAGGGCTCTTTGCAT
SOE PCR primers		
VP1456	VP1456A (XbaI)	**TCTAGA**ATCAATGGGGACAGCGATAA
	VP1456B	*cagctgagatctggtacc*CGAAGCGAATTTTATCACCAA
	VP1456C	*ggtaccagatctcagctg*CGTACCGAACTTTCCGCTTA
	VP1456D (SacI)	**GAGCTC**CAACCATTTTCGCGTTTGTTC
	VP1456FLF	GTCGATTACAATGGCGGATT
	VP1456FL-R	GTGGCACATTGTGAATGCTC
VP1723	VP1723A (XbaI)	**TCTAGA**ACGATATGGTCTGCCAGCTT
	VP1723B	*cagctgagatctggtacc*GGGACGTTTAATCCCACCAT
	VP1723C	*ggtaccagatctcagctg*GGTCTAATGGATGAACCTCGTC
	VP1723D (SacI)	**GAGCTC**CCAATTTCTGGATAAAGCACCC
	VP1273FL-F	TGCGCTTTTAAACACCATTG
	VP11723FL-R	ATGTCCAACGGAGGACAATC
VP1905	VP1905A (XbaI)	**TCTAGA**GAGGAACGATGACAAAGGGTA
	VP1905B	*cagctgagatctggtacc*CGAGCCAAGACATGAATGAA
	VP1905C	*ggtaccagatctcagctg*ATGTTTGATGTGCTGCCATTT
	VP1905D (SacI)	**GAGCTC**TTGATCGATTATTGACGCTCTG
	VP1905FL-F	AATAGCGCGGATGATCTGAC
	VP1905FL-R	TTGAATGCGCTTGCAATATC
VPA0356	VPA0356A (XbaI)	**TCTAGA**CTTGATGTGAGGGGAAATGC
	VPA0356B	*cagctgagatctggtacc*TGTGTCGATGTCTGGTTTCG
	VP0356C	*ggtaccagatctcagctg*ATCATTTCGGTGCTGTTCTTG
	VP0356D (SacI)	**GAGCTC**TTTGCATTTTATGGGGTTGG
	VPA0356FL-F	GCCCACTTCAAACTGTCGTT
	VPA0356FL-R	CTCGATTCGATGTCATTCCA
RT-QPCR primers	**Primer Name**	**Sequence (5'→3')**
VP1456	VP1456RT-F	GTTCGGTCTTGCGACTTCTC
	VP1456RT-R	CCCATCGCAGTATCAAAGGT
VP1723	VP1723RT-F	AACAAAGGGTTGCCACTGAC
	VP1723RT-R	TTCAAACCTGTTGCTGCTTG
VP1905	VP1905RT-F	TGGACGGTATTCTACTGGGC
	VP1905RT-R	CGCCTAACTCGCCTACTTTG
VPA0356	VPA0356RT-F	CAAGGCGTAGGCCGCATGGT
	VPA0356RT-R	ACCGCCCACGATGCTGAACC

Underlined sequences: restriction enzymes sites; Abbreviations: F: Forward; R: Reverse; RT: Reverse Transcriptase; Italicized sequence (bold): complementary tag sequences.

Table 5 **Amino acid identity of the betaine-carnitine-choline transporters.** *V. parahaemolyticus* VP1456, VP1723, VP1905, andVPA0356, *V. cholerae* OpuD (VC1279), and *Escherichia coli* BCCT (ProP, PutP, and BetT) were compared

					% Identity			
ORF	**VP1456**	**VP1723**	**VP1905**	**VPA0356**	**VC1279**	**ProP**	**PutP**	**BetT**
VP1456	100	50.5	67.8	30	67.8	43.5	25.5	37.5
VP1723	50.5	100	52.7	29.6	49.1	26.8	27.5	35.2
VP1905	67.8	52.7	100	30.5	81.8	38.2	23.7	35.3
VPA0356	30	29.6	30.5	100	30.5	36.8	58.3	30

Chapter 4

**THE ROLE OF THE PROU COMPONENT SYSTEMS IN THE OSMOTIC
STRESS TOLORANCE OF THE HALOPHILE VIBRIO
PARAHAEMOLYTICUS**

Introduction

Vibrio parahaemolyticus is a Gram-negative, halophilic bacterium, ubiquitous

in brackish and salt waters around the world [7-9]. The prevalence of this bacterium

in the marine environment has been shown to rely on both high temperature and

salinity, two parameters that control the numbers and proliferation of *V.*

parahaemolyticus in oysters destined for consumption [11, 12, 14-18]. Consequently,

V. parahaemolyticus causes gastrointestinal illness in humans when infected oysters

are consumed raw or undercooked, and has become a public health concern in recent

years [20-23, 172].

The propensity of *V. parahaemolyticus* to thrive and survive in a wide range of

host ecologies and salinity fluctuations has led to the identification of homologues of

osmoregulated proteins predicted to play a role in the growth and survival of this

species under high salinity conditions [3, 85, 94]. Two synthesis systems (ectoine and

betaine), four betaine-carnitine-choline transporters (BCCTs), and two ATP-Binding

Cassette (ABC) transporters have been described in *V. parahaemolyticus* [3, 85, 94].

Previous examination of the roles of the synthesis systems in *V. parahaemolyticus*

demonstrated their role in synthesis of compatible solutes in high salinity [3, 90].

Furthermore, it was demonstrated that addition of ectoine, glycine betaine and proline

in media of high osmolarity resulted in their transport into the cell presumably by uncharacterized osmo-regulated transporters resulting in protection [90].

Typically, a sudden increase in the osmolarity of the external environment, also known as osmotic stress, elicits in most bacteria a set of adaptive responses, aimed at controlling cellular volume and restoring homoeostasis; the uptake and synthesis of low molecular weight organic compounds termed compatible solutes have been shown to be among some of the strategies used by most bacteria [29-32, 35, 37, 41, 51, 61, 64, 75]. In bacteria these responses are carried out via specific membrane-embedded transporters such as the Betaine-Carnitine-Choline Transporter (BCCT) and ATP-Binding Cassette (ABC) family of transporters, and by the biosynthesis systems [33, 113, 124, 131].

The ATP-Binding Cassette (ABC) transporters, also known as ProU transporters, constitute a vast family of carriers that couples the energy generated by ATP hydrolysis with the uptake of substrates across the cell membrane [119, 136]. They are organized in three separate proteins (multicomponent systems) encoded by genes organized in operon (the *proXWX* operon) that includes a periplasmic binding protein component (ProX), a transmembrane component or permease (ProW), and a nucleotide-binding component or ATPase (ProV). Additional signature motifs common to these transporters include a Q-loop, an H-loop/switch region, a Walker A motif/P-loop, and a Walker B motif [119]. Some of these proteins uptake very specific substrates, while others undiscriminatingly uptake structurally diverse compounds [119]. Bioinformatics analysis of *V. parahaemolyticus* genome previously identified two ProU transporters [3, 94]. The ProU1 (locus tag: VP1726-VP1728) located on chromosome I is homologous to the ProU encoded by ProXWV operon of

87

Escherichia coli, and the ProU2 (locus tag: VPA1109-VPA1111) located in chromosome II shows homology to that of *Pseudomonas syringae* [3, 94].

The role of the ProUs in the osmotolerance of *V. parahaemolyticus* remains currently unknown, though a ProU1 mutant was previously constructed and showed no distinguishable phenotype compared to the wild-type in media of high osmolarity [3]. In Gram-negative and -positive bacteria possessing homologous systems, the roles of the ProU in osmotic stress tolerance have been extensively studied. For instance, in *E. coli* and *Salmonella typhimurium* the ProU transporters were shown to be osmotically stimulated and mediated uptake of glycine betaine, proline betaine, choline, dimethylsulfoniopropionate (DMSP) and other compounds [43 , 58, 124, 134, 135, 190, 191]. Unlike the ProU system of *E. coli*, the ProU of *P.aeruginosa* encoded by *cbcXWV* operon was shown to be involved primarily in the transport of choline [117]. Likewise, in *Bacillus subtilis*, a Gram-positive bacterium, three multicomponent transporters (OpuA, OpuB, and OpuC) have been shown to play a role in osmotolerance [192]. Recently, a study examining induction of osmotic-stress-dependent genes in *Vibrio vulnificus*, a close relative of *V. parahaemolyticus*, demonstrated significant up-regulation of the *proU* genes reaching up to 3- to 4.7-fold increase under hyperosmotic stress [193].

In this study, we undertook the examination of the two putative osmoregulated ATP-binding cassette (ABC) transporters of *V. parahaemolyticus* with focus on their roles in the uptake of compatible solutes during growth in media of high osmolarity. We demonstrated that the *proU* genes are induced by NaCl. Moreover, we provided evidence that indicated a role of the ProUs in the uptake of choline, ectoine, and proline. We created in-frame deletion mutations in the two *proU* genes and showed

that the double ProU mutant exhibited an extended lag phase at high osmolarity. This phenotype may imply the possibility of additional role for the ProU systems.

Materials and Methods

Bacterial strains, plasmids, and growth conditions

Bacterial strains and plasmids used in these studies are listed in Table 6. A clinical isolate of *Vibrio parahaemolyticus* RIMD2210633, O3:K6 serotype was used for growth analyses and construction of the mutants [85, 155]. *V. parahaemolyticus* RIMD2210633 wild-type and related mutant strains were routinely grown under aerobic conditions (250 rpm) at 37°C in complex Luria-Bertani (LB) broth (Fisher Scientific, Fair Lawn, NJ) or in defined M9 salts defined medium supplied with 0.4% (w/v) glucose as sole carbon source. Growth analysis in the presence the of compatible solutes was performed in defined M9 salts medium amended with 6 % (w/v) NaCl and energized with 0.4% glucose as sole carbon source. Growth on plates was carried out on LB containing 1.5% agar and adjusted to a final NaCl concentration as indicated. When deemed necessary, the following antibiotics were added to the media to a final concentration: 200 µg/ml streptomycin (Fisher Scientific), 100 µg/ml ampicillin, and 25 µg/ml chloramphenicol. *Escherichia coli* strains, including the DH5α λpir, and β2155 λpir DAP auxotroph were routinely cultured at 37°C in either LB or M9 minimal media adjusted to a NaCl final concentration as indicated. Throughout the text the M9 minimal medium containing 0.4% glucose as carbon source was designated M9G, followed by the NaCl concentration in percentage (w/v).

Bacterial growth analysis

Vibrio parahaemolyticus wild-type and derivative mutant strains used for the examination of compatible solute uptake were grown in defined M9 minimal media containing 0.4% glucose as carbon source. A single bacterial colony was used to inoculate 5 ml of M9 minimal media containing 1%, 3% NaCl and grown overnight at 37ºC under aerobic conditions. An aliquot from the overnight culture was subsequently used to inoculate M9 media of equal salinity and grown aerobically for 5 h at 37ºC. The resulting culture was inoculated at 2.5% (v/v) final dilution into wells of a 96-well microtiter plate filled with 200 µl of defined M9 salts minimal media adjusted to 6% NaCl, and in the absence or presence of exogenously supplied compatible solutes/precursors. Growth analysis was carried out at 37°C for 24 h using a Tecan Sunrise microplate reader (Tecan US Inc.). The hourly optical densities (OD_{595}) measured in the course of a 24 h period were processed and plotted as average of means ± standard errors of means (SEM) using experimental data from at least two biological replicates.

RNA extraction and real-time PCR analysis

RNA materials were isolated from *V. parahaemolyticus* RIMD2210633 wild-type cultures grown to both logarithmic (4 h) and stationary (10 h) phase cultures in complex (LB) and defined M9 media under non upshock (3% NaCl) and NaCl upshock conditions (6 and 9% NaCl) using RNeasy mini kit (Qiagen). Following the elution step, the isolated total RNA was subjected to DNase treatment with Turbo DNA-free kit (Invitrogen) to remove DNA contaminants, and quantified with a NanoDrop spectrophotometer (Thermo Fisher Scientific). The first strand cDNA was synthesized with 500 ng of RNA template using Superscript II reverse transcriptase

(Invitrogen) in the presence of 200 ng of random hexamer primers (Invitrogen).

Reverse Transcriptase (RT)-PCR and Quantitative real-time PCR were used to

quantifiy fold change in gene expression following NaCl upshock; the assay was

performed with diluted cDNA as template in a reaction tube containing *proU*-gene-

specific primers (Table 7) and Hot Start-IT SYBR Green qPCR Master Mix reagent

(USB). The amplification was carried out with an Applied Biosystems 7500 Fast real-

time PCR system (Foster City, CA). The threshold cycle (C_T) values determined

using the 7500 Software v2.0 (ABI) were normalized to 16S rRNA control level using

$\Delta\Delta C_T$ method [160-162]. The transcript levels relative to culture grown in 3% NaCl

were plotted as average of means ± SEM from at least two biological replicates.

Mutant construction

Splicing by Overlap extension Polymerase Chain Reaction (SOE PCR) and

homologous recombination were used to create in-frame deletions in the *proU* genes

as previously described [3, 90, 155]. *V. parahaemolyticus* RIMD2210633 wild-type

genomic DNA template and SOE primers listed in Table 7 were used in the SOE PCR

amplification to create a truncated *proU2* PCR fragment of 750 bp in size by removing

~1,150 bp nucleotides from the wild-type *proU2* gene (1,900 bp). The truncated

proU2 fragment was subsequently cloned into a pDS132 suicide vector[165],

transformed in *E. coli* β2155 λpir DAP auxotroph, and mobilized into a recipient *V.

parahaemolyticus* RIMD2210633 wild-type strain by contact-dependent conjugation.

Following a series of selections using selective markers and homologous

recombination, the truncated *proU2* fragment was integrated into chromosome II of

the recipient *V. parahaemolyticus* RIMD2210633 strain. The generated *V.

parahaemolyticus* RIMD2210633 mutant strain harboring a truncated version of the

proU2 gene was designated Δ*proU2*. To create the double mutant Δ*proU1*Δ*proU2* strain, *V. parahaemolyticus* RIMD2210633 Δ*proU2* strain was used as background, and a previously created Δ*proU1* strain [3] inserted into the Δ*proU2* background by conjugation and homologous recombination. All the created deletions were confirmed by PCR and sequencing.

Amino acid alignment and conserved domain search

Protein sequences were retrieved from the National Center for Biotechnology Information (NCBI) website (http://www.ncbi.nlm.nih.gov) using their designated locus tags. EMBOSS Water-Pairwise Protein Sequence Alignment from the European Molecular Biology Laboratory (EMBL) and the European Bioinformatics Institute (EBI) was used for multiple sequence alignment and determination of percentages amino acid identity. Search for specific conserved domains within the ATP-binding components (ProV) of ProU1 and ProU2 proteins was performed using NCBI's interface online tool for searching the Conserved Domain Database (NCBI). The locus tags for the ProUs are listed in parentheses. ProU1 operon (VP1726-VP1728) located in chromosome I contains ProV (VP1726), ProW *(*VP1727), and ProX *(*VP1728). ProU2 operon (VPA1109-VPA1111) located in chromosome II contains ProV (VPA1109), ProW *(*VPA1110), and ProX *(*VPA1111).

Statistical analysis

An unpaired student's t-test was used to compare the means between two treatments (treated and untreated). The significance of the data was computed as P-values and represented by the asterisk. *, P<0.05; **, P<0.01; ***, P<0.001. Graphing and statistical analyses of the data was performed using Prism 5.

Results

ProU homologues present in *V. parahaemolyticus* are unrelated

Previously, two ProU transporters were identified on the genome of *V. parahaemolyticus* RIMD2210633, VP1726-VP1728 (ProXWV) on chromosome I and VPA1109-VPA1111 (ProXWV) on chromosome II, which we designated ProU1 and ProU2, respectively [3]. In order to determine the degree of relatedness between the two ProUs of *V. parahaemolyticus* amino acid alignment of ProX, ProW, and ProV subunits was performed. It was found that the different subunits shared amino acid identities of 21.5 % for ProX, 42.4% for ProW, and 39.6 % for ProV between each other (Table 8). These data show that the ProUs of *V. parahaemolyticus* RIMD2210633 are unrelated. BLAST homology searches determined that ProU1 is more closely related to ProU from *E. coli* and ProU2 shows homology to ProU in *P. syringae*.

The ProU systems are induced by NaCl upshock in log phase cells

Vibrio parahaemolyticus possesses two putative osmotically-controlled ProU transport systems whose activating cues have not been previously determined. To examine whether the ProU transporter genes are constitutively expressed or induced by high osmolarity, RT-PCR and qPCR analyses of cDNA synthesized from log and stationary phase cultures of *V. parahaemolyticus* in LB before and after NaCl upshock were performed. Both ProU systems are constitutively expressed in LB 3% NaCl (Fig. 22A). It was found that the level of VP1726 (ProU1) transcript was down-regulated by -1.9 $\log_2$ fold in log phase during 6% NaCl upshock but up-regulated by 3.3 $\log_2$ fold (P<0.001) during 9% NaCl upshock in log phase (Fig. 22B). VP1726 was down-regulated in stationary phase at both NaCl concentrations (Fig. 22B).

Expression of VPA1111 (ProU2) was significantly (P<0.001) up-regulated in log phase cells by 5 and 3.8 $\log_2$ fold during 6% and 9% NaCl upshock (Fig. 22C). In stationary phase cells, VPA1111 expression was significantly down-regulated during both 6% and 9% NaCl upshock (Fig. 22C). Overall, these results indicated that ProU systems were constitutively expressed and were up-regulated by NaCl upshock in log phase cells.

The ProU systems of *V. parahaemolyticus* are functionally redundant

Previously, a *V. parahaemolyticus* Δ*proU1* strain was constructed and showed no distinguishable phenotype compared to the WT under high osmolarity [3]. In order to expand the examination of the role of the ProU systems from *V. parahaemolyticus*, a second Δ*proU2* strain was created by deleting VPA1109 (Fig. 23). Like the previously created *V. parahaemolyticus* Δ*proU1* strain, Δ*proU2* showed no distinguishable phenotype compared to WT in media of high osmolarity in the absence or presence of exogenously supplied compatible solutes, indicating that these systems are functionally redundant under the conditions examined.

Δ*proU1*Δ*proU2* has a defect in high osmolarity in defined medium

To further examine the redundancy observed in the single mutants, a *V parahaemolyticus* Δ*proU1*Δ*proU2* strain was constructed (Fig. 23). The Δ*proU1*Δ*proU2* strain was assessed for growth under optimal M9G 3% NaCl and LB media 3%, 6%, 9% and 11% NaCl (Fig. 24E and F). Under these conditions, both the double mutant and the wild-type (WT) strains grew similar to one another with no apparent overall growth defect observed for the mutant. We then performed a comparative growth analysis of WT and Δ*proU1*Δ*proU2* in M9G 6% NaCl with and

94

without compatible solutes. For these assays, WT and mutant were grown overnight in M9G 3% NaCl and then inoculated into M9G 6% NaCl. We found that the *ΔproU1ΔproU2* strain had an extended lag phase of ~11 h, twice that of the WT (Fig. 24). The extended lag time observed in the *ΔproU1ΔproU2* strain indicates that this strain has a defect in high osmolarity in defined medium.

Compatible solutes reduced lag phase of *ΔproU1ΔproU2* strain at high osmolarity

Comparative growth analyses was performed in M9G 6% NaCl in the presence of glycine betaine (Fig. 24A), proline (Fig. 24B), choline (Fig. 24C), and ectoine (Fig. 24D). The uptake of glycine betaine was similar for both WT and *ΔproU1ΔproU2* (Fig. 24A) with a reduction of the lag phase for both to 2 h, which indicates that the defect in the mutant is NaCl stress related. The uptake of glycine betaine in the mutant is as expected since we have shown that the four BCCT transporters are involved in this process and this result indicates that neither of the ProUs is required for the uptake of glycine betaine. The uptake of proline, choline and ectoine was also found in the double mutant with a reduction in the lag phase but in all cases it was never to the same level as WT lag phase reduction (Fig. 24B, C, and D). These data suggest that for proline, choline and ectoine, the ProU systems are not essential for uptake but one or more of these systems likely have the ability to uptake these compatible solutes.

Discussion

In an attempt to elucidate the physiological significance of the two putative osmoregulatory ATP-Binding Cassette (ABC) transporters of *V. parahaemolyticus,* we investigated the role of these systems in the osmotic stress tolerance in media of high

osmolarity. We demonstrated that the ProU transporters were inducible by NaCl upshock in log phase cells; this result is in agreement with osmoregulated transporters behavior in both *E. coli* and *Salmonella* species where the transcription of the *proU* genes was shown to be stimulated in response to increases in external osmolarity [190, 194]. A double mutant Δ*proU1*Δ*proU2* was created and exhibited an extended lag time (11 h) compared to WT in M9G 6% NaCl but not in M9G 3% or LB 3, 6, 9% NaCl. These data suggested that the ProU systems may be involved in something other than compatible solute uptake. In fact, additional roles for the ProU systems and other osmoregulated transporters (BCCTs) have been previously described [167, 195-197]. For example, in *E. coli* the ProP protein was shown to play a role in osmosensing, while the BetP of *C. glutanicum* was shown to act both as osmosensor and osmoregulator [198, 199]. The OpuA of *Lactobacillus lactis,* an ABC type transporter, was found to play a role in sensing changes in osmolarity in this species and this function was mainly attributed to the presence of two the Cystathionine β-synthetase (CBS) domains arranged in tandem and located the in C-terminal portion of this protein [118, 200-202]. Likewise, in *Pseudomonas* species the presence of the CBS domains was found to be important for osmoregulatory function of the OpuC [123]. Thus, it is possible that the extended lag time exhibited by the double *proU* mutant in this study could be due to a defect in osmosensing. In support of this, we identified within the sequence of the ATP binding component (ProV) a pair of CBS domains in ProU1 located between amino acids 284 and 391, and one CBS domain in the ATPase subunit of the ProU2 between 334 and 386 amino acids (Fig. 25A-B). These CBS domains were deleted during the creation of Δ*proU1*Δ*proU2* strain.

The osmotic stress tolerance of *V. parahaemolyticus* was examined in this study, focusing on the role of the proU transport systems. We showed that the ProU systems in *V. parahaemolyticus* are unrelated to each other, and are induced by NaCl. A Δ*proU1*Δ*proU2* was constructed and showed extended lag phase in high osmolarity in defined medium. This phenotype raises the possibility of additional roles for the ProU systems. Furthermore, the Cystathionine β-synthetase (CBS) domains in association with the ProV subunits of the ProU1 and ProU2 described in this study raised additional questions on how this *V. parahaemolyticus* senses in osmolarity.

A. LB 3% NaCl
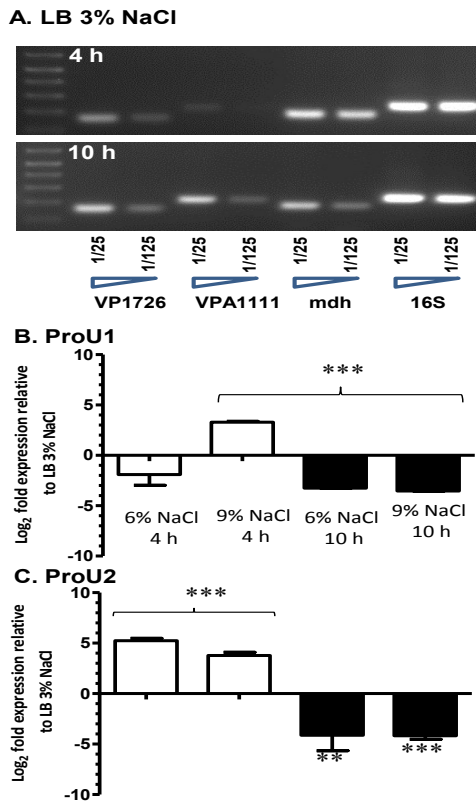
Figure 22 **RT-QPCR expression analysis of the ProU systems**. Cultures were grown in LB broth containing 3% NaCl to log or stationary phase and subjected to 30 min NaCl upshock. Total RNA was extracted from the NaCl upshocked cells and cDNA synthesized. **A**. RT-PCR analysis of VP1726 and VPA1111 in LB 3% NaCl. **B**. ProU1 QPCR analysis. **C**. ProU2 QPCR analysis. QPCR data are plotted relative to untreated cells grown in LB 3% NaCl with two biological replicates. An unpaired Student's *t*-test was used to compare the means between two treatments (treated and untreated). The significance of the data was computed as P-values and represented by the asterisk sign. *, $P<0.05$; **, $P<0.01$; ***, $P<0.001$.
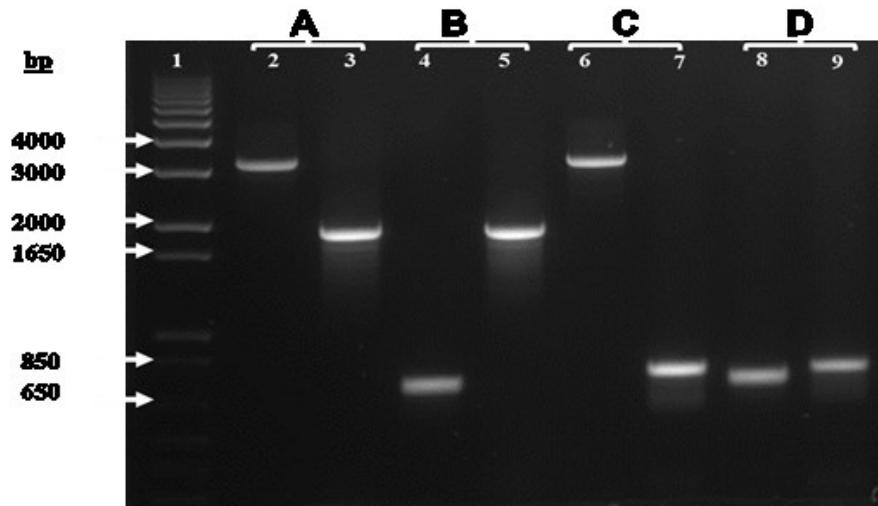
Figure 23   **PCR gel confirmation of *V. parahaemolyticus* WT and Δ*proU* knockouts**. SOE PCR and homologous recombination were used to create the deletions. Legend. lane 1: 1kb molecular weight marker (Invitrogen); (**A**) *V. parahaemolyticus* WT containing in lane 2: a *proU1* WT band (3,200 bp) and in lane 3: a *proU2* WT band (1,900 bp); (**B**):*V. parahaemolyticus* Δ*proU2* harboring in lane 4: a truncated *proU2* band (750 bp) and in lane 5: an intact *proU2* WT band (1,900 bp); (**C**): *V. parahaemolyticus* Δ*proU1* harboring in lane 6: an intact *proU1* WT band (3,200 bp) and in lane 7: a *proU1* truncated band (700 bp); (**D**): *V. parahaemolyticus* Δ*proU2* Δ*proU1* harboring in lane 8: a *proU2* truncated band (750 bp) and in lane 9: a *proU1* truncated band (700 bp).bp: base pair.
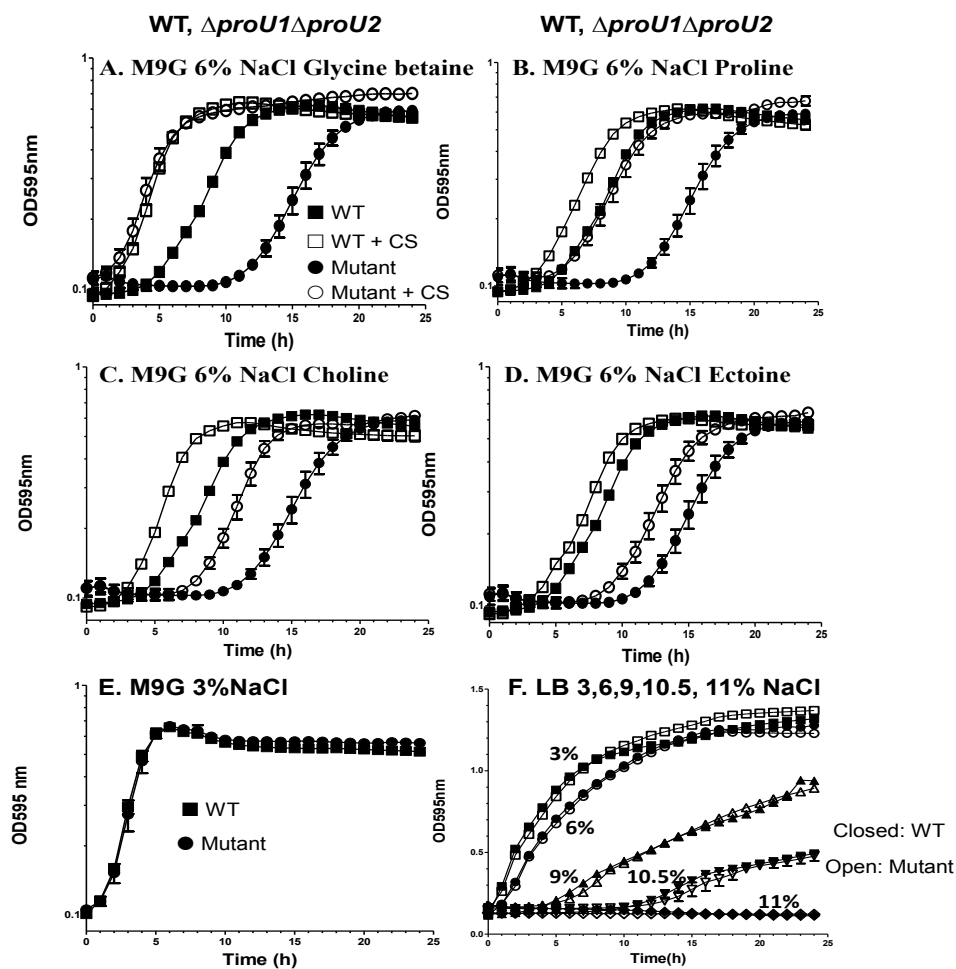
Figure 24   **Growth analyses of *V.parahaemolyticus* WT and Δ*proU2*Δ*proU1*. A**.
M9G 6% NaCl+Glycine betaine; **B**. M9G 6% NaCl+Proline; **C**. M9G
6%NaCl+Choline; **D**. M9G 6% NaCl+Ectoine; **E**. M9G 3% NaCl. **F**.
LB 3, 6, 9, 10.5, 11% (w/v) NaCl. Analyses were performed in triplicate
per condition, and the data are shown as pooled of two biological
replicates.

A   Conserved domains of ProV(VP1726) of ProU1

B   Conserved domains of ProV (VPA1109) of ProU2
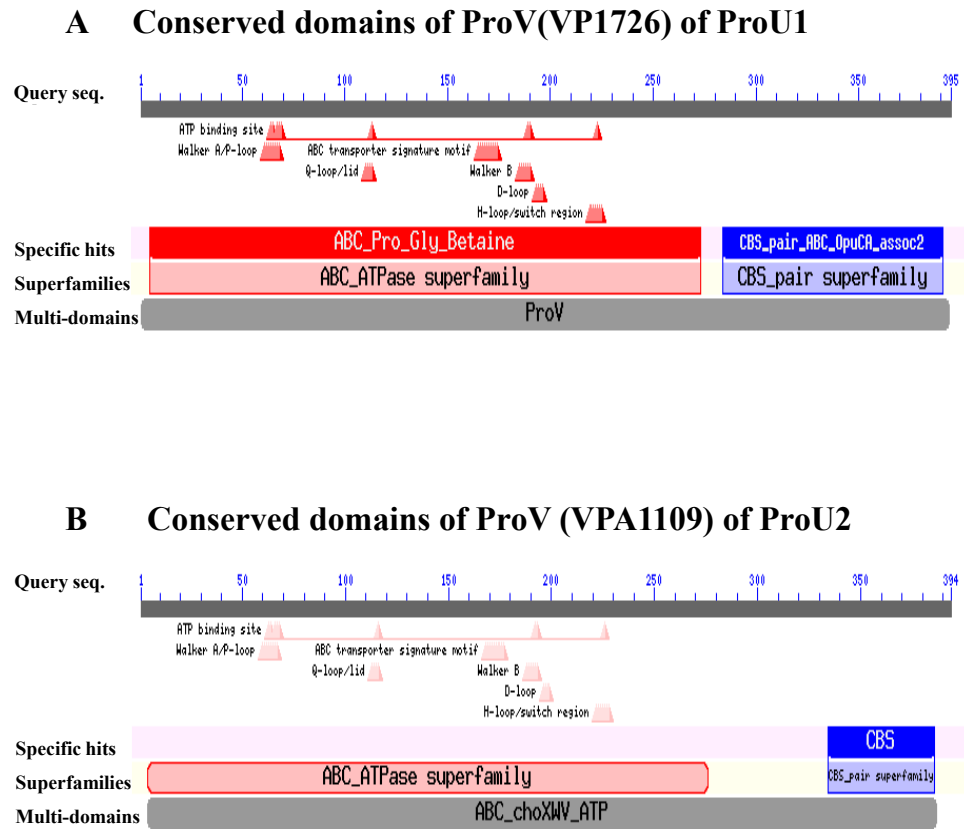
Figure 25   **Conserved domains of the ProV subunits of the ProU systems**. NCBI
Conserved Domain (CDD) Database for the functional annotation of
proteins was used for CDD search [203-205].**A**. ATP-binding subunit
ProV (VP1726) of ProU1.**B**. ATP-binding subunit ProV (VPA1109) of
ProU2.

Table 6   **Bacterial strains and plasmids used in this study**

Strain or Plasmid	Genotypes	Reference
Strains		
Vibrio parahaemolyticus		
RIMD2210633	O3:K6 clinical isolate	[3]
Δ*proU1*	RIMD2210633 harboring *proU1*(VP1726-1728) deletion	[3]
Δ*proU2*	RIMD2210633 harboring *proU2* (VPA1109) deletion	This study
Δ*proU1*Δ*proU2*	RIMD2210633 harboring *proU1* and *proU2* deletions	This study
Escherichia coli		
MKH13	*E. coli* MC4100, Δ*putPA*, Δ*proP*, Δ*proU,* Sp^R	[135]
pDS-132-Δ*proU1β2155*	*E. coli* β2155 strain harboring pDS-132- Δ*proU1*	[3]
Plasmids		
pJET1.2	General cloning vector, Amp^R	Fermentas
pDS132	Suicide vector for allelic exchange, *sacB*, Cm^R	[165]
pDS132- Δ*proU1*	Deleted *proU1* SOE product cloned into pDS132	
pDS132- Δ*proU2*	Deleted *proU2* SOE product cloned into pDS132	This study

Table 7   **Primers used in this study**

SOE-PCR primers

Target	Primer name	Sequence (5' →3')
VPA1109	VPA1109A	GCATGCTGCCATTGCCGCACCAATC
	VPA1109B	CAGCTGAGATCTGGTACCGTCCATTAAGCCTCCT
	VPA1109C	GGTACCAGATCTCAGCTGGCTTAGTTGAGATAAACGT
	VPA1109D	GAGCTCCTTCAACGGTCATTGGAC
	VPA1109FL-F	CATTGTACCGGGACT
	VPA1109FL-R	AGCAGATATGTACAACACC

qPCR primers

Target	Primer name	Sequence (5' →3')
VP1726	VP726F	GCATCGTTTCTCTCGACTCC
	VP1726R	TGCTCATCGACTACTGGCAC
VPA1111	VPA1111F	ATCGTTACCTGGTTCGATGC
	VPA1111R	TTCCTTGGTAACTGGATGCC
VPr001 (16S rRNA)	VPr001F	ACCGCCTGGGGAGTACGGTC
	VPr001R	TTGCGCTCGTTGCGGGACTT
VP0325(*mdh*)	VP0325F	GGCGTTGTTGAGTGTGCTTA
	VP0325R	ACACCAATGTTGATGTCGCCA

Underlined sequences: restriction enzymes sites; Abbreviations: F: Forward; R: Reverse; RT: Reverse Transcriptase.

Table 8   **Amino acid identity of ProU systems of *V. parahaemolyticus*.** The amino acid sequences of the ProU components were retrieved from The National Center for Biotechnology Information (NCBI) website and aligned using EMBOSS Water-Pairwise Protein Sequence Alignment (EMBL-EBI). The percentage identity between the different subunits was deduced from the alignments. The locus tags for the different subunit are listed in parentheses.

ProU1 (Chromosome 1)	% Identity	ProU2 (Chromosome 2)
ProX (VP1728)	21.5	ProX (VPA1111)
ProW (VP1727)	42.4	ProW (VPA1110)
ProV (VP1726)	39.6	ProV (VPA1109)

Chapter 5

CONCLUSION AND FUTURE DIRECTIONS

Vibrio parahaemolyticus growth and survival in high salinity conditions was examined in this study. We focused on the roles of the putative osmoregulated systems that included two synthesis systems (ectoine and betaine) and six transporters (four BCCTs and two ProUs). We demonstrated that the ectoine and betaine synthesis systems are functional and used by *V. parahaemolyticus* to synthesize compatible solutes at high osmolarity. Moreover, we showed that these systems are NaCl-inducible, but the ectoine system (not the betaine synthesis) was critical for growth at high osmolarity. We demonstrated that growth in complex media extended the salinity range of *V. parahaemolyticus*. We examined the role of the four betaine-carnitine-choline transporters in the osmotic stress tolerance of *V. parahaemolyticus* and demonstrated their functionality and role in the uptake of compatible solutes at high osmolarity. We demonstrated that the four betaine-carnitine-choline transporters had a diversified range in the uptake of the compatible solutes; however, VP1456 had the most extended substrate range, up-taking glycine betaine, ectoine, proline, and choline. Examination of the two ProU component systems revealed that they are also induced by NaCl upshock and involved in the uptake of compatible solutes. Interestingly, the proU double knockout exhibited an extended lag phase at high osmolarity in defined media, implying the possibility of additional roles for the ProU systems.

Altogether, this study demonstrated the functionality of the synthesis and transport systems in *V. parahaemolyticus* and showed that their function was NaCl-dependent, a behavior reminiscent of osmoregulated systems.

Despite these interesting results, many questions still remain unanswered. For instance, we still do not know how this organism senses changes in the osmolarity and orchestrates the overall osmoadaptation response. The regulation of these different systems is also currently unknown. Future studies will be needed to address these questions. So far, our bioinformatics analyses of the ProU systems have revealed the presence of two Cystathionine β-Synthetase (CBS) domains in association with the ProV subunit of the ProU1 and one CBS with the ProV of the ProU2. The presence of these modules has been associated with osmosensory and osmoregulatory functions in a number of bacterial species. Therefore, it would be interesting to investigate whether these domains are used by *V. parahaemolyticus* to sense changes in osmolarity. One way to examine the roles of these domains in osmosensing would be to clone and purify individual CBS proteins, followed by point mutation analyses to determine critical residues.

We had previously used a different route in the attempt to answer the same question (osmosensing) by examining the role of two components EnvZ/OmpR in the ability of *V. parahaemolyticus* to sense changes in salinity. Purposely, *V. parahaemolyticus* strains harboring a deletion in either the *ompR* gene (Δ*ompR*) or in both *envZ* and *ompR* genes (Δ*envZ*Δ*ompR*) were created. An Initial assessment of their functionality relative to *V. parahaemolyticus* wild-type in media of high osmolarity showed no distinguishable phenotype. These results raised additional questions on how this organism senses changes in osmolarity and relays the osmotic

signal. It is possible that the mechanisms by which *V. parahaemolyticus* senses and responds to the change*s* in external osmolarity are either independent of the EnvZ/OmpR two-component system, solely dependent of the ProU systems, or perhaps even more complex and occurring via an as-yet unknown mechanism. Future studies will be needed to fully elucidate these questions fundamental to the ubiquitous lifestyle of this important marine organism.

Finally, we have shown throughout this document that NaCl was the trigger for induction of most of the synthesis and transport system genes in *V. parahaemolyticus*. However, we have no knowledge of the mechanisms that control the transcription of these systems. Preliminary data of the alignment of the 200 nucleotide sequences (DNA) located upstream of the start codon of the four betaine-carnitine-choline transporters and the two ProU component systems have revealed very disparate patterns with very low degree of sequence conservations. Moreover, two of the BCCT genes (VP1456 and VP1723) start with alternate start codons GTG, while the other two (VP1905 and VPA0356) start with the ATG codons. Furthermore, promoter prediction analyses of these sequences found -10 and -35 sequence motifs corresponding to sigma 70, sigma 38 and sigma 32. Further investigations of the upstream regions of these genes using primer extension analysis could help determine the transcription start site and the different transciption factors involved.

REFERENCES

1. Schiefner A, Breed J, Bosser L, Kneip S, Gade J, Holtmann G, Diederichs K, Welte W, Bremer E: **Cation-pi interactions as determinants for binding of the compatible solutes glycine betaine and proline betaine by the periplasmic ligand-binding protein ProX from** *Escherichia coli*. *J Biol Chem* 2004, **279**(7):5588-5596.

2. Oswald C, Smits SH, Hoing M, Sohn-Bosser L, Dupont L, Le Rudulier D, Schmitt L, Bremer E: **Crystal structures of the choline/acetylcholine substrate-binding protein ChoX from** *Sinorhizobium meliloti* **in the liganded and unliganded-closed states**. *J Biol Chem* 2008, **283**(47):32848-32859.

3. Naughton LM, Blumerman SL, Carlberg M, Boyd EF: **Osmoadaptation among Vibrio species and unique genomic features and physiological responses of** *Vibrio parahaemolyticus*. *Appl Environ Microbiol* 2009, **75**(9):2802-2810.

4. Joseph SW, Colwell RR, Kaper JB: *Vibrio parahaemolyticus* **and related halophilic Vibrios**. *Crit Rev Microbiol* 1982, **10**(1):77-124.

5. Fujino T, Miwatani T, Takeda Y, Shinoda S, Yoshihara A: **Characterization of** *Vibrio parahaemolyticus* **isolated in the USA**. *Biken J* 1972, **15**(4):223-228.

6. Thompson FL, Iida T, Swings J: **Biodiversity of vibrios**. *Microbiol Mol Biol Rev* 2004, **68**(3):403-431, table of contents.

7. Krantz GE, Colwell RR, Lovelace E: *Vibrio parahaemolyticus* **from the blue crab Callinectes sapidus in Chesapeake Bay**. *Science* 1969, **164**(3885):1286-1287.

8. Kaneko T, Colwell RR: **Ecology of** *Vibrio parahaemolyticus* **in Chesapeake Bay**. *J Bacteriol* 1973, **113**(1):24-32.

9. Colwell RR, Kaper J, Joseph SW: ***Vibrio cholera*e, *Vibrio parahaemolyticus*, and other vibrios: occurrence and distribution in Chesapeake Bay**. *Science* 1977, **198**(4315):394-396.

10. Powell A, Baker-Austin C, Wagley S, Bayley A, Hartnell R: **Isolation of pandemic *Vibrio parahaemolyticus* from UK water and shellfish produce**. *Microb Ecol* 2013, **65**(4):924-927.

11. Martinez-Urtaza J, Blanco-Abad V, Rodriguez-Castro A, Ansede-Bermejo J, Miranda A, Rodriguez-Alvarez MX: **Ecological determinants of the occurrence and dynamics of *Vibrio parahaemolyticus* in offshore areas**. *ISME J* 2012, **6**(5):994-1006.

12. Martinez-Urtaza J, Huapaya B, Gavilan RG, Blanco-Abad V, Ansede-Bermejo J, Cadarso-Suarez C, Figueiras A, Trinanes J: **Emergence of Asiatic Vibrio diseases in South America in phase with El Nino**. *Epidemiology* 2008, **19**(6):829-837.

13. Martinez-Urtaza J, Lozano-Leon A, Varela-Pet J, Trinanes J, Pazos Y, Garcia-Martin O: **Environmental determinants of the occurrence and distribution of *Vibrio parahaemolyticus* in the rias of Galicia, Spain**. *Appl Environ Microbiol* 2008, **74**(1):265-274.

14. Audemard C, Kator HI, Rhodes MW, Gallivan T, Erskine AJ, Leggett AT, Reece KS: **High salinity relay as a postharvest processing strategy to reduce *Vibrio vulnificus* levels in Chesapeake Bay oysters (*Crassostrea virginica*)**. *J Food Prot* 2011, **74**(11):1902-1907.

15. Depaola A, Jones JL, Noe KE, Byars RH, Bowers JC: **Survey of postharvest-processed oysters in the United States for levels of *Vibrio vulnificus* and *Vibrio parahaemolyticus***. *J Food Prot* 2009, **72**(10):2110-2113.

16. Ellis CN, Schuster BM, Striplin MJ, Jones SH, Whistler CA, Cooper VS: **Influence of seasonality on the genetic diversity of *Vibrio parahaemolyticus* in New Hampshire shellfish waters as determined by multilocus sequence analysis**. *Appl Environ Microbiol* 2012, **78**(10):3778-3782.

17. Phuvasate S, Chen MH, Su YC: **Reductions of *Vibrio parahaemolyticus* in Pacific oysters (*Crassostrea gigas*) by depuration at various temperatures**. *Food Microbiol* 2012 **31**(1):51-56.

18. Sarkar BL, Nair GB, Banerjee AK, Pal SC: **Seasonal distribution of *Vibrio parahaemolyticus* in freshwater environs and in association with freshwater fishes in Calcutta**. *Appl Environ Microbiol* 1985, **49**(1):132-136.

19.   Kaneko T, Colwell RR: **Incidence of *Vibrio parahaemolyticus* in Chesapeake Bay**. *Appl Microbiol* 1975, **30**(2):251-257.

20.   Daniels NA, MacKinnon L, Bishop R, Altekruse S, Ray B, Hammond RM, Thompson S, Wilson S, Bean NH, Griffin PM *et al*: ***Vibrio parahaemolyticus* infections in the United States, 1973-1998**. *J Infect Dis* 2000, **181**(5):1661-1666.

21.   Velazquez-Roman J, Leon-Sicairos N, de Jesus Hernandez-Diaz L, Canizalez-Roman A: **Pandemic *Vibrio parahaemolyticus* O3:K6 on the American continent**. *Front Cell Infect Microbiol* 2014, **3**:110.

22.   Nair GB, Ramamurthy T, Bhattacharya SK, Dutta B, Takeda Y, Sack DA: **Global dissemination of *Vibrio parahaemolyticus* serotype O3:K6 and its serovariants**. *Clin Microbiol Rev* 2007, **20**(1):39-48.

23.   Newton A, Kendall M, Vugia DJ, Henao OL, Mahon BE: **Increasing rates of vibriosis in the United States, 1996-2010: review of surveillance data from 2 systems**. *Clin Infect Dis* 2012, **54 Suppl 5**:S391-395.

24.   Su YC, Liu C: ***Vibrio parahaemolyticus*: a concern of seafood safety**. *Food Microbiol* 2007, **24**(6):549-558.

25.   DePaola A, Kaysner CA, Bowers J, Cook DW: **Environmental investigations of *Vibrio parahaemolyticus* in oysters after outbreaks in Washington, Texas, and New York (1997 and 1998)**. *Appl Environ Microbiol* 2000, **66**(11):4649-4654.

26.   DePaola A, Nordstrom JL, Bowers JC, Wells JG, Cook DW: **Seasonal abundance of total and pathogenic *Vibrio parahaemolyticus* in Alabama oysters**. *Appl Environ Microbiol* 2003, **69**(3):1521-1526.

27.   Yeung PS, Boor KJ: **Epidemiology, pathogenesis, and prevention of foodborne *Vibrio parahaemolyticus* infections**. *Foodborne Pathog Dis* 2004, **1**(2):74-88.

28.   Yang ZQ, Jiao XA, Li P, Pan ZM, Huang JL, Gu RX, Fang WM, Chao GX: **Predictive model of *Vibrio parahaemolyticus* growth and survival on salmon meat as a function of temperature**. *Food Microbiol* 2009, **26**(6):606-614.

29.   Oren A: **Microbial life at high salt concentrations: phylogenetic and metabolic diversity**. *Saline Systems* 2008, **4**:2.

30. Csonka LN: **Physiological and genetic responses of bacteria to osmotic stress**. *Microbiol Rev* 1989, **53**(1):121-147.

31. Galinski EA: **Osmoadaptation in bacteria**. *Adv Microb Physiol* 1995, **37**:272-328.

32. Oren A: **Bioenergetic aspects of halophilism**. *Microbiol Mol Biol Rev* 1999, **63**(2):334-348.

33. Wood JM: **Bacterial osmosensing transporters**. *Methods Enzymol* 2007, **428**:77-107.

34. Whatmore AM, Reed RH: **Determination of turgor pressure in Bacillus subtilis: a possible role for K^+ in turgor regulation**. *J Gen Microbiol* 1990, **136**(12):2521-2526.

35. Martin DD, Ciulla RA, Roberts MF: **Osmoadaptation in archaea**. *Appl Environ Microbiol* 1999, **65**(5):1815-1825.

36. Ventosa A, Nieto JJ, Oren A: **Biology of moderately halophilic aerobic bacteria**. *Microbiol Mol Biol Rev* 1998, **62**(2):504-544.

37. Goh F, Jeon YJ, Barrow K, Neilan BA, Burns BP: **Osmoadaptive strategies of the archaeon *Halococcus hamelinensis* isolated from a hypersaline stromatolite environment**. *Astrobiology* 2011, **11**(6):529-536.

38. McLaggan D, Naprstek J, Buurman ET, Epstein W: **Interdependence of K^+ and glutamate accumulation during osmotic adaptation of *Escherichia coli***. *J Biol Chem* 1994, **269**(3):1911-1917.

39. Meury J, Robin A, Monnier-Champeix P: **Turgor-controlled K^+ fluxes and their pathways in *Escherichia coli***. *Eur J Biochem* 1985, **151**(3):613-619.

40. Christian JH, Waltho JA: **The sodium and potassium content of non-halophilic bacteria in relation to salt tolerance**. *J Gen Microbiol* 1961, **25**:97-102.

41. Dinnbier U, Limpinsel E, Schmid R, Bakker EP: **Transient accumulation of potassium glutamate and its replacement by trehalose during adaptation of growing cells of *Escherichia coli* K-12 to elevated sodium chloride concentrations**. *Arch Microbiol* 1988, **150**(4):348-357.

42.   Epstein W, Buurman E, McLaggan D, Naprstek J: **Multiple mechanisms, roles and controls of K$^+$ transport in *Escherichia coli***. *Biochem Soc Trans* 1993, **21**(4):1006-1010.

43.   Lucht JM, Bremer E: **Adaptation of *Escherichia coli* to high osmolarity environments: osmoregulation of the high-affinity glycine betaine transport system proU**. *FEMS Microbiol Rev* 1994, **14**(1):3-20.

44.   Jebbar M, Sohn-Bosser L, Bremer E, Bernard T, Blanco C: **Ectoine-induced proteins in *Sinorhizobium meliloti* include an Ectoine ABC-type transporter involved in osmoprotection and ectoine catabolism**. *J Bacteriol* 2005, **187**(4):1293-1304.

45.   Jebbar M, Talibart R, Gloux K, Bernard T, Blanco C: **Osmoprotection of *Escherichia coli* by ectoine: uptake and accumulation characteristics**. *J Bacteriol* 1992, **174**(15):5027-5035.

46.   Saum SH, Muller V: **Salinity-dependent switching of osmolyte strategies in a moderately halophilic bacterium: glutamate induces proline biosynthesis in *Halobacillus halophilus***. *J Bacteriol* 2007, **189**(19):6968-6975.

47.   Galinski EA, Pfeiffer HP, Truper HG: **1,4,5,6-Tetrahydro-2-methyl-4-pyrimidinecarboxylic acid. A novel cyclic amino acid from halophilic phototrophic bacteria of the genus *Ectothiorhodospira***. *Eur J Biochem* 1985, **149**(1):135-139.

48.   Louis P, Galinski EA: **Characterization of genes for the biosynthesis of the compatible solute ectoine from *Marinococcus halophilus* and osmoregulated expression *in Escherichia coli***. *Microbiology* 1997, **143 (Pt 4)**:1141-1149.

49.   Anton J, Oren A, Benlloch S, Rodriguez-Valera F, Amann R, Rossello-Mora R: ***Salinibacter ruber* gen. nov., sp. nov., a novel, extremely halophilic member of the Bacteria from saltern crystallizer ponds**. *Int J Syst Evol Microbiol* 2002, **52**(Pt 2):485-491.

50.   Youssef NH, Savage-Ashlock KN, McCully AL, Luedtke B, Shaw EI, Hoff WD, Elshahed MS: **Trehalose/2-sulfotrehalose biosynthesis and glycine-betaine uptake are widely spread mechanisms for osmoadaptation in the Halobacteriales**. *ISME J* 2014, **8**(3):636-649.

51.   Roberts MF: **Organic compatible solutes of halotolerant and halophilic microorganisms**. *Saline Systems* 2005, **1**:5.

52.   Sleator RD, Hill C: **Compatible solutes: A listerial passe-partout?** *Gut Microbes* 2010, **1**(2):77-79.

53.   Sleator RD, Hill C: **Compatible solutes: the key to Listeria's success as a versatile gastrointestinal pathogen?** *Gut Pathog* 2010, **2**(1):20.

54.   Kapfhammer D, Karatan E, Pflughoeft KJ, Watnick PI: **Role for glycine betaine transport in *Vibrio cholerae* osmoadaptation and biofilm formation within microbial communities**. *Appl Environ Microbiol* 2005, **71**(7):3840-3847.

55.   Smiddy M, Sleator RD, Patterson MF, Hill C, Kelly AL: **Role for compatible solutes glycine betaine and L-carnitine in listerial barotolerance**. *Appl Environ Microbiol* 2004, **70**(12):7555-7557.

56.   Welsh DT: **Ecological significance of compatible solute accumulation by micro-organisms: from single cells to global climate**. *FEMS Microbiol Rev* 2000, **24**(3):263-290.

57.   Sleator RD, Gahan CG, Hill C: **Identification and disruption of the proBA locus in *Listeria monocytogenes*: role of proline biosynthesis in salt tolerance and murine infection**. *Appl Environ Microbiol* 2001, **67**(6):2571-2577.

58.   Kempf B, Bremer E: **Uptake and synthesis of compatible solutes as microbial stress responses to high-osmolality environments**. *Arch Microbiol* 1998, **170**(5):319-330.

59.   Larsen PI, Sydnes LK, Landfald B, Strom AR: **Osmoregulation in *Escherichia coli* by accumulation of organic osmolytes: betaines, glutamic acid, and trehalose**. *Arch Microbiol* 1987, **147**(1):1-7.

60.   Imhoff JF, Rodriguez-Valera F: **Betaine is the main compatible solute of halophilic eubacteria**. *J Bacteriol* 1984, **160**(1):478-479.

61.   Brown AD: **Microbial water stress**. *Bacteriol Rev* 1976, **40**(4):803-846.

62.   da Costa MS, Santos H, Galinski EA: **An overview of the role and diversity of compatible solutes in Bacteria and Archaea**. *Adv Biochem Eng Biotechnol* 1998, **61**:117-153.

63.   Vargas C, Argandona M, Reina-Bueno M, Rodriguez-Moya J, Fernandez-Aunion C, Nieto JJ: **Unravelling the adaptation responses to osmotic and**

temperature stress in *Chromohalobacter salexigens*, **a bacterium with broad salinity tolerance**. *Saline Systems* 2008, **4**:14.

64. Roberts MF: **Osmoadaptation and osmoregulation in archaea: update 2004**. *Front Biosci* 2004, **9**:1999-2019.

65. Lai MC, Hong TY, Gunsalus RP: **Glycine betaine transport in the obligate halophilic archaeon *Methanohalophilus portucalensis***. *J Bacteriol* 2000, **182**(17):5020-5024.

66. Ko R, Smith LT, Smith GM: **Glycine betaine confers enhanced osmotolerance and cryotolerance on *Listeria monocytogenes***. *J Bacteriol* 1994, **176**(2):426-431.

67. Gauthier MJ, Le Rudulier D: **Survival in seawater of *Escherichia coli* cells grown in marine sediments containing glycine betaine**. *Appl Environ Microbiol* 1990, **56**(9):2915-2918.

68. Ghoul M, Bernard T, Cormier M: **Evidence that *Escherichia coli* accumulates glycine betaine from marine sediments**. *Appl Environ Microbiol* 1990, **56**(2):551-554.

69. Reina-Bueno M, Argandona M, Salvador M, Rodriguez-Moya J, Iglesias-Guerra F, Csonka LN, Nieto JJ, Vargas C: **Role of trehalose in salinity and temperature tolerance in the model halophilic bacterium *Chromohalobacter salexigens***. *PLoS One* 2012, **7**(3):e33587.

70. Hoffmann T, Bremer E: **Protection of *Bacillus subtilis* against cold stress via compatible-solute acquisition**. *J Bacteriol* 2011, **193**(7):1552-1562.

71. Kuhlmann AU, Bursy J, Gimpel S, Hoffmann T, Bremer E: **Synthesis of the compatible solute ectoine in *Virgibacillus pantothenticus* is triggered by high salinity and low growth temperature**. *Appl Environ Microbiol* 2008, **74**(14):4560-4563.

72. Fisher MT: **Proline to the rescue**. *Proc Natl Acad Sci U S A* 2006, **103**(36):13265-13266.

73. Yancey PH, Clark ME, Hand SC, Bowlus RD, Somero GN: **Living with water stress: evolution of osmolyte systems**. *Science* 1982, **217**(4566):1214-1222.

74.   England JL, Haran G: **Role of solvation effects in protein denaturation: from thermodynamics to single molecules and back**. *Annu Rev Phys Chem* 2011, **62**:257-277.

75.   Held C, Neuhaus T, Sadowski G: **Compatible solutes: Thermodynamic properties and biological impact of ectoines and prolines**. *Biophys Chem* 2010, **152**(1-3):28-39.

76.   Khan SH, Ahmad N, Ahmad F, Kumar R: **Naturally occurring organic osmolytes: from cell physiology to disease prevention**. *IUBMB Life* 2010, **62**(12):891-895.

77.   Kitko RD, Wilks JC, Garduque GM, Slonczewski JL: **Osmolytes contribute to pH homeostasis of *Escherichia coli***. *PLoS One* 2010, **5**(4):e10078.

78.   Singh LR, Poddar NK, Dar TA, Kumar R, Ahmad F: **Protein and DNA destabilization by osmolytes: the other side of the coin**. *Life Sci* 2011, **88**(3-4):117-125.

79.   Capp MW, Pegram LM, Saecker RM, Kratz M, Riccardi D, Wendorff T, Cannon JG, Record MT, Jr.: **Interactions of the osmolyte glycine betaine with molecular surfaces in water: thermodynamics, structural interpretation, and prediction of m-values**. *Biochemistry* 2009, **48**(43):10372-10379.

80.   Yu I, Jindo Y, Nagaoka M: **Microscopic understanding of preferential exclusion of compatible solute ectoine: direct interaction and hydration alteration**. *J Phys Chem B* 2007, **111**(34):10231-10238.

81.   Arakawa T, Timasheff SN: **The stabilization of proteins by osmolytes**. *Biophys J* 1985, **47**(3):411-414.

82.   Timasheff SN: **Water as ligand: preferential binding and exclusion of denaturants in protein unfolding**. *Biochemistry* 1992, **31**(41):9857-9864.

83.   Bursy J, Kuhlmann AU, Pittelkow M, Hartmann H, Jebbar M, Pierik AJ, Bremer E: **Synthesis and uptake of the compatible solutes ectoine and 5-hydroxyectoine by *Streptomyces coelicolor* A3(2) in response to salt and heat stresses**. *Appl Environ Microbiol* 2008, **74**(23):7286-7296.

84.   Giaever HM, Styrvold OB, Kaasen I, Strom AR: **Biochemical and genetic characterization of osmoregulatory trehalose synthesis in *Escherichia coli***. *J Bacteriol* 1988, **170**(6):2841-2849.

85.   Makino K, Oshima K, Kurokawa K, Yokoyama K, Uda T, Tagomori K, Iijima Y, Najima M, Nakano M, Yamashita A *et al*: **Genome sequence of *Vibrio parahaemolyticus*: a pathogenic mechanism distinct from that of V cholerae**. *Lancet* 2003, **361**(9359):743-749.

86.   Decker K, Gerhardt F, Boos W: **The role of the trehalose system in regulating the maltose regulon of *Escherichia coli***. *Mol Microbiol* 1999, **32**(4):777-788.

87.   Horlacher R, Boos W: **Characterization of TreR, the major regulator of the Escherichia coli trehalose system**. *J Biol Chem* 1997, **272**(20):13026-13032.

88.   Rimmele M, Boos W: **Trehalose-6-phosphate hydrolase of *Escherichia coli***. *J Bacteriol* 1994, **176**(18):5654-5664.

89.   Marechal LR: **Transport and metabolism of trehalose in *Escherichia coli* and Salmonella typhimurium**. *Arch Microbiol* 1984, **137**(1):70-73.

90.   Ongagna-Yhombi SY, Boyd EF: **Biosynthesis of the osmoprotectant ectoine, but not glycine betaine, is critical for survival of osmotically stressed *Vibrio parahaemolyticus* cells**. *Appl Environ Microbiol* 2013 **79**(16):5038-5049.

91.   Goller K, Ofer A, Galinski EA: **Construction and characterization of an NaCl-sensitive mutant of *Halomonas elongata* impaired in ectoine biosynthesis**. *FEMS Microbiol Lett* 1998, **161**(2):293-300.

92.   Ofer N, Wishkautzan M, Meijler M, Wang Y, Speer A, Niederweis M, Gur E: **Ectoine biosynthesis in *Mycobacterium smegmatis***. *Appl Environ Microbiol* 2012, **78**(20):7483-7486.

93.   Kuhlmann AU, Hoffmann T, Bursy J, Jebbar M, Bremer E: **Ectoine and hydroxyectoine as protectants against osmotic and cold stress: uptake through the SigB-controlled betaine-choline-carnitine transporter-type carrier EctT from *Virgibacillus pantothenticus***. *J Bacteriol* 2011 **193**(18):4699-4708.

94.   Reen FJ, Almagro-Moreno S, Ussery D, Boyd EF: **The genomic code: inferring Vibrionaceae niche specialization**. *Nat Rev Microbiol* 2006, **4**(9):697-704.

95.   Lamark T, Kaasen I, Eshoo MW, Falkenberg P, McDougall J, Strom AR: **DNA sequence and analysis of the bet genes encoding the osmoregulatory**

choline-glycine betaine pathway of *Escherichia coli*. *Mol Microbiol* 1991, **5**(5):1049-1064.

96. Landfald B, Strom AR: **Choline-glycine betaine pathway confers a high level of osmotic tolerance in *Escherichia coli*.** *J Bacteriol* 1986, **165**(3):849-855.

97. Styrvold OB, Falkenberg P, Landfald B, Eshoo MW, Bjornsen T, Strom AR: **Selection, mapping, and characterization of osmoregulatory mutants of *Escherichia coli* blocked in the choline-glycine betaine pathway**. *J Bacteriol* 1986, **165**(3):856-863.

98. Pietruszko R, Shah PC, Kikonyogo A, Chern MK, Lehmann T: **New human aldehyde dehydrogenases**. *Adv Exp Med Biol* 1995, **372**:169-172.

99. McNeil SD, Nuccio ML, Ziemak MJ, Hanson AD: **Enhanced synthesis of choline and glycine betaine in transgenic tobacco plants that overexpress phosphoethanolamine N-methyltransferase**. *Proc Natl Acad Sci U S A* 2001, **98**(17):10001-10005.

100. Sakamoto A, Murata N: **Genetic engineering of glycinebetaine synthesis in plants: current status and implications for enhancement of stress tolerance**. *J Exp Bot* 2000, **51**(342):81-88.

101. Boch J, Kempf B, Schmid R, Bremer E: **Synthesis of the osmoprotectant glycine betaine in *Bacillus subtilis*: characterization of the gbsAB genes**. *J Bacteriol* 1996, **178**(17):5121-5129.

102. Boch J, Nau-Wagner G, Kneip S, Bremer E: **Glycine betaine aldehyde dehydrogenase from *Bacillus subtilis*: characterization of an enzyme required for the synthesis of the osmoprotectant glycine betaine**. *Arch Microbiol* 1997, **168**(4):282-289.

103. Wood AJ, Saneoka H, Rhodes D, Joly RJ, Goldsbrough PB: **Betaine aldehyde dehydrogenase in sorghum**. *Plant Physiol* 1996, **110**(4):1301-1308.

104. Rozwadowski KL, Khachatourians GG, Selvaraj G: **Choline oxidase, a catabolic enzyme in *Arthrobacter pascens*, facilitates adaptation to osmotic stress in Escherichia coli**. *J Bacteriol* 1991, **173**(2):472-478.

105. Brouquisse R, Weigel P, Rhodes D, Yocum CF, Hanson AD: **Evidence for a ferredoxin-dependent choline monooxygenase from spinach chloroplast stroma**. *Plant Physiol* 1989, **90**(1):322-329.

106. Lai MC, Wang CC, Chuang MJ, Wu YC, Lee YC: **Effects of substrate and potassium on the betaine-synthesizing enzyme glycine sarcosine dimethylglycine N-methyltransferase from a halophilic methanoarchaeon** *Methanohalophilus portucalensis*. *Res Microbiol* 2006, **157**(10):948-955.

107. von Weymarn N, Nyyssola A, Reinikainen T, Leisola M, Ojamo H: **Improved osmotolerance of recombinant** *Escherichia coli* **by de novo glycine betaine biosynthesis**. *Appl Microbiol Biotechnol* 2001, **55**(2):214-218.

108. Nyyssola A, Kerovuo J, Kaukinen P, von Weymarn N, Reinikainen T: **Extreme halophiles synthesize betaine from glycine by methylation**. *J Biol Chem* 2000, **275**(29):22196-22201.

109. Rebouche CJ, Seim H: **Carnitine metabolism and its regulation in microorganisms and mammals**. *Annu Rev Nutr* 1998, **18**:39-61.

110. Kleber HP: **Bacterial carnitine metabolism**. *FEMS Microbiol Lett* 1997, **147**(1):1-9.

111. Goulas P: **Purification and properties of carnitine dehydrogenase from** *Pseudomonas putida*. *Biochim Biophys Acta* 1988, **957**(3):335-339.

112. Steger R, Weinand M, Kramer R, Morbach S: **LcoP, an osmoregulated betaine/ectoine uptake system from** *Corynebacterium glutamicum*. *FEBS Lett* 2004, **573**(1-3):155-160.

113. Ziegler C, Bremer E, Kramer R: **The BCCT family of carriers: from physiology to crystal structure**. *Mol Microbiol* 2010, **78**(1):13-34.

114. Peter H, Burkovski A, Kramer R: **Isolation, characterization, and expression of the** *Corynebacterium glutamicum* betP **gene, encoding the transport system for the compatible solute glycine betaine**. *J Bacteriol* 1996, **178**(17):5229-5234.

115. Khafizov K, Perez C, Koshy C, Quick M, Fendler K, Ziegler C, Forrest LR: **Investigation of the sodium-binding sites in the sodium-coupled betaine transporter BetP**. *Proc Natl Acad Sci USA* 2012, **109**(44):E3035-3044.

116. Kappes RM, Kempf B, Bremer E: **Three transport systems for the osmoprotectant glycine betaine operate in** *Bacillus subtilis***: characterization of OpuD**. *J Bacteriol* 1996, **178**(17):5071-5079.

117.   Malek AA, Chen C, Wargo MJ, Beattie GA, Hogan DA: **Roles of three transporters, CbcXWV, BetT1, and BetT3, in *Pseudomonas aeruginosa* choline uptake for catabolism**. *J Bacteriol* 2011, **193**(12):3033-3041.

118.   Biemans-Oldehinkel E, Doeven MK, Poolman B: **ABC transporter architecture and regulatory roles of accessory domains**. *FEBS Lett* 2006, **580**(4):1023-1035.

119.   Davidson AL, Chen J: **ATP-binding cassette transporters in bacteria**. *Annu Rev Biochem* 2004, **73**:241-268.

120.   Dattananda CS, Gowrishankar J: **Osmoregulation in *Escherichia coli*: complementation analysis and gene-protein relationships in the proU locus**. *J Bacteriol* 1989, **171**(4):1915-1922.

121.   Gul N, Poolman B: **Functional reconstitution and osmoregulatory properties of the ProU ABC transporter from *Escherichia coli***. *Mol Membr Biol* 2013 **30**(2):138-148.

122.   Chen C, Malek AA, Wargo MJ, Hogan DA, Beattie GA: **The ATP-binding cassette transporter Cbc (choline/betaine/carnitine) recruits multiple substrate-binding proteins with strong specificity for distinct quaternary ammonium compounds**. *Mol Microbiol* 2010, **75**(1):29-45.

123.   Chen C, Beattie GA: **Characterization of the osmoprotectant transporter OpuC from *Pseudomonas syringae* and demonstration that cystathionine-beta-synthase domains are required for its osmoregulatory function**. *J Bacteriol* 2007, **189**(19):6901-6912.

124.   van der Heide T, Poolman B: **Osmoregulated ABC-transport system of *Lactococcus lactis* senses water stress via changes in the physical state of the membrane**. *Proc Natl Acad Sci USA* 2000, **97**(13):7102-7106.

125.   Shinoda S: **Sixty years from the discovery of *Vibrio parahaemolyticus* and some recollections**. *Biocontrol Sci* 2011, **16**(4):129-137.

126.   Takeda Y: **[Discovery of *Vibrio parahaemolyticus* by Tsunesaburo Fujino]**. *Nihon Naika Gakkai Zasshi* 2002, **91**(10):2903-2906.

127.   Baker-Austin C, Stockley L, Rangdale R, Martinez-Urtaza J: **Environmental occurrence and clinical impact of *Vibrio vulnificus* and *Vibrio parahaemolyticus*: a European perspective**. *Environ Microbiol Rep* 2010, **2**(1):7-18.

128. Alam M, Chowdhury WB, Bhuiyan NA, Islam A, Hasan NA, Nair GB, Watanabe H, Siddique AK, Huq A, Sack RB *et al*: **Serogroup, virulence, and genetic traits of *Vibrio parahaemolyticus* in the estuarine ecosystem of Bangladesh**. *Appl Environ Microbiol* 2009, **75**(19):6268-6274.

129. Ansede-Bermejo J, Gavilan RG, Trinanes J, Espejo RT, Martinez-Urtaza J: **Origins and colonization history of pandemic *Vibrio parahaemolyticus* in South America**. *Mol Ecol* 2010, **19**(18):3924-3937.

130. Sleator RD, Hill C: **Bacterial osmoadaptation: the role of osmolytes in bacterial stress and virulence**. *FEMS Microbiol Rev* 2002, **26**(1):49-71.

131. Sleator RD, Wouters J, Gahan CG, Abee T, Hill C: **Analysis of the role of OpuC, an osmolyte transport system, in salt tolerance and virulence potential of *Listeria monocytogenes***. *Appl Environ Microbiol* 2001, **67**(6):2692-2698.

132. Culham DE, Lu A, Jishage M, Krogfelt KA, Ishihama A, Wood JM: **The osmotic stress response and virulence in pyelonephritis isolates of *Escherichia coli*: contributions of RpoS, ProP, ProU and other systems**. *Microbiology* 2001, **147**(Pt 6):1657-1670.

133. Verheul A, Wouters JA, Rombouts FM, Abee T: **A possible role of ProP, ProU and CaiT in osmoprotection of *Escherichia coli* by carnitine**. *J Appl Microbiol* 1998, **85**(6):1036-1046.

134. Gouesbet G, Jebbar M, Talibart R, Bernard T, Blanco C: **Pipecolic acid is an osmoprotectant for *Escherichia coli* taken up by the general osmoporters ProU and ProP**. *Microbiology* 1994, **140 (Pt 9)**:2415-2422.

135. Haardt M, Kempf B, Faatz E, Bremer E: **The osmoprotectant proline betaine is a major substrate for the binding-protein-dependent transport system ProU of *Escherichia coli* K-12**. *Mol Gen Genet* 1995, **246**(6):783-786.

136. Gowrishankar J: **Nucleotide sequence of the osmoregulatory proU operon of Escherichia coli**. *J Bacteriol* 1989, **171**(4):1923-1931.

137. May G, Faatz E, Villarejo M, Bremer E: **Binding protein dependent transport of glycine betaine and its osmotic regulation in *Escherichia coli* K12**. *Mol Gen Genet* 1986, **205**(2):225-233.

138. Daniels NA, Ray B, Easton A, Marano N, Kahn E, McShan AL, 2nd, Del Rosario L, Baldwin T, Kingsley MA, Puhr ND *et al*: **Emergence of a new

Vibrio parahaemolyticus **serotype in raw oysters: A prevention quandary**. *JAMA* 2000, **284**(12):1541-1545.

139. McLaughlin JB, DePaola A, Bopp CA, Martinek KA, Napolilli NP, Allison CG, Murray SL, Thompson EC, Bird MM, Middaugh JP: **Outbreak of *Vibrio parahaemolyticus* gastroenteritis associated with Alaskan oysters**. *N Engl J Med* 2005, **353**(14):1463-1470.

140. Garcia K, Torres R, Uribe P, Hernandez C, Rioseco ML, Romero J, Espejo RT: **Dynamics of clinical and environmental *Vibrio parahaemolyticus* strains during seafood-related summer diarrhea outbreaks in southern Chile**. *Appl Environ Microbiol* 2009, **75**(23):7482-7487.

141. Kalburge SS, Whitaker WB, Boyd EF: **High-salt preadaptation of *Vibrio parahaemolyticus* enhances survival in response to lethal environmental stresses**. *J Food Prot*, **77**(2):246-253.

142. Gotoh K, Kodama T, Hiyoshi H, Izutsu K, Park KS, Dryselius R, Akeda Y, Honda T, Iida T: **Bile acid-induced virulence gene expression of *Vibrio parahaemolyticus* reveals a novel therapeutic potential for bile acid sequestrants**. *PLoS One* 2010 **5**(10):e13365.

143. Pace JL, Chai TJ, Rossi HA, Jiang X: **Effect of bile on *Vibrio parahaemolyticus***. *Appl Environ Microbiol* 1997, **63**(6):2372-2377.

144. Pastor JM, Salvador M, Argandona M, Bernal V, Reina-Bueno M, Csonka LN, Iborra JL, Vargas C, Nieto JJ, Canovas M: **Ectoines in cell stress protection: uses and biotechnological production**. *Biotechnol Adv* 2010, **28**(6):782-801.

145. Sauer T, Galinski EA: **Bacterial milking: A novel bioprocess for production of compatible solutes**. *Biotechnol Bioeng* 1998, **59**(1):128.

146. Bestvater T, Louis P, Galinski EA: **Heterologous ectoine production in *Escherichia coli*: by-passing the metabolic bottle-neck**. *Saline Systems* 2008, **4**:12.

147. Turner JW, Malayil L, Guadagnoli D, Cole D, Lipp EK: **Detection of *Vibrio parahaemolyticus*, *Vibrio vulnificus* and *Vibrio cholerae* with respect to seasonal fluctuations in temperature and plankton abundance**. *Environ Microbiol* 2013.

148. Turner JW, Paranjpye RN, Landis ED, Biryukov SV, Gonzalez-Escalona N, Nilsson WB, Strom MS: **Population structure of clinical and environmental**

Vibrio parahaemolyticus **from the Pacific Northwest coast of the United States**. *PLoS One* 2013, **8**(2):e55726.

149.   Colwell RR: **Global climate and infectious disease: the cholera paradigm**. *Science* 1996, **274**(5295):2025-2031.

150.   Colwell RR, Epstein PR, Gubler D, Maynard N, McMichael AJ, Patz JA, Sack RB, Shope R: **Climate change and human health**. *Science* 1998, **279**(5353):968-969.

151.   Harvell CD, Kim K, Burkholder JM, Colwell RR, Epstein PR, Grimes DJ, Hofmann EE, Lipp EK, Osterhaus AD, Overstreet RM *et al*: **Emerging marine diseases--climate links and anthropogenic factors**. *Science* 1999, **285**(5433):1505-1510.

152.   Pascual M, Rodo X, Ellner SP, Colwell R, Bouma MJ: **Cholera dynamics and El Nino-Southern Oscillation**. *Science* 2000, **289**(5485):1766-1769.

153.   Lobitz B, Beck L, Huq A, Wood B, Fuchs G, Faruque AS, Colwell R: **Climate and infectious disease: use of remote sensing for detection of Vibrio cholerae by indirect measurement**. *Proc Natl Acad Sci U S A* 2000, **97**(4):1438-1443.

154.   Johnson CN, Bowers JC, Griffitt KJ, Molina V, Clostio RW, Pei S, Laws E, Paranjpye RN, Strom MS, Chen A *et al*: **Ecology of *Vibrio parahaemolyticus* and *Vibrio vulnificus* in the coastal and estuarine waters of Louisiana, Maryland, Mississippi, and Washington (United States)**. *Appl Environ Microbiol* 2012 **78**(20):7249-7257.

155.   Whitaker WB, Parent MA, Naughton LM, Richards GP, Blumerman SL, Boyd EF: **Modulation of responses of V*ibrio parahaemolyticus* O3:K6 to pH and temperature stresses by growth at different salt concentrations**. *Appl Environ Microbiol* 2010, **76**(14):4720-4729.

156.   Mahoney JC, Gerding MJ, Jones SH, Whistler CA: **Comparison of the pathogenic potentials of environmental and clinical *Vibrio parahaemolyticus* strains indicates a role for temperature regulation in virulence**. *Appl Environ Microbiol* 2010, **76**(22):7459-7465.

157.   Boyd EF, Cohen AL, Naughton LM, Ussery DW, Binnewies TT, Stine OC, Parent MA: **Molecular analysis of the emergence of pandemic *Vibrio parahaemolyticus***. *BMC Microbiol* 2008, **8**:110.

158. Galinski EA, Oren A: **Isolation and structure determination of a novel compatible solute from the moderately halophilic purple sulfur bacterium** *Ectothiorhodospira marismortui*. *Eur J Biochem* 1991, **198**(3):593-598.

159. Pflughoeft KJ, Kierek K, Watnick PI: **Role of ectoine in** *Vibrio cholerae* **osmoadaptation**. *Appl Environ Microbiol* 2003, **69**(10):5919-5927.

160. Pfaffl MW: **A new mathematical model for relative quantification in real-time RT-PCR**. *Nucleic Acids Res* 2001, **29**(9):e45.

161. Livak KJ, Schmittgen TD: **Analysis of relative gene expression data using real-time quantitative PCR and the 2(-Delta Delta C(T)) Method**. *Methods* 2001, **25**(4):402-408.

162. Schmittgen TD, Livak KJ: **Analyzing real-time PCR data by the comparative C(T) method**. *Nat Protoc* 2008, **3**(6):1101-1108.

163. Horton RM, Ho SN, Pullen JK, Hunt HD, Cai Z, Pease LR: **Gene splicing by overlap extension**. *Methods Enzymol* 1993, **217**:270-279.

164. Horton RM, Hunt HD, Ho SN, Pullen JK, Pease LR: **Engineering hybrid genes without the use of restriction enzymes: gene splicing by overlap extension**. *Gene* 1989, **77**(1):61-68.

165. Philippe N, Alcaraz JP, Coursange E, Geiselmann J, Schneider D: **Improvement of pCVD442, a suicide plasmid for gene allele exchange in bacteria**. *Plasmid* 2004, **51**(3):246-255.

166. Tamura K, Peterson D, Peterson N, Stecher G, Nei M, Kumar S: **MEGA5: molecular evolutionary genetics analysis using maximum likelihood, evolutionary distance, and maximum parsimony methods**. *Mol Biol Evol* 2011, **28**(10):2731-2739.

167. Wood JM, Bremer E, Csonka LN, Kraemer R, Poolman B, van der Heide T, Smith LT: **Osmosensing and osmoregulatory compatible solute accumulation by bacteria**. *Comp Biochem Physiol A Mol Integr Physiol* 2001, **130**(3):437-460.

168. Saum SH, Muller V: **Regulation of osmoadaptation in the moderate halophile** *Halobacillus halophilus***: chloride, glutamate and switching osmolyte strategies**. *Saline Systems* 2008, **4**:4.

169. Wargo MJ, Hogan DA: **Identification of genes required for** *Pseudomonas aeruginosa* **carnitine catabolism**. *Microbiology* 2009, **155**(Pt 7):2411-2419.

170.   Saitou N, Nei M: **The neighbor-joining method: a new method for reconstructing phylogenetic trees**. *Mol Biol Evol* 1987, **4**(4):406-425.

171.   Tiruvayipati S, Bhassu S, Kumar N, Baddam R, Shaik S, Gurindapalli AK, T*hong KL, Ahmed N: **Genome anatomy of the gastrointestinal pathogen, Vibrio parahaemolyticus* of crustacean origin**. *Gut Pathog* 2013, **5**(1):37.

172.   Martinez-Urtaza J, Baker-Austin C, Jones JL, Newton AE, Gonzalez-Aviles GD, DePaola A: **Spread of Pacific Northwest *Vibrio parahaemolyticus* strain**. *N Engl J Med* 2013, **369**(16):1573-1574.

173.   Cabanillas-Beltran H, E LL-M, Romero R, Espinoza A, Garcia-Gasca A, Nishibuchi M, Ishibashi M, Gomez-Gil B: **Outbreak of gastroenteritis caused by the pandemic *Vibrio parahaemolyticus* O3:K6 in Mexico**. *FEMS Microbiol Lett* 2006, **265**(1):76-80.

174.   Velazquez-Roman J, Leon-Sicairos N, de Jesus Hernandez-Diaz L, Canizalez-Roman A: **Pandemic *Vibrio parahaemolyticus* O3:K6 on the American continent**. *Front Cell Infect Microbiol* 2013, **3**:110.

175.   Ceccarelli D, Hasan NA, Huq A, Colwell RR: **Distribution and dynamics of epidemic and pandemic *Vibrio parahaemolyticus* virulence factors**. *Front Cell Infect Microbiol* 2013, **3**:97.

176.   Chao G, Jiao X, Zhou X, Yang Z, Huang J, Pan Z, Zhou L, Qian X: **Serodiversity, pandemic O3:K6 clone, molecular typing, and antibiotic susceptibility of foodborne and clinical *Vibrio parahaemolyticus* isolates in Jiangsu, China**. *Foodborne Pathog Dis* 2009, **6**(8):1021-1028.

177.   Rehnstam-Holm AS, Atnur V, Godhe A: **Defining the Niche of *Vibrio parahaemolyticus* During Pre- and Post-Monsoon Seasons in the Coastal Arabian Sea**. *Microb Ecol* 2014, **67**(1):57-65.

178.   Sobrinho Pde S, Destro MT, Franco BD, Landgraf M: **Occurrence and distribution of *Vibrio parahaemolyticus* in retail oysters in Sao Paulo State, Brazil**. *Food Microbiol* 2011, **28**(1):137-140.

179.   Fyfe M, Yeung ST, Daly P, Schallie K, Kelly MT, Buchanan S: **Outbreak of *Vibrio parahaemolyticus* related to raw oysters in British Columbia**. *Can Commun Dis Rep* 1997, **23**(19):145-148.

180.   Su YC, Yang Q, Hase C: **Refrigerated seawater depuration for reducing *Vibrio parahaemolyticus* contamination in pacific oyster (*Crassostrea gigas*)**. *J Food Prot* 2010, **73**(6):1111-1115.

181. Wood JM: **Osmosensing by bacteria**. *Sci STKE* 2006, **2006**(357):pe43.

182. Pfluger K, Muller V: **Transport of compatible solutes in extremophiles**. *J Bioenerg Biomembr* 2004, **36**(1):17-24.

183. Sleator RD, Gahan CG, Abee T, Hill C: **Identification and disruption of BetL, a secondary glycine betaine transport system linked to the salt tolerance of *Listeria monocytogenes* LO28**. *Appl Environ Microbiol* 1999, **65**(5):2078-2083.

184. Onraedt A, De Mey M, Walcarius B, Soetaert W, Vandamme EJ: **Transport kinetics of ectoine, an osmolyte produced by *Brevibacterium epidermis***. *Biotechnol Lett* 2006, **28**(21):1741-1747.

185. Chen C, Beattie GA: ***Pseudomonas syringae* BetT is a low-affinity choline transporter that is responsible for superior osmoprotection by choline over glycine betaine**. *J Bacteriol* 2008, **190**(8):2717-2725.

186. Casadaban MJ: **Transposition and fusion of the lac genes to selected promoters in *Escherichia coli* using bacteriophage lambda and Mu**. *J Mol Biol* 1976, **104**(3):541-555.

187. Peters JE, Thate TE, Craig NL: **Definition of the *Escherichia coli* MC4100 genome by use of a DNA array**. *J Bacteriol* 2003, **185**(6):2017-2021.

188. Vermeulen V, Kunte HJ: ***Marinococcus halophilus* DSM 20408T encodes two transporters for compatible solutes belonging to the betaine-carnitine-choline transporter family: identification and characterization of ectoine transporter EctM and glycine betaine transporter BetM**. *Extremophiles* 2004, **8**(3):175-184.

189. Guzman LM, Belin D, Carson MJ, Beckwith J: **Tight regulation, modulation, and high-level expression by vectors containing the arabinose PBAD promoter**. *J Bacteriol* 1995, **177**(14):4121-4130.

190. Cairney J, Booth IR, Higgins CF: **Osmoregulation of gene expression in *Salmonella typhimurium*: proU encodes an osmotically induced betaine transport system**. *J Bacteriol* 1985, **164**(3):1224-1232.

191. Jovanovich SB, Record MT, Jr., Burgess RR: **In an *Escherichia coli* coupled transcription-translation system, expression of the osmoregulated gene proU is stimulated at elevated potassium concentrations and by an extract from cells grown at high osmolality**. *J Biol Chem* 1989, **264**(14):7821-7825.

192.   Kempf B, Bremer E: **OpuA, an osmotically regulated binding protein-dependent transport system for the osmoprotectant glycine betaine in *Bacillus subtilis***. *J Biol Chem* 1995, **270**(28):16701-16713.

193.   Rao NV, Shashidhar R, Bandekar JR: **Comparative analysis of induction of osmotic-stress-dependent genes in *Vibrio vulnificus* exposed to hyper- and hypo-osmotic stress**. *Can J Microbiol* 2013, **59**(5):333-338.

194.   Gunasekera TS, Csonka LN, Paliy O: **Genome-wide transcriptional responses of *Escherichia coli* K-12 to continuous osmotic and heat stresses**. *J Bacteriol* 2008, **190**(10):3712-3720.

195.   Culham DE, Henderson J, Crane RA, Wood JM: **Osmosensor ProP of *Escherichia coli* responds to the concentration, chemistry, and molecular size of osmolytes in the proteoliposome lumen**. *Biochemistry* 2003, **42**(2):410-420.

196.   Keates RA, Culham DE, Vernikovska YI, Zuiani AJ, Boggs JM, Wood JM: **Transmembrane helix I and periplasmic loop 1 of *Escherichia coli* ProP are involved in osmosensing and osmoprotectant transport**. *Biochemistry* 2010, **49**(41):8847-8856.

197.   Wood JM: **Osmosensing by bacteria: signals and membrane-based sensors**. *Microbiol Mol Biol Rev* 1999, **63**(1):230-262.

198.   Kramer R: **Osmosensing and osmosignaling in *Corynebacterium glutamicum***. *Amino Acids* 2009, **37**(3):487-497.

199.   Kramer R, Ziegler C: **Regulative interactions of the osmosensing C-terminal domain in the trimeric glycine betaine transporter BetP from *Corynebacterium glutamicum***. *Biol Chem* 2009, **390**(8):685-691.

200.   Mahmood NA, Biemans-Oldehinkel E, Patzlaff JS, Schuurman-Wolters GK, Poolman B: **Ion specificity and ionic strength dependence of the osmoregulatory ABC transporter OpuA**. *J Biol Chem* 2006, **281**(40):29830-29839.

201.   Karasawa A, Erkens GB, Berntsson RP, Otten R, Schuurman-Wolters GK, Mulder FA, Poolman B: **Cystathionine beta-synthase (CBS) domains 1 and 2 fulfill different roles in ionic strength sensing of the ATP-binding cassette (ABC) transporter OpuA**. *J Biol Chem* 2011, **286**(43):37280-37291.

202.   Biemans-Oldehinkel E, Mahmood NA, Poolman B: **A sensor for intracellular ionic strength**. *Proc Natl Acad Sci U S A* 2006, **103**(28):10624-10629.

203. Marchler-Bauer A, Anderson JB, Chitsaz F, Derbyshire MK, DeWeese-Scott C, Fong JH, Geer LY, Geer RC, Gonzales NR, Gwadz M *et al*: **CDD: specific functional annotation with the Conserved Domain Database**. *Nucleic Acids Res* 2009, **37**(Database issue):D205-210.

204. Marchler-Bauer A, Bryant SH: **CD-Search: protein domain annotations on the fly**. *Nucleic Acids Res* 2004, **32**(Web Server issue):W327-331.

205. Marchler-Bauer A, Lu S, Anderson JB, Chitsaz F, Derbyshire MK, DeWeese-Scott C, Fong JH, Geer LY, Geer RC, Gonzales NR *et al*: **CDD: a Conserved Domain Database for the functional annotation of proteins**. *Nucleic Acids Res* 2011, **39**(Database issue):D225-229.

206. Combet C, Blanchet C, Geourjon C, Deleage G: **NPS@: network protein sequence analysis**. *Trends Biochem Sci* 2000, **25**(3):147-150.

207. Altschul SF, Gish W, Miller W, Myers EW, Lipman DJ: **Basic local alignment search tool**. *J Mol Biol* 1990, **215**(3):403-410.

208. Remmert M, Biegert A, Hauser A, Soding J: **HHblits: lightning-fast iterative protein sequence searching by HMM-HMM alignment**. *Nat Methods* 2011, **9**(2):173-175.

209. Peitsch MC: **ProMod and Swiss-Model: Internet-based tools for automated comparative protein modelling**. *Biochem Soc Trans* 1996, **24**(1):274-279.

210. Eswar N, Eramian D, Webb B, Shen MY, Sali A: **Protein structure modeling with MODELLER**. *Methods Mol Biol* 2008, **426**:145-159.

211. Sali A, Potterton L, Yuan F, van Vlijmen H, Karplus M: **Evaluation of comparative protein modeling by MODELLER**. *Proteins* 1995, **23**(3):318-326.

212. Fiser A, Sali A: **Modeller: generation and refinement of homology-based protein structure models**. *Methods Enzymol* 2003, **374**:461-491.

213. Benkert P, Biasini M, Schwede T: **Toward the estimation of the absolute quality of individual protein structure models**. *Bioinformatics* 2011, **27**(3):343-350.

214. Mariani V, Kiefer F, Schmidt T, Haas J, Schwede T: **Assessment of template based protein structure predictions in CASP9**. *Proteins* 2011, **79 Suppl 10**:37-58.

Appendix A

CONSERVED MOTIFS OF THE PROV SUBUNITS OF THE PROUS

The ATP-binding subunits (ProV) amino acid sequences of *V. parahaemolyticus* RIMD2210633 locus tags VPA1726 (395 residues) and VPA1109 (394 residues), *Pseudomonas syringae* pv. tomato DC3000 locus tag PSPTO_0462 (392 residues), *E. coli* K-12 MG1655 locus tag b2677 (400 residues), and *Sinorhizobium meliloti* 2011 locus tag SM2011_c02739 (349 residues) were aligned with NPS@: Network Protein Sequence Analysis [206]. The residues conserved for 90 % or more are represented by upper-case letters (~105 is 25.86 %); residues conserved for 50 % and less than 90 % are represented by lower-case letters (108 is 26.60 %); residues conserved less than 50 % are denoted by the white space (173 is 42.61 %); IV conserved positions are shown by (!) (5 is 1.23 %); LM conserved positions ($) (5 is 1.23 %); FY conserved positions (%) (0 is 0.00 %); NDQEBZ conserved positions (#): 10 is 2.46 %. The following motifs are highlighted in yellow (bold): (a) Walker A/P-loop (GLSGSGKS) that forms a loop that binds to the alpha and β-phosphates of di-and tri-nucleotides; (b) Q-loop/lid motif (MVFQ) that contains an invariant Gln that is thought to be the attacking nucleophile in ATP hydrolysis; (c) Walker B motif (ILLMDE) thought to coordinate the Mg2^{+} ion or polarize the attacking water molecule in ATP hydrolysis like the switch region. This motif also contains four aliphatic residues followed by two negatively charged residues; (d) D-loop motif (SALD) contains an invariant Asp; (e) H-loop/switch region (VFISHDL) contains an invariant Histdine (His) that is thought to polarize the attacking water molecule during ATP hydrolysis. Together Walker A, Walker B, Q-loop, D-loop, and H-loop form the nucleotide binding site/ ATP binding site (chemical binding site). The ATPase multiple sequence alignment also contains additional conserved domains: (1) Two CBS domains for *E. coli* positions 284 and 391; (2) Two CBS for *V.*

parahaemolyticus (ProU1) positions 284 and 391; (3) One CBS domain for *V. parahaemolyticus* (ProU2) positions 340 and 393.
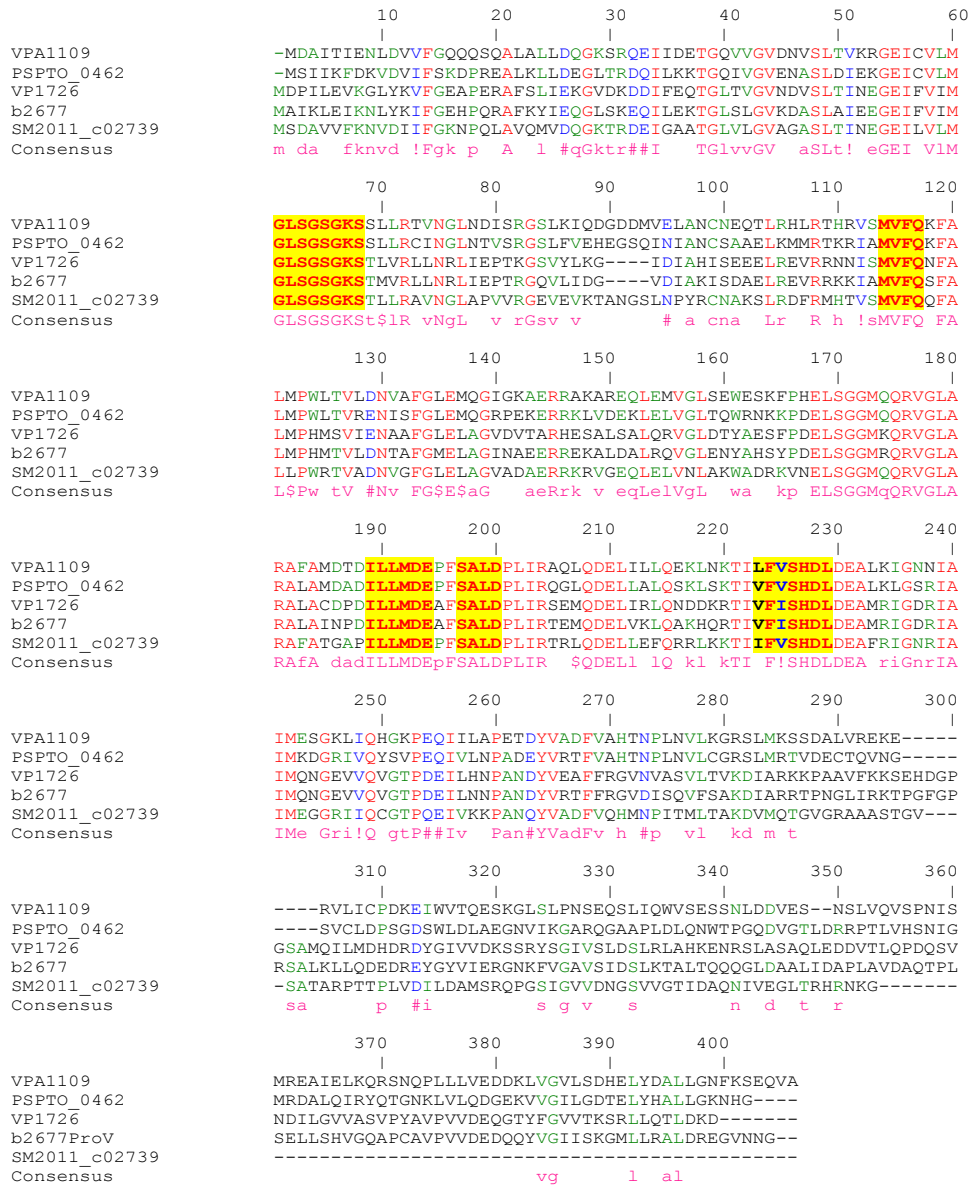
```
                    10         20         30         40         50         60
                    |          |          |          |          |          |
VPA1109       -MDAITIENLDVVFGQQQSQALALLDQGKSRQEIIDETGQVVGVDNVSLTVKRGEICVLM
PSPTO_0462    -MSIIKFDKVDVIFSKDPREALKLLDEGLTRDQILKKTGQIVGVENASLDIEKGEICVLM
VP1726        MDPILEVKGLYKVFGEAPERAFSLIEKGVDKDDIFEQTGLTVGVNDVSLTINEGEIFVIM
b2677         MAIKLEIKNLYKIFGEHPQRAFKYIEQGLSKEQILEKTGLSLGVKDASLAIEEGEIFVIM
SM2011_c02739 MSDAVVFKNVDIIFGKNPQLAVQMVDQGKTRDEIGAATGLVLGVAGASLTINEGEILVLM
Consensus     m da  fknvd !Fgk p  A  l #qGktr##I    TGlvvGV  aSLt! eGEI VlM

                    70         80         90        100        110        120
                    |          |          |          |          |          |
VPA1109       GLSGSGKSSLLRTVNGLNDISRGSLKIQDGDDMVELANCNEQTLRHLRTHRVSMVFQKFA
PSPTO_0462    GLSGSGKSSLLRCINGLNTVSRGSLFVEHEGSQINIANCSAAELKMMRTKRIAMVFQKFA
VP1726        GLSGSGKSTLVRLLNRLIEPTKGSVYLKG----IDIAHISEEELREVRRNNISMVFQNFA
b2677         GLSGSGKSTMVRLLNRLIEPTRGQVLIDG----VDIAKISDAELREVRRKKIAMVFQSFA
SM2011_c02739 GLSGSGKSTLLRAVNGLAPVVRGEVEVKTANGSLNPYRCNAKSLRDFRMHTVSMVFQQFA
Consensus     GLSGSGKSt$lR vNgL  v rGsv v         # a cna  Lr  R h !sMVFQ FA

                   130        140        150        160        170        180
                    |          |          |          |          |          |
VPA1109       LMPWLTVLDNVAFGLEMQGIGKAERRAKAREQLEMVGLSEWESKFPHELSGGMQQRVGLA
PSPTO_0462    LMPWLTVRENISFGLEMQGRPEKERRKLVDEKLELVGLTQWRNKKPDELSGGMQQRVGLA
VP1726        LMPHMSVIENAAFGLELAGVDVTARHESALSALQRVGLDTYAESFPDELSGGMKQRVGLA
b2677         LMPHMTVLDNTAFGMELAGINAEERREKALDALRQVGLENYAHSYPDELSGGMRQRVGLA
SM2011_c02739 LLPWRTVADNVGFGLELAGVADAERRKRVGEQLELVNLAKWADRKVNELSGGMQQRVGLA
Consensus     L$Pw tV #Nv FG$E$aG  aeRrk v eqLelVgL  wa  kp ELSGGMqQRVGLA

                   190        200        210        220        230        240
                    |          |          |          |          |          |
VPA1109       RAFAMDTDILLMDEPFSALDPLIRAQLQDELILLQEKLNKTILFVSHDLDEALKIGNNIA
PSPTO_0462    RALAMDADILLMDEPFSALDPLIRQGLQDELLALQSKLSKTIVFVSHDLDEALKLGSRIA
VP1726        RALACDPDILLMDEAFSALDPLIRSEMQDELIRLQNDDKRTIVFISHDLDEAMRIGDRIA
b2677         RALAINPDILLMDEAFSALDPLIRTEMQDELVKLQAKHQRTIVFISHDLDEAMRIGDRIA
SM2011_c02739 RAFATGAPILLMDEPFSALDPLIRTRLQDELLEFQRRLKKTIIFVSHDLDEAFRIGNRIA
Consensus     RAfA dadILLMDEpFSALDPLIR  $QDELl  lQ  kl kTI F!SHDLDEA riGnrIA

                   250        260        270        280        290        300
                    |          |          |          |          |          |
VPA1109       IMESGKLIQHGKPEQIILAPETDYVADFVAHTNPLNVLKGRSLMKSSDALVREKE-----
PSPTO_0462    IMKDGRIVQYSVPEQIVLNPADEYVRTFVAHTNPLNVLCGRSLMRTVDECTQVNG-----
VP1726        IMQNGEVVQVGTPDEILHNPANDYVEAFFRGVNVASVLTVKDIARKKPAAVFKKSEHDGP
b2677         IMQNGEVVQVGTPDEILNNPANDYVRTFFRGVDISQVFSAKDIARRTPNGLIRKTPGFGP
SM2011_c02739 IMEGGRIIQCGTPQEIVKKPANQYVADFVQHMNPITMLTAKDVMQTGVGRAAASTGV---
Consensus     IMe Gri!Q gtP##Iv  Pan#YVadFv h #p  vl  kd m t

                   310        320        330        340        350        360
                    |          |          |          |          |          |
VPA1109       ----RVLICPDKEIWVTQESKGLSLPNSEQSLIQWVSESSNLDDVES--NSLVQVSPNIS
PSPTO_0462    ----SVCLDPSGDSWLDLAEGNVIKGARQGAAPLDLQNWTPGQDVGTLDRRPTLVHSNIG
VP1726        GSAMQILMDHDRDYGIVVDKSSRYSGIVSLDSLRLAHKENRSLASAQLEDDVTLQPDQSV
b2677         RSALKLLQDEDREYGYVIERGNKFVGAVSIDSLKTALTQQQGLDAALIDAPLAVDAQTPL
SM2011_c02739 -SATARPTTPLVDILDAMSRQPGSIGVVDNGSVVGTIDAQNIVEGLTRHRNKG-------
Consensus     sa     p  #i      s g v  s        n  d  t  r

                   370        380        390        400
                    |          |          |          |
VPA1109       MREAIELKQRSNQPLLLVEDDKLVGVLSDHELYDALLGNFKSEQVA
PSPTO_0462    MRDALQIRYQTGNKLVLQDGEKVVGILGDTELYHALLGKNHG----
VP1726        NDILGVVASVPYAVPVVDEQGTYFGVVTKSRLLQTLDKD-------
b2677ProV     SELLSHVGQAPCAVPVVDEDQQYVGIISKGMLLRALDREGVNNG--
SM2011_c02739 ---------------------------------------------
Consensus                       vg     l  al
```

Figure 26   **Sequence alignment of the ProV subunits of the ProU systems**. *V. parahaemolyticus* VP1726 (ProU1) and VPA1109 (ProU2), *P. syringae* pv. tomato DC3000 (PSPTO_0462), *E. coli* K-12 MG1655 (b2677), and *Sinorhizobium meliloti* 2011 (SM2011_c02739).

Appendix B

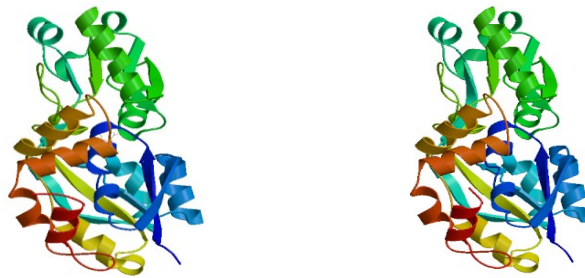**MODELING PREDICTION OF 3D STRUCTURE OF THE PROX**

The ProU component systems have been shown to uptake proline, glycine betaine and related molecules in a wide range of bacterial species. Our examination of the role of two ProUs in *V. parahaemolyticus* suggested that they are involved in the uptake of proline, but not glycine betaine. The lack of glycine betaine uptake by the ProU component systems observed in this study is perplexing, given what has been widely reported in the literature. In an attempt to get preliminary insight on the binding site of these proteins, we performed a modeling homology prediction of the periplasmic ligand-binding protein (ProX) of ProU1 and ProU2 present in *V. parahaemolyticus*. We utilized 3D protein homology modeling tool from SWISS-MODEL Workspace (a fully automated protein structure homology-modeling server, accessible via the ExPASy web server, or from the program Deepview [Swiss Pdb-Viewer]). Different steps as implemented by SWISS-MODEL Workspace were used for 3D modeling process. First, template search was performed with amino acid sequences of periplasmic-binding protein (ProX) targets of ProU1 (VP1728) and ProU2 (VPA1111) proteins using BLAST search [207] against the primary amino acid sequences contained in the SWISS-MODEL Template Library (SMTL). A total of 10 templates was found for VP1728 and 14 templates for VPA1109. An initial HHblits profile was built using the procedure outlined in [208], followed by one iteration of HHblits against NR20. The obtained profile was then searched against all profiles of the SMTL. A total of 262 templates was found for VP1728 (ProU1) and 383 for VPA1109 (ProU2). Next, template selection was performed using the quality of target-template alignment. The templates with the highest alignment quality were then selected for model building, which was carried out based on the target-template alignment using Promod [209]. Coordinates which were conserved between the target

131

and the template were copied from the template to the model. In case Promod was unable to build a model, models were built with MODELLER as a fallback [210-212]. Estimation of the quality of the model was assessed using the QMEAN scoring function [213]. Ligand modeling was subsequently performed by transferring ligands present in the template structure and copied to the model following specific criteria[214]. Finally, oligomeric state conservation for homo-oligomeric structure of the target protein was predicted based on the analysis of pairwise interfaces of the identified template structures using a QscoreOligomer.

A Template: ProX from *E.coli* (PDB id: 1r9l.1) [1]   Target ProX (VP1728)
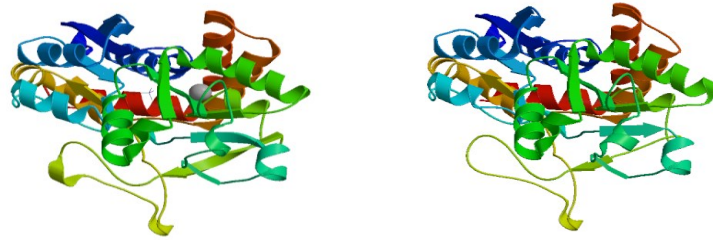
B

Template: ChoX from S. meliloti (PDB id: **2rin.1)** [2]   Target ProX (VPA111)

Figure 27   **Modeling 3D prediction of the ProX subunits of the ProU systems**.
3D modeling predictions of ProU1 and ProU2 of *V. parahaemolyticus*
were achieved using amino acids sequences of ProU1 (VP1728) and
ProU2 (VPA1111) as targets. Template searches with Blast and HHBlits
were performed against the SWISS-MODEL template library SMTL;
selected templates were automatically aligned based on the percentage
amino identity and used to predict the model of the target proteins. **A**.
Template protein (ProX) (PDB id: 1r9l.1) of *E. coli* [1] used for 3D
structure prediction of the target VP1728 (ProU1). **B**. Template protein
(ChoX) (PDB id: 2rin.1) from *S. meliloti* [2] used for 3D structure
prediction of the target VPA1111 (ProU2).

Appendix C

^{1}H-NMR PROFILES OF COMPOUNDS USED AS CONTROLS

Controls used for ^{1}H-NMR analyses were prepared using chemical compounds purchased from SIGMA. Control compounds (proline, glutamate, choline, glycine betaine, and ectoine) were prepared and adjusted to a working concentration of 500 μM. These compounds were then individually dissolved in ethanol. After an evaporation step to remove ethanol, the resulting dried material was dissolved in D2O slovent. ^{1}H-NMR data were acquired with a Bruker AVANCE III-400 MHz spectrophotometer and processed using the ACD/Labs processing software.
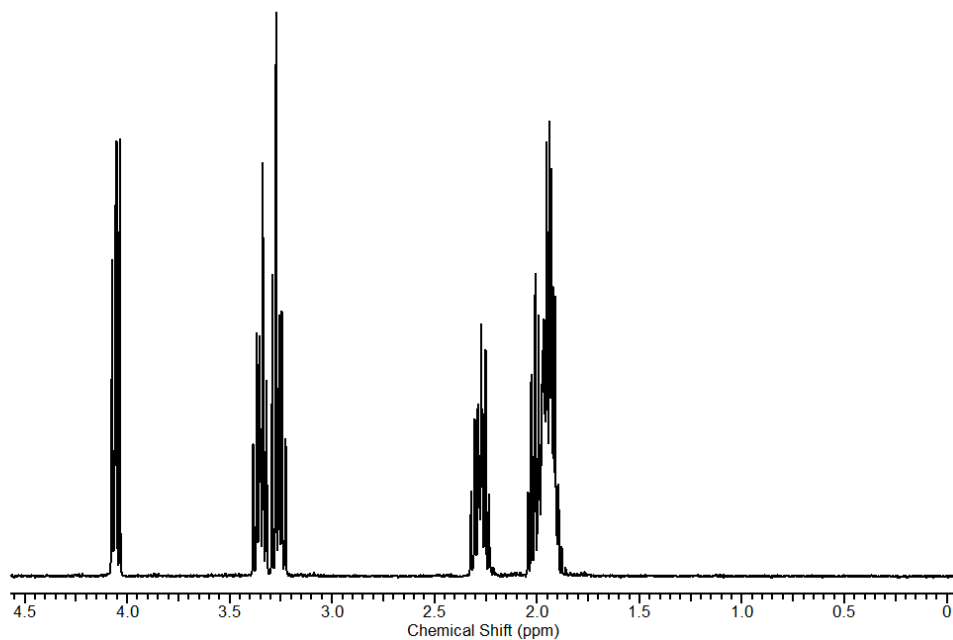
Figure 28   **¹H-NMR analysis of Proline**. A working concentration of 500 μM
Proline (SIGMA) dissolved in D2O was used as control. 1H-NMR was
acquired with a Bruker AVANCE III-400 MHz NMR Spectrometer and
processed with the ACD/Labs processing software. The chemical shifts
(δ) are expressed in ppm in the figure. Peaks corresponding to the
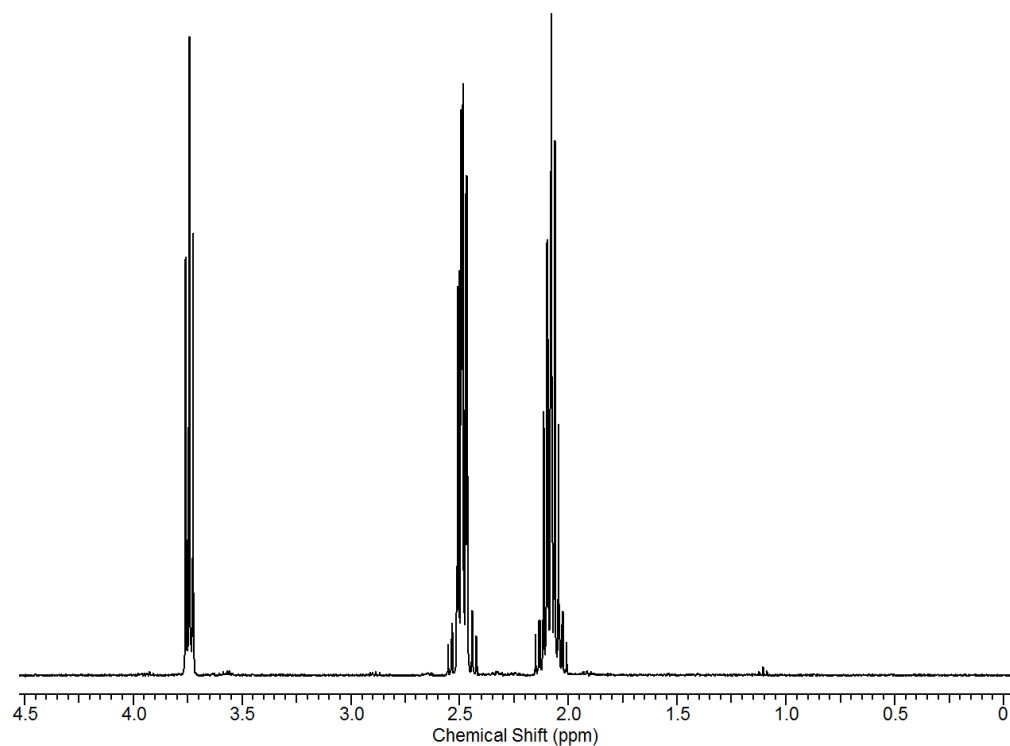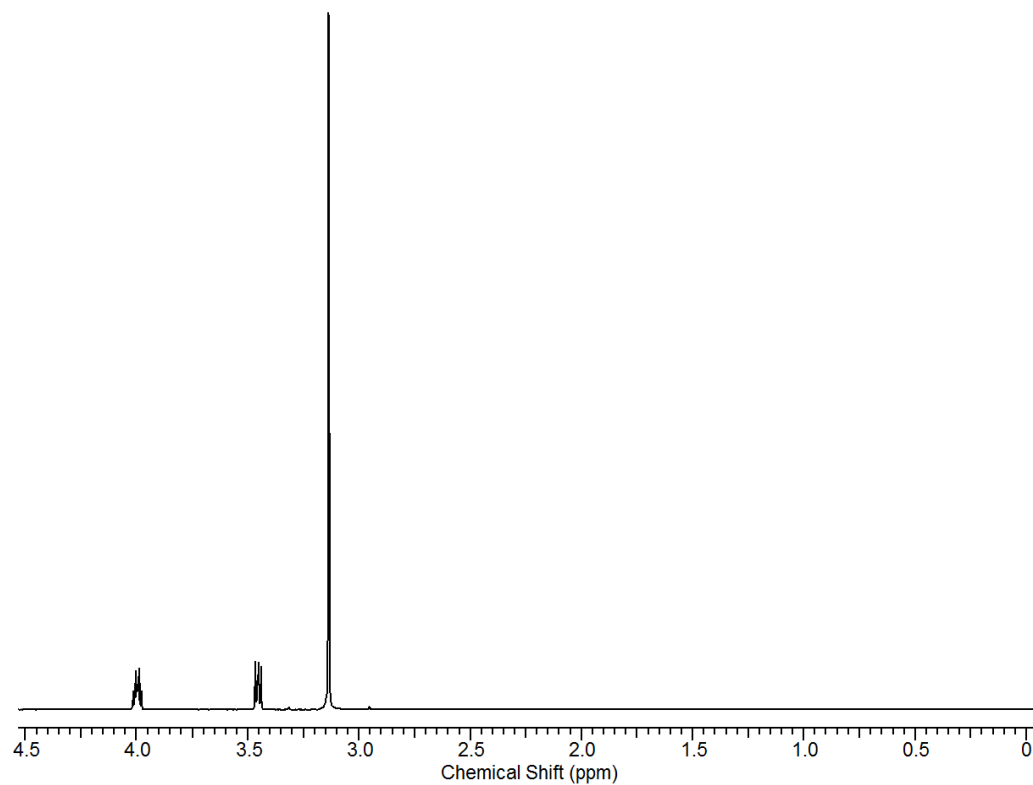compound of interest are shown in the figure.

Figure 29   **^{1}H-NMR analysis of Glutamate**. A working concentration of 500 μM of Glutamate (SIGMA) dissolved in D_2O was prepared and used as control. ^{1}H-NMR analysis was acquired with a Bruker AVANCE III-400 MHz NMR Spectrometer and processed with the ACD/Labs processing software. The chemical shifts (δ) are expressed in ppm in the figure. Peaks corresponding to the compound of interest are shown in the figure.

Figure 30   **¹H-NMR analysis of Choline**. A working concentration of 500 μM of
Choline (SIGMA) dissolved in D_2O was prepared and used as control.
¹H-NMR analysis was acquired with a Bruker AVANCE III-400 MHz
NMR Spectrometer and processed with the ACD/Labs processing
software. The chemical shifts (δ) are expressed in ppm in the figure.
Peaks corresponding to the compound of interest are shown in the figure.

Figure 31   **¹H-NMR analysis of Glycine betaine**. A working concentration of 500 µM of Glycine betaine (SIGMA) dissolved in D_2O was prepared and used as control. ¹H-NMR analysis was acquired with a Bruker AVANCE III-400 MHz NMR Spectrometer and processed with the ACD/Labs processing software. The chemical shifts (δ) are expressed in ppm in the figure. Peaks corresponding to the compound of interest are shown in the figure.
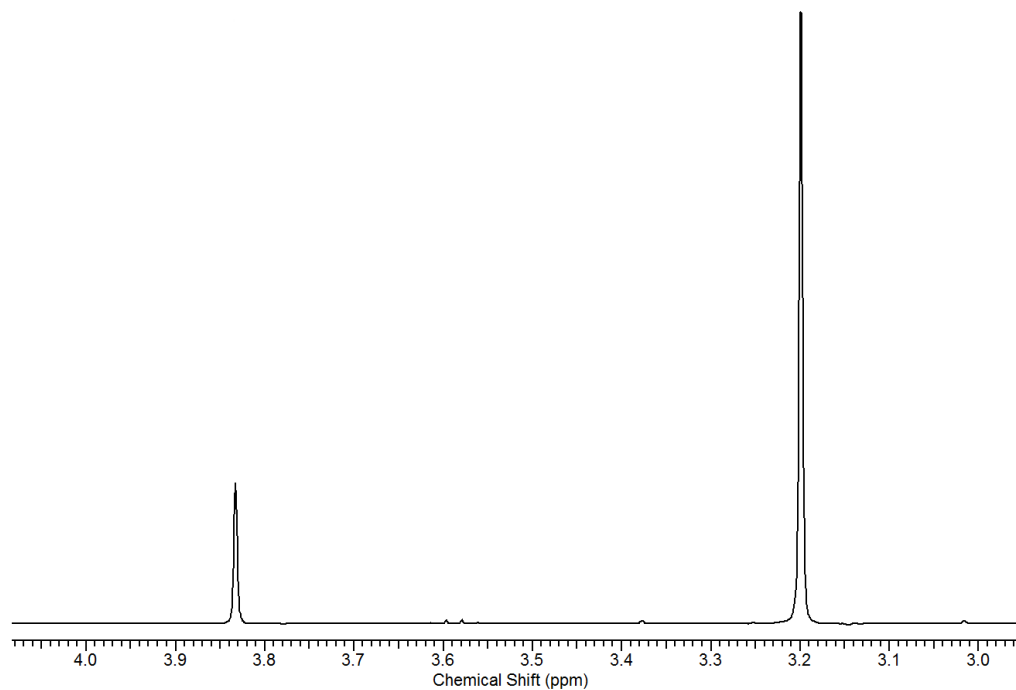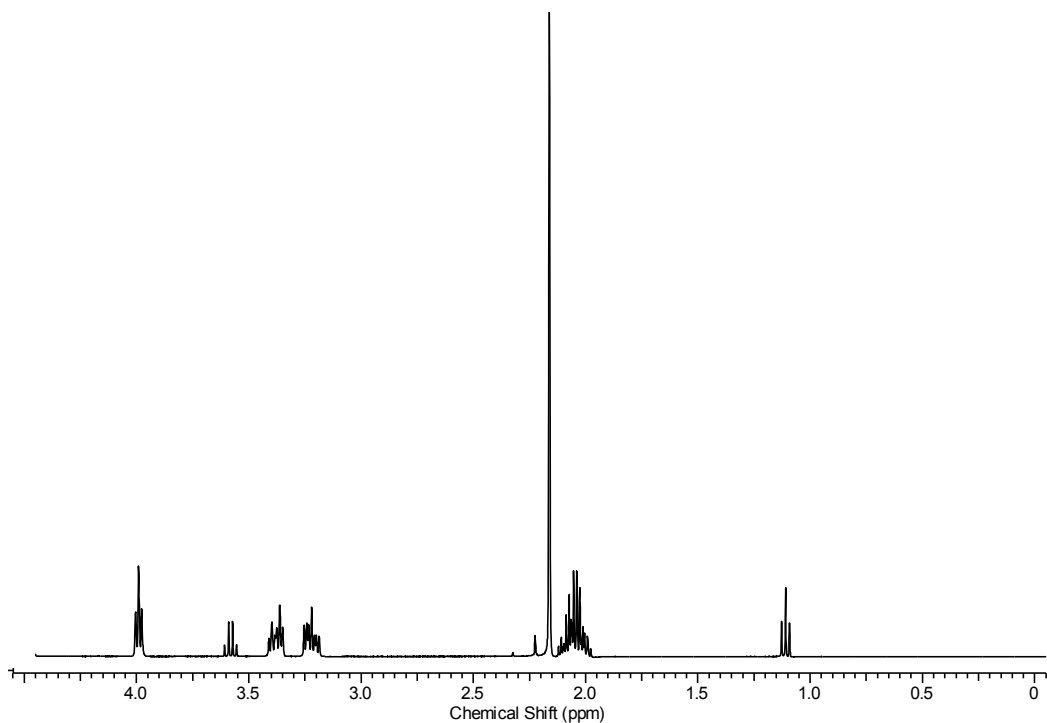
Figure 32   **¹H-NMR analysis of Ectoine**. A working concentration of 500 μM of
Ectoine (SIGMA) dissolved in D_2O was prepared and used as control.
¹H-NMR analysis was acquired with a Bruker AVANCE III-400 MHz
NMR Spectrometer and processed with the ACD/Labs processing
software. The chemical shifts (δ) are expressed in ppm in the figure.
Peaks corresponding to ectoine are labeled in the figure.